



HAL
open science

A glossary of plant cell structures: Current insights and future questions

Byung-Ho Kang, Charles T Anderson, Shin-Ichi Arimura, Emmanuelle Maria Bayer, Magdalena Bezanilla, Miguel A Botella, Federica Brandizzi, Tessa M Burch-Smith, Kent D Chapman, Kai Dünser, et al.

► To cite this version:

Byung-Ho Kang, Charles T Anderson, Shin-Ichi Arimura, Emmanuelle Maria Bayer, Magdalena Bezanilla, et al.. A glossary of plant cell structures: Current insights and future questions. *The Plant cell*, 2022, 34 (1), pp.10-52. 10.1093/plcell/koab247 . hal-03374829v1

HAL Id: hal-03374829

<https://hal.science/hal-03374829v1>

Submitted on 12 Oct 2021 (v1), last revised 7 Feb 2023 (v2)

HAL is a multi-disciplinary open access archive for the deposit and dissemination of scientific research documents, whether they are published or not. The documents may come from teaching and research institutions in France or abroad, or from public or private research centers.

L'archive ouverte pluridisciplinaire **HAL**, est destinée au dépôt et à la diffusion de documents scientifiques de niveau recherche, publiés ou non, émanant des établissements d'enseignement et de recherche français ou étrangers, des laboratoires publics ou privés.

REVIEW ARTICLE

A glossary of plant cell structures: Current insights and future questions

Byung-Ho Kang^{a*}, Charles T. Anderson^b, Shin-ichi Arimura^c, Emmanuelle Bayer^d, Magdalena Bezanilla^e, Miguel A. Botella^f, Federica Brandizzi^{g,h,i}, Tessa M. Burch-Smith^j, Kent D. Chapman^k, Kai Dünser^{l,m}, Yangnan Guⁿ, Yvon Jaillais^o, Helmut Kirchhoff^p, Marisa S. Otegui^q, Abel Rosado^r, Yu Tangⁿ, Jürgen Kleine-Vehn^{l,m}, Pengwei Wang^s, Bethany Karlin Zolman^t

^aSchool of Life Sciences, Centre for Cell & Developmental Biology and State Key Laboratory of Agrobiotechnology, The Chinese University of Hong Kong, Shatin, New Territories, Hong Kong, China

^bDepartment of Biology and Center for Lignocellulose Structure and Formation, The Pennsylvania State University, University Park, PA 16802 USA

^cGraduate School of Agricultural and Life Sciences, University of Tokyo, Japan

^dUniv. Bordeaux, CNRS, Laboratoire de Biogenèse Membranaire, UMR 5200, F-33140 Villenave d'Ornon, France

^eDepartment of Biological Sciences, Dartmouth College, Hanover, NH 03755, USA

^fDepartamento de Biología Molecular y Bioquímica, Instituto de Hortifruticultura Subtropical y Mediterránea "La Mayora," Universidad de Málaga-Consejo Superior de Investigaciones Científicas (IHSM-UMA-CSIC), Universidad de Málaga, Campus Teatinos, 29071 Málaga, Spain

^gMSU-DOE Plant Research Lab, Michigan State University, East Lansing, MI, 48824 USA

^hDepartment of Plant Biology, Michigan State University, East Lansing, MI, 48824 USA

ⁱGreat Lakes Bioenergy Research Center, Michigan State University, East Lansing, MI, 48824 USA

^jDepartment of Biochemistry & Cellular and Molecular Biology, University of Tennessee, Knoxville, TN 37996 USA

^kBioDiscovery Institute and Department of Biological Sciences, University of North Texas, Denton, TX, 76203 USA

^lFaculty of Biology, Chair of Molecular Plant Physiology (MoPP) University of Freiburg, 79104 Freiburg, Germany

^mCenter for Integrative Biological Signalling Studies (CIBSS), University of Freiburg, 79104 Freiburg, Germany

ⁿDepartment of Plant and Microbial Biology, Innovative Genomics Institute, University of California, Berkeley, CA 94720, USA

^oLaboratoire Reproduction et Développement des Plantes (RDP), Université de Lyon, ENS de Lyon, UCB Lyon 1, CNRS, INRAE, Lyon, France

^pInstitute of Biological Chemistry, Washington State University, Pullman, WA, 99164 USA

^qDepartment of Botany and Center for Quantitative Cell Imaging, University of Wisconsin-Madison, WI 53706 USA

^rDepartment of Botany, University of British Columbia, V6T1Z4 Vancouver, BC, Canada

^sKey Laboratory of Horticultural Plant Biology (MOE), College of Horticulture and Forestry Sciences, Huazhong Agricultural University, Wuhan 430070, Hubei Province, China

^tDepartment of Biology, University of Missouri – St. Louis, St. Louis MO 63121 USA

*Corresponding author: bkang@cuhk.edu.hk

Short title: A glossary of plant cell organelles

One-sentence summary: A collection of short reviews of plant cell organelles covering our up-to-date understanding, novel findings, and future research outlooks.

ABSTRACT

In this glossary of plant cell structures, we asked experts to summarize a present-day view of plant organelles and structures, including a discussion of outstanding questions. In the following short reviews, the authors discuss the complexities of the plant cell endomembrane system, exciting connections between organelles, novel insights into peroxisome structure and function, dynamics of mitochondria, and the mysteries that need to be unlocked from the plant cell wall. These discussions are focused through a lens of new microscopy techniques. Advanced imaging has uncovered unexpected shapes, dynamics, and intricate membrane formations. With a continued focus in the next decade, these imaging modalities coupled with functional studies are sure to begin to unravel mysteries of the plant cell.

1 INTRODUCTION

2 For the Cell Biology Special Focus Issue, we wanted readers to have a modern view of
3 plant cell structures that are sure to come up in research articles and other reviews. A
4 common theme found throughout is how advancements in microscopy have illuminated
5 fascinating new aspects of the plant cell, in particular the ability to generate 3-dimensional
6 images using electron tomography whereby thicker specimens are imaged through a tilt
7 series in the electron microscope, enabling the generation of a 3-dimensional image. In
8 this glossary, we gathered experts in the field to share their striking images as well as
9 their intellectual insights on how plant cell structures are understood today. This journey
10 through the plant cell begins at the nucleus, where new insights into the protein
11 composition of the nuclear envelope and its connections with the cytoplasm are beginning
12 to decipher the functional diversity of the nucleus and how the nucleus is organized and
13 linked to cytoplasmic status. The plant nucleus also hosts many phase-separated

14 biomolecular condensates, making it an ideal place to study this exciting new cell
15 biological phenomenon.

16
17 Continuous with the nuclear envelope, the endoplasmic reticulum (ER) in all of its spatial
18 and temporal complexity holds many unresolved questions. The Golgi, of central
19 importance in polysaccharide biosynthesis for building the plant body, has several plant-
20 specific features. The trans-Golgi network (TGN) and endosomes comprise a nexus of
21 membrane-intricate compartments with vastly different shaping mechanisms, ultimately
22 linking trafficking to the plasma membrane (PM) or the vacuole. The vacuole is the largest
23 organelle in mature plant cells, playing multiple roles from cellular homeostasis, storage,
24 growth, and development to plant responses to biotic/abiotic stresses. Long known to be
25 a reservoir for lipids, lipid droplets (LDs) are emerging as important for plant responses
26 to environmental stress. New insights into the molecular mechanisms driving LD
27 formation from the ER are discussed.

28
29 Recent imaging of peroxisomes in developing seedlings has revealed strikingly complex
30 membrane topologies. Imaging of live mitochondria demonstrates how dynamic plant
31 mitochondria are, with many fusion and fission events occurring to generate a syncytial
32 mitochondrial network within cells. High-resolution imaging of chloroplasts during
33 developmental transitions underscores the structural complexity of these organelles and
34 provides new models for populating the essential thylakoid membranes. Contact sites
35 couple organelles to each other, creating a mechanism to communicate status across
36 different subcellular structures. Plasmodesmata (PD) connect cells to each other,
37 providing routes for short and long-distance communication. Finally, the cell wall not only
38 patterns the cell but also builds the plant body and protects the plant from both abiotic
39 and biotic stresses. The research described in this review has been performed in
40 *Arabidopsis thaliana* unless otherwise stated.

41

42 **THE PLANT NUCLEUS: A GIANT IN THE ORGANELLE GALAXY**

43

44 (Written by Yu Tang and Yangnan Gu)

45
46 The nucleus can be thought of as a gigantic organelle defined by a double-layered
47 membrane structure called the nuclear envelope. The nuclear envelope sequesters the
48 nuclear genome and spatially separates transcription from translation, an evolutionary
49 invention that enables remarkable functions and regulatory mechanisms that are
50 fundamentally important to the eukaryotic cell (e.g. intricate spatial-temporal regulation of
51 gene expression and signal transduction). Here, we briefly summarize current views in
52 key aspects of the plant nucleus, including structure, composition, dynamics, and
53 function, from the surface to the interior.

54

55 **Nuclear envelope protein composition and function**

56 The nuclear envelope surrounds the nucleus (Figure 1A) and is composed of the outer
57 and inner nuclear membranes (Figure 1B), both of which harbor distinct collections of
58 proteins that make the nuclear envelope a platform for versatile functions and
59 communication. Plant nuclear envelope proteins have been reported to function in nuclear
60 calcium signaling (Capoen et al., 2011; Charpentier et al., 2016), chromatin organization
61 and dynamics (Pawar et al., 2016; Gumber et al., 2019), immune activation (Gu et al.,
62 2016), cell cycle progression (Wang et al., 2019), mechanical shielding (Goswami et al.,
63 2020), and so on (Figure 1D). Among these protein complexes, the LINC (linker of
64 nucleoskeleton and cytoskeleton) complex is one of the best characterized. The LINC
65 complex is composed of the inner nuclear membrane-localized SUN (Sad1/UNC48
66 homology) protein and the outer nuclear membrane-localized KASH (Klarsicht/ANC-
67 1/Syne Homology) protein, with the former associated with the nucleoskeleton and
68 chromatin and the latter bound with cytoskeleton and motor proteins (Figure 1D). SUN
69 and KASH physically interact in the perinuclear region, thus establishing a molecular
70 structure that enables the translation of cytoplasmic mechanical forces into nuclear
71 movement and chromatin activities. The plant LINC complexes have been shown to play
72 critical roles in stomatal development and responses to light and hormone signals
73 (Gumber et al., 2019; Biel et al., 2020a, b), male gametophyte development (Tamura et
74 al., 2013; Varas et al., 2015; Zhou et al., 2015; Moser et al., 2020), and plant-microbe
75 interactions (Zhou et al., 2014; Newman-Griffis et al., 2019). Nonetheless, compared with

76 animals and yeast, we still lack a comprehensive understanding of nuclear envelope
77 protein composition and function in plants. Recent applications of advanced proteomic
78 tools in plants (e.g. proximity labeling proteomics), however, have empowered the
79 identification of novel nuclear envelope components (Goto et al., 2019; Tang et al.,
80 2020a) and nuclear envelope-specific biological processes (e.g. inner nuclear
81 membrane-associated membrane protein degradation (Huang et al., 2020)). Future
82 studies using continuously evolving proteomics and microscopy techniques will greatly
83 expand our view of the global protein landscape of the plant nuclear envelope and unravel
84 both eukaryote-conserved and plant-specific nuclear envelope functions.

85

86 **The nuclear pore complex: more than a conduit for nucleocytoplasmic transport**

87 The nucleus, a special membrane compartment, evolved a sophisticated communication
88 system that allows remarkably efficient but highly selective exchange of materials across
89 the nuclear envelope. The outer and inner nuclear membranes fuse at numerous sites to
90 form physical openings, each ~120 nm in diameter, termed nuclear pores (Figure 1C).
91 The surface of individual plant nuclear pores is covered by ~1,000 nucleoporin proteins
92 of ~40 different types, which are assembled into a structurally conserved mega protein
93 complex called the nuclear pore complex (Tamura et al., 2010; Mosalaganti et al., 2018)
94 (Figure 1D). The central channel of the nuclear pore complex is filled with a protein
95 meshwork made up of intrinsically disordered phenylalanine-glycine (FG)-rich
96 nucleoporins, which are capable of interacting with nuclear transport receptors (importin
97 and exportin) that carry out selective transport of cargo molecules. Besides playing a
98 conserved role in mediating nucleocytoplasmic transport, individual plant nucleoporins
99 have been reported to play specific roles in regulating flowering time, hormone signaling,
100 and activation of abiotic and biotic stress responses, suggesting that the nuclear pore
101 complex may function as a versatile signaling platform in addition to a conserved
102 trafficking apparatus in plants (Meier et al., 2017; Gu, 2018; de Leone et al., 2020; Li and
103 Gu, 2020). Efforts in identifying novel nucleoporins and dissecting their functional
104 importance in different aspects of plant physiology are still undergoing (Tang et al.,
105 2020b), which may help to address fundamental biological principles underlying the
106 nuclear pore complex in both plants and animals.

107

108 **The nucleoskeleton**

109 Underneath the inner nuclear membrane lies the plant nucleoskeleton, assembled by long
110 coiled-coil lamin-like proteins (e.g., CRWNs, named for the crowded nuclei mutants) and
111 CRWN-associated proteins (e.g. KAKU4), which bear no sequence homology with animal
112 lamin proteins. These proteins are required for proper nuclear morphology (Wang et al.,
113 2013; Goto et al., 2014; McKenna et al., 2021) and potentially interact extensively with
114 the nuclear pore complex basket (Mermet et al., 2021) and membrane-bound inner
115 nuclear membrane proteins to form the plant nuclear lamina. CRWNs were recently
116 shown to also interact with histone modifiers and to be necessary for tethering chromatin
117 to the inner nuclear membrane to suppress stress-related gene expression (Hu et al.,
118 2019; Mikulski et al., 2019; Choi and Richards, 2020; Sakamoto et al., 2020; Wang et al.,
119 2021). These studies suggest a critical role of the plant nuclear lamina in maintaining
120 heterochromatin organization and repression at the nuclear rim, similar to what was found
121 in animals. Future studies will determine whether other plant nuclear lamina components,
122 such as inner nuclear membrane proteins, also contribute to this process.

123

124 **Organization of the nuclear interior**

125 Within the nucleus, the genome is organized three-dimensionally with chromosomes
126 occupying specific territories and active and inactive chromatin regions separated from
127 each other. Most heterochromatic regions and chromocenters are typically positioned
128 near the nuclear periphery. However, the distribution of telomeres and some other
129 transcriptionally quiescent regions varies between plant species (Figure 1D). For
130 example, most telomeres are attached to the nuclear surface in wheat and barley but are
131 associated with the nucleolus in *Arabidopsis* and maize (*Zea mays*) (Pontvianne et al.,
132 2016). Recent genome-wide high throughput chromosome conformation capture (Hi-C)
133 analyses in both diploid and polyploid plant species revealed extensive inter- and intra-
134 chromosomal interactions that define higher-order chromosomal packing during
135 interphase (Bi et al., 2017; Liu et al., 2017; Dong et al., 2018; Concia et al., 2020). Both
136 the spatial positioning (nuclear envelope tethering) and the three-dimensional
137 organization of chromatin are tightly linked to local epigenetic states and can profoundly

138 influence chromatin activities, such as transcription regulation and the timing of DNA
139 replication (Grob et al., 2014; Wear et al., 2017; Karaaslan et al., 2020; Sakamoto et al.,
140 2020; Bishop et al., 2021).

141
142 Like chromatin, many biomolecules are also organized in a dynamic and heterogeneous
143 manner within the nucleus. Spontaneous nucleation of biomolecules drives the formation
144 of many membrane-less compartments observed in plant nuclei, including nucleoli, Cajal
145 bodies, photobodies, dicing bodies, splicing speckles, DNA damage foci, and immune-
146 activated condensates (Emenecker et al., 2020; Zavaliev et al., 2020; Huang et al.,
147 2021b) (Figure 1D). In these nuclear bodies, multivalent proteins/nucleic acids capable
148 of forming extensive inter- and intra-molecular interactions undergo liquid-liquid phase
149 separation, a physical principle that compositionally demixes a homogenous solution into
150 distinct liquid phases, to concentrate functionally relevant molecules and create a specific
151 subnuclear environment that is integral to nuclear functions such as ribosome biogenesis,
152 mRNA and miRNA processing, transcription activation, and signaling (Liu et al., 2012;
153 Van Buskirk et al., 2012; Fang et al., 2019; Powers et al., 2019; Jung et al., 2020; Zavaliev
154 et al., 2020; Huang et al., 2021a; Huang et al., 2021b). Further exploring the role of phase
155 separation-promoted biomolecular condensates in plants and elucidating how phase
156 separation may be regulated by internal and external signals represents an exciting new
157 research area for plant science in the next decade.

158

159 **Movement and dynamics of the nucleus**

160 Like most other organelles, the entire nucleus is capable of directional movement
161 triggered by environmental and developmental cues (e.g., towards pathogen-invading loci
162 or with the rapid elongation of pollen tubes) (Griffis et al., 2014) and can establish
163 connections with other organelles (e.g. chloroplast stromules) for signal exchange
164 (Caplan et al., 2015; Gu and Dong, 2015). Plant nuclei also exhibit distinct morphology in
165 different cell types and membrane dynamics during cell cycle progression. As an extreme
166 example, the nuclear envelope undergoes a complete breakdown and subsequent
167 reformation during mitosis. These aspects of plant nuclear dynamics have been
168 extensively reviewed elsewhere (Meier et al., 2016; Meier et al., 2017; Groves et al., 2018;

169 Groves et al., 2020; Goto et al., 2021), and mechanisms that regulate plant nuclear
170 movement, nuclear envelope dynamics, inter-organellar communication, and their
171 functional importance are currently under active investigation.

172

173 **OPEN QUESTIONS ON THE NETWORK STRUCTURE OF THE PLANT ER**

174

175 (Written by Federica Brandizzi)

176

177 The ER is a large membrane-extension organelle at the core of the secretory pathway.
178 The ER is responsible for several important processes that are essential for the life of the
179 cell and the entire organism. For example, the ER initiates the biosynthesis of secretory
180 proteins and essential lipids, functions as a calcium storage organelle, and houses
181 several receptors of hormone signaling. Morphologically, the plant ER network is
182 composed of interconnected tubules and cisternae that form a highly dynamic membrane
183 network (Figure 2), which is anchored to the PM, similar to a spider web hanging off
184 surfaces. ER tubules connect with other tubules and flatten themselves in enlarged areas,
185 also known as cisternae, forming small, triangular sheets that are called three-way
186 junctions (Shemesh et al., 2014) (Figure 2). In fully expanded plant cells, much of the cell
187 volume is occupied by the vacuole. As a consequence, the bulk of the plant ER is
188 distributed at the cell cortex where it is sandwiched between the PM and the tonoplast
189 (vacuolar membrane), in continuum with the nuclear envelope and the transvacuolar
190 strands. The transvacuolar strands form a tightly packed meshwork of ER tubules and
191 cisternae that connect distal portions of the ER across the cell through tonoplast
192 invaginations. The nature of the plant ER cisternae is unknown: they may be continuous
193 membrane sheets and tightly packed tubules or perforated sheets of membranes, as
194 described in non-plant species (Nixon-Abell et al., 2016; Schroeder et al., 2019).

195

196 The ER network undergoes continuous remodeling through processes that include
197 homotypic fusion of ER tubules and the interconversion of ER tubules and cisternae due
198 to the action of ER shapers, the cytoskeleton and associated motors, and ER-
199 cytoskeleton connectors (Brandizzi, 2021). Together, these processes and ER shapers

200 contribute to the overall movement or streaming of the ER. This is distinct from the
201 movement of other organelles (e.g., peroxisomes, mitochondria, endosomes), which
202 translocate across the cytoplasm. The relative abundance of ER tubules and cisternae
203 varies during cell growth. As cells expand, the ER shape transitions from a more
204 predominantly cisternal form, typical of non-expanded cells, to a more tubular form that
205 is visible in mature cells (Ridge et al., 1999; Stefano et al., 2014), through mechanisms
206 that are yet to be established.

207

208 In vitro and in vivo experiments have demonstrated that the ER membrane-associated
209 GTPase ROOT HAIR DEFECTIVE3 (RHD3) is responsible for the homotypic fusion of
210 the ER membrane (Chen et al., 2011; Stefano et al., 2012; Zhang et al., 2013; Ueda et
211 al., 2016) in a manner similar to the mammalian and yeast homologs atlastins and Sey1p,
212 respectively (McNew et al., 2013); however, the mechanisms underlying the fast and
213 dynamic interconversion of ER tubules and cisternae are yet to be discovered. A
214 redistribution of membrane curvature-inducing proteins, such as the conserved reticulons
215 (Tolley et al., 2008; Sparkes et al., 2009b), and the three-way junction-stabilizing
216 LUNAPARK proteins (Lnps; named for the amino acid sequence LNPARK)
217 (Kriechbaumer et al., 2018; Ueda et al., 2018; Sun et al., 2020a), is likely responsible for
218 the dynamic interconversion of ER forms, but the underlying regulatory mechanisms
219 remain largely unknown.

220

221 The biological function of the reshaping of the plant ER is still unclear. Confocal
222 microscopy analyses have demonstrated that ER movement increases during cell growth
223 concomitant with an increase in the streaming of other organelles with whom the ER is in
224 close association, such as Golgi stacks, mitochondria, peroxisomes, and endosomes.
225 Furthermore, defects in ER network structure due to the loss of RHD3 compromise cell
226 expansion as well as the streaming of the ER and closely associated organelles (Stefano
227 et al., 2014; Stefano et al., 2015). Therefore, the ER contributes to the dynamics and
228 spatial organization of other organelles, possibly through ER-organelle contact sites, and
229 this may be necessary for the organelles' functions. This is supported by the finding that
230 in an *rhd3* loss-of-function mutant, the streaming of endosomes is reduced and clathrin-

231 mediated endocytosis is compromised (Stefano et al., 2015). These results support the
232 hypothesis that the streaming of the ER and closely associated organelles is ultimately
233 important for cell growth, but the underlying mechanisms are yet to be fully elucidated.

234

235 A double loss-of-function mutant of the two Arabidopsis *Lnps* shows an increased
236 abundance of ER sheets with dense fenestration and ER conglomerates (Kriechbaumer
237 et al., 2018; Ueda et al., 2018; Sun et al., 2020a). Combined, the finding that the localized
238 distribution of *Lnps* in the ER depends on the cellular availability of their interacting protein
239 RHD3, and that *Lnps* antagonize the role of RHD3 in ER shaping and induce RHD3
240 degradation via the proteasome pathway (Sun et al., 2020a) mechanistically support the
241 notion that certain ER shapers are dependent on the abundance of other ER shapers for
242 their distribution and function in the ER. Curiously, mutants with a loss of RHD3 alone are
243 viable and show only limited phenotypic defects in plant growth (Stefano et al., 2012);
244 however, the loss of RHD3 with either member of the RHD3-like family of proteins, RHD3-
245 like 1 or RHD3-like 2, is either lethal or causes pollen defects, respectively (Zhang et al.,
246 2013). Conversely, mutants with the loss of both *Lnps* are viable, with only minor defects
247 in plant growth (Sun et al., 2020a). Therefore, certain ER shapers may have a more
248 relevant role in the life of the cell than others, either because associated ER shaping
249 events are essential compared to others or because the shapers carry out other functions,
250 in addition to ER reshaping. For example, maize reticulons 1 and 2 function in shaping
251 the ER but also as autophagy receptors and are involved in degradation of the ER through
252 the regulated process known as ER-phagy (Zhang et al., 2020). Furthermore, RHD3 has
253 been found to interact with ARK1, an armadillo-repeat containing kinesin, which is thought
254 to pull an ER tubule toward another tubule (Sun et al., 2020b). While these findings
255 support the earlier discovery that the remodeling of a subset of ER tubules depends on
256 their sliding on pre-existing microtubules (Hamada et al., 2014), they also highlight
257 additional functions of RHD3 besides its fusogenic activity of the plant ER membranes.

258

259 Future characterization of the broader roles of the plant ER shapers may provide
260 opportunities to establish how physiologically and developmentally relevant processes
261 are connected to ER network integrity. For example, the loss of RHD3 leads to an

262 attenuation of signaling in the unfolded protein response (Lai et al., 2014), a conserved
263 cytoprotective pathway that is designed to attenuate proteotoxic stress in the ER (Pastor-
264 Cantizano et al., 2020). While these findings support the idea that the homeostasis of the
265 ER network structure is critical for cell health, a challenge for the future is to establish a
266 mechanistic framework connecting ER shape integrity with the functions of essential
267 signaling pathways.

268
269 Despite the functional conservation of shapers such as RHD3, reticulons, and Lnps, the
270 plant ER structure depends on plant-unique factors. For example, a minor role for
271 microtubules in ER reshaping is consistent with the predominant role of actin in this
272 process (Sparkes et al., 2009a); this is markedly different from the dependence of ER
273 network shaping on microtubules in mammalian cells (Waterman-Storer and Salmon,
274 1998; English et al., 2009). The existence of plant-unique ER-actin interactors (i.e.,
275 SYP73 and NETWORKED 3B) (Cao et al., 2016; Wang and Hussey, 2017), plant-specific
276 molecular motors (i.e. Myosin XI family) (Peremyslov et al., 2010; Ueda et al., 2010), and
277 the absence in plants of CLIMP63, the connector of the mammalian ER to microtubules
278 and a spacer of the cisternal lumen (Klopfenstein et al., 2001; Shibata et al., 2010), further
279 support the notion that plants have developed specific mechanisms of ER shaping across
280 kingdoms. An obvious challenge for the future is to determine the nature or such
281 mechanisms via the identification of additional players. For example, proteomics of
282 cellular compartments or targeted proteomics based on pull-downs of ER shapers have
283 yielded opportunities to identify proteins making up the plant ER (Dunkley et al., 2006;
284 Kriechbaumer et al., 2018), but the challenge ahead is to define a functional pipeline to
285 identify proteins specifically involved in ER structure. Forward genetics screening based
286 on confocal microscopy analyses of Arabidopsis seedlings expressing fluorescent
287 markers to identify mutants with defective organization of secretory organelles (Faso et
288 al., 2009; Nakano et al., 2009; Takagi et al., 2013) offers a realistic opportunity to identify
289 mutations that compromise the ER, although an innate limitation of these screens is their
290 labor-intensive nature. Automation of this type of screen, along with the implementation
291 of software capable of quantitatively analyzing the dynamics of the ER (Pain et al., 2019),

292 will likely offer a platform for the rapid identification of modifiers of ER shape and
293 dynamics.

294

295 **PLANT GOLGI STACKS: VERSATILE GLYCOSYLATION FACTORIES ON THE** 296 **MOVE**

297

298 (Written by Byung-Ho Kang)

299

300 The Golgi lies at the center of the secretory pathway, importing cargoes from the ER,
301 adding glycosyl groups, and exporting these cargoes to post-Golgi compartments or the
302 extracellular space (Alberts et al., 2014). The role of the Golgi as a processing trader is
303 illustrated in its polarized stack architecture, where entry (*cis*) and exit (*trans*) sides can
304 be discerned (Figure 3A and C) (Farquhar and Palade, 1981; Moore et al., 1991). In
305 addition to serving as the site of protein and lipid glycosylation, the plant Golgi synthesizes
306 non-cellulosic cell wall polysaccharides (Zhang and Staehelin, 1992; Carpita and
307 McCann, 2000). The Golgi in plants consists of many discrete stacks (Figure 3B) whose
308 numbers per cell vary from dozens to hundreds (Dupree and Sherrier, 1998). Each stack
309 is thought to function independently (Nebenfuhr and Staehelin, 2001). The stacks travel
310 in the cytosol at speeds of up to several microns per second; this movement is dependent
311 on myosin motors (Boevink et al., 1998; Madison et al., 2015). The decentralized
312 organization of plant Golgi contrasts with that of mammalian Golgi, whose stacks are
313 stitched side-by-side to form a ribbon or a complex next to the nucleus (Ito et al., 2014).
314 Therefore, ER-to-Golgi transport and post-Golgi secretion require long-distance vesicular
315 trafficking to and from the Golgi (Gillingham and Munro, 2016). Mobile Golgi stacks in
316 plants, by contrast, can visit ER export sites (ERES), concentrate to sites of secretion,
317 and redistribute for cell division (Nebenfuhr et al., 2000; Kang and Staehelin, 2008;
318 Ndinyanka Fabrice et al., 2017).

319

320 **Transport through the plant Golgi**

321 During ER-to-Golgi transport, Golgi stacks slow down at ERES and receive COPII-type
322 vesicles (Nebenfuhr et al., 1999; Yang et al., 2005). In mammalian cells, the ER-to-Golgi

323 intermediate compartment (ERGIC) assembles at the ERES, and ER-resident proteins
324 are retrieved from the ERGIC (Appenzeller-Herzog and Hauri, 2006). Plant cells lack
325 ERGICs, as COPII vesicles are directly transferred to the cis-side of Golgi stacks in
326 association with the ER. ERES in mammalian cells are marked by ERGICs (Weigel et al.,
327 2021). Due to the absence of discrete ERGICs, plant ERES are spotted under an electron
328 microscope based on their COPII buds and Golgi stacks in their vicinity. Biosynthetic
329 activities are observed from the medial Golgi after the recycling of ER proteins is complete
330 in the cis-Golgi (Donohoe et al., 2013), indicating that the cis cisternae take the place of
331 the ERGIC in plant cells (Ito and Boutte, 2020).

332

333 Among the models describing intra-Golgi transport, the cisternal progression/maturation
334 model has been supported by electron microscopy studies of the plant Golgi (Robinson,
335 2020). It is evident from electron micrographs of plant Golgi stacks that Golgi cisternae
336 are peeled off from the trans-side, supporting the notion that Golgi cisternae are transient
337 entities (Day et al., 2013). Electron tomography analysis has revealed assembly
338 intermediates of new cisternae on the *cis*-side that exhibit highly diverse sizes and shapes
339 (Donohoe et al., 2013). Cell wall polysaccharides were detected in the cisternal lumen
340 but not in COPI-type vesicles at the cisternal margins, which are thought to retrieve Golgi-
341 resident proteins against the cisternal membrane flux (Donohoe et al., 2007).

342

343 On the trans-side, TGN compartments arise from the trans-most cisternae. This
344 transformation involves a significant reduction in the amount of membrane, suggesting
345 that Golgi-resident proteins are retrieved from the TGN (Kang et al., 2011). Secretory
346 vesicles carrying cell wall polysaccharides, clathrin-coated vesicles, and COPI vesicles
347 arise from the TGN. In cotyledon cells, darkly stained vesicles, termed dense vesicles,
348 transport globulins from the TGN to protein storage vacuoles (Robinson, 2020).

349

350 The aforementioned transport steps occur within a ribosome-excluding matrix that
351 encloses the region from COPII vesicles to TGN cisternae (Figure 3D) (Staelin and
352 Kang, 2008). The matrix likely corresponds to a dense network of proteins involved in
353 Golgi membrane assembly, maturation, TGN formation, and fastening cisternae into a

354 stack. Golgins are Golgi-localized long coiled-coil proteins, and some of them are
355 tethering factors (Latijnhouwers et al., 2005) and, given their rod-like shape, they
356 constitute scaffolds for the matrix. Mammalian Golgins are required for Golgi integrity,
357 vesicular trafficking to the Golgi, and protein glycosylation (Wong and Munro, 2014; Liu
358 et al., 2017; Witkos et al., 2019). Arabidopsis Golgins have been shown to play roles in
359 COPII vesicular transport (Kang and Staehelin, 2008) and interactions of cis-Golgi with
360 ERES (Osterrieder et al., 2017).

361

362 **Biosynthesis in the plant Golgi**

363 Production and export of cell wall matrix polysaccharides distinguish the plant Golgi from
364 its animal counterpart. The reaction cascades for polysaccharide synthesis are arranged
365 sequentially over the stack from the *cis-to-trans* direction. As the amounts of
366 glycosyltransferases and sugar transporters per stack are small, their localization within
367 the Golgi has been investigated using overexpressor lines or by localizing reaction
368 products (Chevalier et al., 2010; Meents et al., 2019). The constitutive secretion of cell
369 wall polysaccharides and several mechanisms for retaining Golgi proteins from the bulk
370 flow have been characterized (Brandizzi, 2002; Gao et al., 2014; Schoberer et al., 2019).

371

372 TGN cisternae consist of distinct domains where secretory and vacuolar cargoes are
373 separately packaged (Shimizu et al., 2021). Electron tomography imaging of Golgi/TGN
374 complexes revealed that varying ratios of secretory and clathrin-coated vesicle buds in a
375 TGN cisterna, suggesting that the biosynthetic functions of each Golgi stack are not
376 uniform in a plant cell (Staehelin and Kang, 2008). Golgi stacks appear to be versatile
377 factories whose activities are determined by the proteins imported from the ER. Golgi
378 stacks enriched with enzymes for synthesizing cell wall polysaccharides would give rise
379 to more secretory vesicles than Golgi stacks that process proteins for the vacuole.

380

381 **Future research perspectives**

382 The structures and functions of Golgi stacks change as plant cells differentiate, but the
383 molecular mechanisms governing their remodeling remain elusive. For example, small
384 Golgi stacks in root meristem cells undergo sequential remodeling as meristem cells

385 develop into gravity-sensing columella cells and eventually into mucilage-secreting
386 border cells in the root cap (Figure 3E and F) (Wang et al., 2017). Since several cell-
387 specific markers for the Arabidopsis root cap have been identified (Kamiya et al., 2016),
388 it would be possible to uncover novel genes involved in cell type-specific polysaccharide
389 synthesis and protein targeting in the Golgi after performing single-cell sequencing of root
390 cap isolates (Shaw et al., 2021). Indeed, a proteomic analysis of fractions enriched with
391 cis-, medial-, or trans-Golgi expanded the list of Golgi-resident proteins with their cisternal
392 localization (Parsons et al., 2019). Expression profiling of genes encoding Golgi proteins
393 during cell differentiation will provide insights into the regulation of Golgi functions.

394

395 Correlative light and electron microscopy refers to protocols in which macromolecules are
396 first localized with fluorescence microscopy and the volume enclosing the
397 macromolecules is then imaged by electron microscopy. This correlative approach will be
398 useful for analyzing organelles composed of heterogeneous members (Wang et al.,
399 2019). Golgi stacks labeled by specific fluorescent markers could be examined by
400 electron microscopy to characterize their nanoscale architectures and interactions with
401 other organelles. Examining the dynamics of Golgi subpopulations under stress
402 conditions will shed light on how the secretory pathway reorganizes in response to threats
403 from the outside. As export from the Golgi is mediated by the TGN, this analysis should
404 be combined with exploring TGN dynamics (Uemura et al., 2019).

405

406 Advances in cryo-electron microscopy and sample processing technology allowed for
407 electron tomography analysis of frozen-hydrated cells to visualize macromolecular
408 complexes *in situ* (Otegui and Pennington, 2018). Due to the limitation in section
409 thickness for electron microscopy, frozen cells must either be sliced or thinned by focused
410 ion beam milling (FIB). Golgi vesicles and intraluminal filaments were delineated in
411 Chlamydomonas cells by cryo-electron tomography (Engel et al., 2015). Although intact
412 plant tissues are too thick for FIB, *in vitro* germinated pollen tube tips are amenable to
413 FIB thinning (Liu et al., 2021). As Golgi stacks produce numerous secretory vesicles to
414 sustain tip growth, it would be exciting to capture images of plant Golgi stacks by cryo-

415 electron tomography to uncover novel features not observed in plastic-embedded
416 electron microscopy samples.

417

418 **PLANT ENDOSOMES: PROTEIN SORTING MASTERS**

419

420 (Written by Marisa Otegui)

421

422 The ability to regulate the composition of the PM and the endomembrane system is critical
423 for cell survival. Endosomes play a central role in this process by regulating protein and
424 lipid (cargo) trafficking in the endomembrane system through both the anterograde and
425 retrograde pathways. As part of the anterograde pathways, that is, transport from the site
426 of synthesis to the place of residence and function, proteins and lipids synthesized in the
427 ER are typically transported in vesicles to the Golgi, to the TGN, and from there, either to
428 the PM (exocytosis) or to the vacuole. Retrograde pathways mediate the transport of
429 cargo or trafficking factors in the opposite direction from the anterograde pathway, usually
430 back to their original donor compartments. Proteins removed from the PM in vesicles
431 through clathrin-mediated endocytosis are delivered to early endosomes, where they can
432 be either recycled to the PM or carried to multivesicular endosomes (MVEs, also referred
433 to as multivesicular bodies or prevacuolar compartments) for further sorting into
434 intraluminal vesicles and subsequent degradation in the vacuolar lumen (Valencia et al.,
435 2016) (Figure 4A-D). In plants, the TGN functions as the early endosome since it is the
436 first compartment that receives endocytosed cargo (Dettmer et al., 2006; Lam et al.,
437 2007). Thus, in contrast to animal cells, plant cells do not have separate early endosomes
438 but instead combine both endocytic and biosynthetic sorting at the TGN (Viotti et al.,
439 2010).

440

441 TGNs and MVEs, the two types of plant endosomes, arise, mature, and are consumed
442 as part of their membrane trafficking function. Therefore, both types of organelles are in
443 continuous flux and can be found as subpopulations at different stages of maturation.

444

445 **The TGN**

446 As part of the endosomal pathway, the TGN receives PM cargo, which is either recycled
447 back to the PM or retained for further sorting in MVEs and degradation in vacuoles. As
448 part of the secretory pathway, the TGN produces both vesicles carrying cargo (proteins,
449 membrane lipids, and cell wall polysaccharides) to the PM and vesicles containing
450 vacuolar cargo (Rosquete et al., 2018). The TGN mediates retrograde recycling back to
451 the Golgi and ER through COPI- (Bykov et al., 2017) and retromer-mediated trafficking
452 (Niemes et al., 2010).

453

454 The TGN forms largely through cisternal maturation of the trans-most Golgi cisterna
455 (Golgi-associated TGN or GA-TGN) but eventually detaches from the Golgi, becoming an
456 independent organelle (free or Golgi-independent TGN) that fragments into vesicles
457 (Toyooka et al., 2009; Kang et al., 2011; Uemura et al., 2014; Uemura et al., 2019) (Figure
458 4A and B). There are approximately 35 Golgi stacks and GA-TGNs in an Arabidopsis
459 shoot apical meristematic cell at interphase (Segui-Simarro and Staehelin, 2006). In
460 Arabidopsis root cells, as the *trans*-most cisterna matures into the TGN, it develops
461 numerous vesicle buds, loses 30-35% of its total membrane surface area, and becomes
462 enriched in the Rab GTPases RAB-A2a and RAB-A4b, the phosphatidylinositol 4-kinase
463 PI4Kb1, the vacuolar V-ATPase subunit VHA1a (Figure 4D), and the SNAREs (Soluble
464 N-ethylmaleimide sensitive factor Attachment protein Receptor) SYP61 (Syntaxin of
465 Plants 61), SYP43, VAMP721 (Vesicle-Associated Membrane Protein 721), VAMP722,
466 and VAMP727 (Dettmer et al., 2006; Chow et al., 2008; Kang et al., 2011; Zhang et al.,
467 2011). As the Golgi-associated TGN detaches from the Golgi stacks to become
468 free/Golgi-independent TGNs, the budding profiles become more abundant (Figure 4B).

469

470 These Golgi-associated and Golgi-independent TGN subpopulations play distinct roles in
471 trafficking (Renna et al., 2018; Uemura et al., 2019; Ito and Boutte, 2020). For example,
472 GA-TGN but not free/Golgi-independent TGNs label with the endocytic tracer FM4-64
473 (Uemura et al., 2019), suggesting that endosomal function is carried out by the GA-TGN,
474 whereas free Golgi-independent TGNs seem to be primarily involved in exocytosis. The
475 different trafficking functions of the TGN are spatially separated in subdomains that differ
476 both in their protein and membrane lipid composition (Wattelet-Boyer et al., 2016; Shimizu

477 et al., 2021) and their ability to recruit specific vesicle-forming coat proteins, such as
478 clathrin. Thus, within the GA-TGN, there are at least two “zones”, the secretory (exocytic)
479 and the vacuolar-trafficking zones. The secretory zone generates exocytic vesicles and
480 is enriched in the SNARE VAMP721, the adaptor complex AP-1, the accessory protein
481 EPSIN1, and clathrin. The vacuolar trafficking zone sends vesicles to MVEs for vacuolar
482 delivery and is enriched in VAMP727, the adaptor complex AP-4, and the accessory
483 protein MODIFIED TRANSPORT TO THE VACUOLE1 (MTV1) (Heinze et al., 2020;
484 Shimizu et al., 2021). In addition, a plant-specific TRAPPII complex is thought to mediate
485 the recruitment/tethering of endocytosed vesicles to subdomains of the TGN (Rosquete
486 et al., 2019).

487
488 The TGN not only has subdomains for exocytic, endocytic, and vacuolar trafficking, but it
489 also associates with protein complexes that control the trafficking of specific cargo
490 proteins. Thus, for example, the TGN-localized protein ECHIDNA controls the secretion
491 of only a subset of PM proteins, such as the auxin influx carrier AUX1 (Boutte et al., 2013).
492 By contrast, a module formed by seven transmembrane domain-containing proteins
493 (7TM) and components of guanine nucleotide-binding (G) protein signaling function
494 together at the Golgi and TGN to regulate the exocytosis of cellulose synthases, but not
495 the endocytosis or general exocytosis of soluble or PM cargoes (McFarlane et al., 2021).

496

497 **MVEs**

498 MVEs arise from membranes derived from the TGN and are characterized by a rounded
499 shape, the presence of intraluminal vesicles (Figure 4A and B), and their association with
500 RAB-F GTPases such as ARA6, ARA7, and RHA1 (Figure 4C) (Haas et al., 2007). There
501 are approximately 17-20 MVEs in interphase meristematic cells, which are usually found
502 in close proximity to the GA-TGN (Segui-Simarro and Staehelin, 2006). PM proteins
503 targeted for degradation are usually ubiquitinated at the PM, internalized by endocytosis,
504 and delivered first to the TGN and then to MVEs (Figure 4A).

505

506 The MVE intraluminal vesicles contain cargo proteins targeted for degradation in the
507 vacuole. Failure to properly sort PM components into intraluminal vesicles results in the

508 accumulation of PM proteins in the vacuolar membrane (Figure 4A), which leads to
509 severe developmental defects, and most frequently, to lethality.

510

511 At the surface of the MVE limiting membrane (the single membrane that surrounds the
512 MVE), a group of cytosolic proteins called ESCRTs (Endosomal Sorting Complex
513 Required for Transport) bind, cluster, and sort the ubiquitinated cargo into membrane
514 domains that bend away from the cytoplasm, forming the intraluminal vesicles typical of
515 these organelles. This membrane bending event occurs in the reverse (negative) topology
516 of the better understood process of vesiculation, such as clathrin-mediated endocytosis.
517 Although it has long been assumed that ESCRTs orchestrate the formation and release
518 of a single endosomal vesicle at a time, studies performed in *Arabidopsis* have shown
519 that at least in plants, these vesicles do not bud off individually but form in concatenated
520 networks (Buono et al., 2017; Goodman et al., 2021).

521

522 In general, ESCRT proteins are well conserved across organisms, from Archaea
523 (Makarova et al., 2010; Dobro et al., 2013; Pulschen et al., 2020) to Eukarya. In fungi and
524 metazoans, five multimeric ESCRT complexes have been identified: ESCRT-0 to III and
525 the triple AAA ATPase SKD1 (SUPPRESSOR OF K⁺ TRANSPORT GROWTH
526 DEFECT1) with its activator LIP5. Plants contain putative orthologs for most of the
527 ESCRT proteins originally identified in metazoans and fungi (Spitzer et al., 2006; Haas et
528 al., 2007; Spitzer et al., 2009; Kalinowska et al., 2015; Buono et al., 2016; Yu et al., 2016;
529 Wang et al., 2017a), with the exception of ESCRT-0 (Winter and Hauser, 2006), which is
530 an early acting complex that binds phosphoinositide-3-phosphate (PI3P), a lipid enriched
531 in endosomal membranes that is critical for the recruitment of ESCRT proteins to
532 endosomes. However, a group of proteins called TOL (TOML1-LIKE) are likely to play the
533 role of ESCRT-0 in plants (Korbei et al., 2013; Moulinier-Anzola et al., 2020).

534

535 How do ESCRT proteins mediate intraluminal vesicle formation and sequestration of
536 cargo proteins? ESCRT-0, -I, and -II contain ubiquitin-binding domains and contribute to
537 the clustering of ubiquitinated cargo on the endosomal membrane and to membrane
538 deformation (Liese et al., 2020). De-ubiquitinating enzymes remove the ubiquitin on cargo

539 before their final sequestration into intraluminal vesicles. Critical for the final steps in
540 vesicle formation is the presence of membrane cargo (Chiaruttini et al., 2015) as well as
541 ESCRT-III and ESCRT-III-associated proteins, which are able to trigger membrane
542 deformation and neck constriction (Hanson et al., 2008; Fyfe et al., 2011; McCullough et
543 al., 2013; Chiaruttini et al., 2015).

544

545 Plants commonly contain several isoforms for each ESCRT subunit and even have
546 evolved plant-specific ESCRT proteins, such as PROS (Positive Regulator of SKD1,
547 which enhances SKD1 activity) (Reyes et al., 2014), FREE1/FYVE1 (Gao et al., 2014),
548 and FYVE4 (Liu et al., 2021a). Interestingly, both proteins contain FYVE domains able to
549 bind PI3P. FREE1 interacts with ESCRT-I subunits and is essential for endosomal sorting
550 (Gao et al., 2014), whereas FYVE4 is required for the recruitment of ESCRT-III subunits
551 (Liu et al., 2021a).

552

553 In Arabidopsis, the loss of critical ESCRT subunits such as CHMP1 and FREE1 results
554 in serious protein mis-sorting defects and embryo and/or seedling lethality (Spitzer et al,
555 2009; Gao et al 2014), whereas the loss of the SKD1-activator LIP5 causes abnormal
556 root gravitropic responses (Buono et al 2016), reduced tolerance to heat and drought
557 stress (Wang et al 2015; Xia et al 2016), and compromised resistance to pathogens
558 (Wang et al 2014).

559

560 **Future perspectives**

561 Our understanding of endosomal biogenesis and the molecular machinery mediating its
562 multiple sorting functions has increased dramatically during the past decades. However,
563 new regulatory and sorting components are being discovered and many more remain
564 elusive, making it still challenging to comprehend how sorting functions are both
565 segregated and integrated in TGNs and MVEs. The plant endosomes have many distinct
566 features that make them different from their counterparts in other organisms. For
567 example, whether the concatenation of MVE intraluminal vesicles in complex networks
568 is unique to plants or is a universal mechanism in all eukaryotes is presently unknown. It
569 is tempting to speculate that the evolution of unique ESCRT components and the drastic

570 diversification of some ESCRT isoforms may have contributed to the unique features of
571 intralumenal vesicle formation in plants.

572

573

574 **THE MULTIFUNCTIONAL VACUOLE**

575

576 (Written by Kai Dünser and Jürgen Kleine-Vehn)

577

578 The plant vacuole fulfills a plethora of indispensable and sometimes seemingly
579 contradictory functions. This multifunctional compartment ensures lytic degradation, but
580 also stores proteins, carbohydrates, and secondary metabolites. The vacuole is a place
581 for detoxification of harmful molecules, but also accumulates allelochemicals for plant
582 defense against herbivory. It is central in pH as well as ion homeostasis, thereby also
583 contributing to the control of turgor pressure (reviewed in Wink 1993; Marty, 1999;
584 Eisenach and De Angeli 2017; de Brito Francisco and Martinoia 2018; Krüger and
585 Schumacher 2018; Hara-Nishimura and Hatsugai, 2011) (Figure 5A and B). Besides all
586 this, the vacuole fulfills a remarkable space-filling function, enabling enormously rapid
587 plant cell enlargement with little *de novo* production of cytosolic components (reviewed in
588 Dünser and Kleine-Vehn, 2015; Kaiser and Scheuring, 2020), but on the other hand must
589 get out of the way to allow cell division (Figure 5A and B).

590

591 **Vacuolar biogenesis**

592 Genetic interference with vacuole biogenesis, as observed in *Arabidopsis vacuoleless1*
593 mutants, leads to embryonic lethality, which indicates that the formation of vacuoles is
594 essential for plant cells (Rojo et al., 2001). Depending on the cell type and developmental
595 context, vacuoles may be formed *de novo* or inherited to daughter cells during cell division
596 (reviewed in Cui et al., 2020). Mechanisms for vacuole biogenesis in roots include the so
597 called provacuoles and the small vacuoles. Provacuoles are double membrane, tubular
598 structures that bud off from the ER, constituting a major membrane source for the
599 establishment of large vacuolar structures (Viotti et al. 2013). On the other hand, whole-
600 cell electron tomography proposed that multivesicular bodies (also called Pre-Vacuolar

601 Compartments (PVC) in plants) undergo homotypic fusion to form small vacuoles prior to
602 their fusion, resulting in the development of large central vacuoles (Cui et al., 2019).

603

604 **Specialized vacuoles and their functions**

605 Although some vacuoles fulfill multiple roles simultaneously, others specialize. Different
606 types of vacuoles carry distinct sets of vacuolar membrane (tonoplast) marker proteins,
607 and different types can co-exist in some plant cells (Frigerio et al., 2008). The lytic
608 vacuole, often considered equivalent to the animal lysosome, is most common and plays
609 central roles in virtually all tissues. By contrast, protein storage vacuoles are
610 predominantly found in seeds and serve as nutrient reservoirs during germination
611 (Ludevid et al., 1992; Höfte et al., 1992; Rojo et al., 2001). Vacuolar identity can be
612 dynamic and undergo transitions, such as lytic vacuole to protein storage vacuole or *vice*
613 *versa*, often marking crucial developmental fate changes (Gattolin et al., 2011; Zheng and
614 Staehlin, 2011; Feeney et al., 2018).

615

616 Autophagy is the regulated degradation of proteins and organelles. During autophagy,
617 the autophagic body is released into the vacuole lumen for degradation by hydrolytic
618 enzymes. Hence, lytic vacuoles contribute to the autophagic processes that maintain
619 basal cellular homeostasis, act in environmental stress responses, or play roles during
620 pathogen defense, not the least of which is the vacuolar contribution to programmed cell
621 death (reviewed in Su et al., 2020; Bassham et al., 2006; Yoshimoto and Ohsumi 2018;
622 Merkulova et al., 2014; Phillips et al., 2008; Chung et al., 2010). Age-related
623 developmental transitions are marked by senescence-associated vacuoles, which are
624 implicated in the degradation of chloroplasts by autophagy (Otegui et al., 2005).

625

626 **pH, ion, and water homeostasis**

627 Vacuolar pH, ion, and water homeostasis are crucial for all of its functions. Vacuole
628 acidification is essential for the lytic degradation of various cellular components. The
629 vacuolar H⁺-pyrophosphatase (V-PPase) AVP1 and two vacuolar H⁺-ATPase (V-ATPase)
630 proton pumps are the main actors in vacuolar pH. In addition, the P-type H⁺-ATPase
631 AHA10 contributes to vacuolar acidification in some cell types (Appelhagen et al., 2015).

632 V-ATPase VHA-a1 activity at the TGN likely contributes to vesicle-based delivery of
633 protons to the vacuole, suggesting that other endomembranes can also affect the pH of
634 the vacuole (Kriegel et al., 2015).

635
636 Cellular ion homeostasis is maintained by a myriad of transporters and channels that are
637 energized by either the proton gradient (ΔpH) or the membrane potential difference ($\Delta\psi$)
638 (reviewed in Martinoia et al., 2012; Martinoia 2018). The vacuolar contribution to cellular
639 ion homeostasis is, among other processes, important for the regulation of turgor
640 pressure (Barragán et al., 2012). Reversible stomatal movements are controlled by
641 changes in guard cell volume, accompanied by drastic changes in vacuole morphology
642 and volume (Franks et al., 2001; Shope et al., 2003; Tanaka et al., 2007; Gao et al., 2009;
643 Bak et al., 2013; Eisenach and De Angeli, 2017). Stomatal opening has mainly been
644 linked to the accumulation of K^+ within the vacuole, whereas stomatal closure is facilitated
645 by K^+ release from the vacuole (Barragán et al., 2012; Andrés et al., 2014; Wege et al.,
646 2014; De Angeli et al., 2013; Gobert et al., 2007; Isner et al., 2018). Water channels
647 (aquaporins) such as TIP1;1 contribute to the water permeability of the tonoplast and
648 buffering the water content of the cytoplasm. Because the expression of TIP1;1 correlates
649 with the onset of cell elongation, it may link intracellular water exchange with cellular
650 enlargement (Beebo et al., 2009).

651

652 **Vacuolar size and its impact on cell size control**

653 The size of the vacuole correlates with cell size in plants, implying that vacuoles are
654 involved in cell size determination (Owens and Poole 1979; Berger et al., 1998; Löffke et
655 al., 2013; Dünser and Kleine-Vehn, 2015). Comparisons of whole-cell 3-D reconstructions
656 in the meristem and elongation zone show that the cellular space occupied by the vacuole
657 gradually increases during cellular elongation, while the cytoplasmic volume remains
658 relatively constant. Therefore, the space-filling function of vacuoles enables rapid cell
659 expansion in a metabolically cost-effective way by obviating the need for considerable *de*
660 *novo* production of cytosolic content (Dünser and Kleine-Vehn, 2015; Dünser et al., 2019)
661 (Figure 5B). Vacuolar size is controlled by the phytohormone auxin, which restricts the
662 rate of cellular expansion (Löffke et al., 2015). Auxin interferes with the delivery and fusion

663 of vesicles to the tonoplast, as well as with actin/myosin-dependent constriction of the
664 vacuole, contributing to the volume of the vacuole and its cellular occupation (Löpfke et al.,
665 2015; Scheuring et al., 2016; Kaiser et al., 2019). A cell wall sensing mechanism allows
666 for the alignment of cell wall acidification/loosening with intracellular vacuole expansion,
667 consequently ensuring cytosol homeostasis required for rapid cell expansion (Dünser et
668 al., 2019; reviewed in Herger et al., 2019).

669

670 **Multiple cargos and multiple trafficking routes towards the vacuole**

671 The vacuolar membrane is a highly connected part of the endomembrane system that
672 receives cargos and membrane from various trafficking routes. Anterograde vacuolar
673 cargo sorting to the vacuole occurs early in the secretory pathway, at the level of the ER
674 and the Golgi apparatus, and includes cargo binding to vacuolar sorting receptors. Upon
675 reaching the TGN, cargo proteins are typically released, and the vacuolar sorting
676 receptors are recycled back to the Golgi and the ER (Künzli et al., 2016), although
677 vacuolar storage proteins in dense vesicles may already be sorted at the cis-cisternae of
678 the Golgi (Hillmer et al., 2001).

679

680 Multiple trafficking routes from the TGN to the vacuole exist, including delivery via PVCs
681 in a RAB5 and RAB7-dependent manner as well as through clathrin-coated vesicles,
682 which are formed in an adaptor protein complex-dependent fashion (Cui et al., 2014;
683 Ebine et al., 2014; Singh et al. 2014; Heinze et al. 2020; Feraru et al., 2010; Zwiewka et
684 al., 2011) (Figure 5A). Notably, two of the most abundant tonoplast proteins, the vacuolar
685 H⁺-ATPase VHA-a3 and the vacuolar H⁺-pyrophosphatase AVP1/VHP1, completely
686 bypass the PVC and/or Golgi trafficking route and are delivered to the vacuole via ER-
687 derived provacuoles (Viotti et al. 2013).

688

689 The vacuole is the endpoint of the endocytic pathway, through which ubiquitylated
690 membrane proteins are likely directed to sub-compartments of the TGN. These sub-
691 compartments mature into or transit towards the PVC (Scheuring et al., 2011).

692

693 The incorporation of PVCs, AP1-, AP4-, and AP-3/RAB5 vesicles, provacuoles, small
694 vacuoles, and autophagosomes into the central vacuole requires membrane tethering,
695 and finally membrane fusion. Recent findings confirm that class c core vacuole/endosome
696 tethering (CORVET) and homotypic fusion and protein sorting (HOPS) complexes are
697 involved in mediating tethering events for different vacuolar transport pathways in plants.
698 They ultimately activate the vacuolar soluble N-ethylmaleimide-sensitive-factor
699 attachment receptor (SNARE) complex, which selectively catalyzes the fusion of adjacent
700 membranes (Takemoto et al., 2018; Ebine et al., 2008; Uemura et al., 2010).

701

702 **Open questions about vacuolar functions**

703 Due to its multifunctional roles, the vacuole needs to process multiple and possibly
704 conflicting information. As such, it is a central integrative signaling hub for plant cells. Very
705 little is known about how its functions evolved over time. Evolutionary analysis could shed
706 further light on this and could also tackle some conceptual questions on vacuolar
707 biogenesis.

708

709 The multitude of trafficking pathways reflects the plethora of cargoes that need to traffic
710 independently to the vacuole; these processes have been subject to intense study,
711 leading to our quite detailed understanding. On the other hand, mechanisms that control
712 the dimension of the vacuole and its contribution to the plant-specific lifestyle are less well
713 understood. We don't yet understand how plant cells monitor the size of the vacuole,
714 which seems especially challenging considering the dazzling complexity of membrane
715 flow towards the vacuole and the dynamic housekeeping processes that the vacuole
716 coordinates.

717

718 The control of vacuole size is not only crucial for its role in rapid cell expansion but also
719 cell division, if only because the vacuole can physically occupy the location specified for
720 cell plate formation. Formative, asymmetric cell divisions that initiate distinct cell fates
721 require the dedicated control of intracellular space and nuclear migration. Therefore, it is
722 not surprising that cells undergoing formative/asymmetric cell divisions contain small,
723 fragmented vacuoles (as seen in lateral root founder cells) or polarized vacuoles (as seen

724 in zygotes (Jansen et al., 2012; Kimata et al., 2019; Matsumoto et al., 2021). Interestingly,
725 the steric control of vacuolar shape during cell division or nuclear migration is somewhat
726 reminiscent of statolith sedimentation in gravitropic shoots, which also requires constant
727 reshaping of the central vacuole (Kato et al., 2002).

728

729 It is apparent that a feedback-based, dynamic remodeling of the vacuole is required to
730 ensure basic cellular functions, but the underlying mechanisms are largely unknown.
731 These open questions ensure that research on vacuoles will continue to amaze us in the
732 future.

733

734

735 **LIPID DROPLETS: SPECIALIZED SUBCELLULAR HYDROPHOBIC** 736 **COMPARTMENTS**

737

738 (Written by Kent Chapman)

739

740 Like all cells, plant cells accumulate storage lipids in their cytoplasm as discrete LDs,
741 most often consisting of a hydrophobic core of non-bilayer forming lipids such as
742 triacylglycerols (TAGs) or sterol esters surrounded by an emulsifying monolayer of
743 phospholipids (Pyc et al., 2017a; Huang, 2018; Ischebeck et al., 2020). Although less
744 commonly considered, rubber particles of rubber-producing plant species with a
745 polyisoprenoid hydrophobic core share the same overall structure (Yamashita and
746 Takahashi, 2020). This thermodynamically stable structure was originally observed in
747 transmission electron microscopy (TEM) micrographs and described by various terms
748 such as lipid bodies, oil bodies, spherosomes, or oleosomes (Wanner and Theimer,
749 1978). However, the contemporary, unifying terminology of “lipid droplets” emphasizes
750 the evolutionary conservation of this compartment across kingdoms of life where there
751 are increasing reports of functions beyond the efficient storage of carbon (Lundquist et
752 al., 2020).

753

754 In plants, LDs are most commonly associated with oilseeds and oleaginous fruits, where
755 they compartmentalize the well-known “vegetable oils” (Chapman et al., 2012). However,
756 LDs are present in essentially all cell types in plants, ranging from a few LDs per cell in
757 leaves to thousands of LDs per cell in seeds. Because the most abundant LD proteins in
758 seeds—oleosins—are not produced in most plant cell types, recent efforts to identify LD
759 proteins through proteomics approaches in non-seed tissues (Horn et al., 2013; Brocard
760 et al., 2017; Kretzschmar et al., 2018; Fernandez-Santos et al., 2020) have expanded the
761 inventory of LD proteins in plant cells. These proteins and their partners have begun to
762 suggest previously unrecognized participants in LD formation, stability, turnover, and
763 functions.

764
765 Among the recently recognized LD proteins are the so-called LDAPs (LIPID DROPLET-
766 ASSOCIATED PROTEINS), which share homology with small rubber particle proteins
767 from rubber producing plants. LDAPs were identified as prominent proteins in purified
768 LDs isolated from avocado (*Persea americana*) mesocarp (Horn et al., 2013) and have
769 since become appreciated for their widespread occurrence throughout the plant kingdom
770 (Gidda et al., 2016; Brocard et al., 2017; de Vries and Ischebeck, 2020) as well as for
771 their induction by drought stress (Kim et al., 2016). The LDAPs are relatively small
772 proteins without extended hydrophobic regions, and they have been shown to localize
773 specifically to the LD surface, perhaps through their extensive amphipathic helices.
774 Screens for potential protein interactors, which might serve as protein recognition sites
775 for LDAPs on the organelle surface, identified the protein LDIP (LDAP-INTERACTING
776 PROTEIN), which also is widely distributed in the plant kingdom (Pyc et al., 2017b; Coulon
777 et al., 2020) (de Vries and Ischebeck, 2020). LDAPs and LDIP are expressed in both
778 seed and non-seed tissues of plants and are suspected of playing broader roles in
779 compartmentalization of neutral lipids in cells beyond those found in seed tissues.

780
781 Another recently identified LD protein is the PLANT UBX DOMAIN-CONTAINING
782 PROTEIN10 (PUX10). PUX10 localizes to LDs through a hydrophobic polypeptide
783 sequence and recruits the AAA-type ATPase CELL DIVISION CYCLE48 (CDC48) protein
784 to the LD surface (Deruyffelaere et al., 2018; Kretzschmar et al., 2018). This interaction

785 is believed to support the selective extraction of LD surface proteins, such as oleosins
786 and LDAPs, for their ubiquitin-mediated protein degradation. This LD-associated
787 degradation pathway likely operates in all cells of plants to repurpose the surface and/or
788 contents of the LD compartment during development or in response to environmental
789 stresses.

790

791 **LD formation at the ER**

792 Like in most eukaryotes, LD formation in plant cells originates in the ER where the
793 enzymes for storage lipid assembly are present (Figure 6). Ultrastructural studies
794 frequently reveal intimate connections of LDs with the ER (Figure 6B) (Herman, 2009;
795 Brocard et al., 2017), which can also be captured by confocal fluorescence laser scanning
796 microscopy (Figure 6A). The process of LD proliferation can be capitulated at the
797 subcellular level in *Nicotiana benthamiana* cells. In these cells, LDs are normally low in
798 abundance, and the transient expression of cDNAs encoding proteins implicated in LD
799 formation can readily be studied, such as the transcription factor LEAFY COTYLEDON 2
800 (LEC2), which is preferentially expressed in developing seeds (Figure 6A). A transient
801 system for LD studies also has been developed using tobacco pollen tubes (Muller et al.,
802 2017), which has been particularly useful for protein localization studies due to the large
803 number of LDs normally present in these cells.

804

805 Existing models for LD formation suggest that newly synthesized TAGs aggregate and
806 form foci or “lipid lens” structures between the two leaflets of the ER bilayer (Figure 6C)
807 (Pyc et al., 2017a). An oligomeric protein complex comprising SEIPIN subunits in the ER
808 bilayer coordinates these TAG foci as they grow (Chapman et al., 2019). SEIPIN proteins
809 direct a bulge of newly accumulating neutral lipids to emerge into the cytoplasm covered
810 with a monolayer of ER-derived phospholipid. Unlike fungi and metazoans, plants have
811 multiple genes encoding SEIPIN isoforms (Cai et al., 2015). In Arabidopsis, *SEIPIN1* is
812 expressed mostly in seed and seedling tissues, whereas *SEIPIN2* and *SEIPIN3* are
813 expressed in essentially all tissues. While loss-of-function mutants in a single *SEIPIN* gene
814 in Arabidopsis resulted in negligible phenotypes, double and especially triple *seipin*
815 mutants showed dramatic cellular disruptions in normal LD formation (Taurino et al.,

816 2018). Seeds and pollen of *sei1 sei2 sei3* mutants accumulated large aberrant-shaped
817 LDs, sometimes observable in the nucleus and ER lumen in addition to the cytoplasm.
818 These results indicate that SEIPINs play critical and partially redundant roles in the
819 normal formation of LDs in plant cells. Structural models based on homology with known
820 structures of *Drosophila* and human SEIPIN suggest that the three *Arabidopsis* SEIPINs
821 can form homo-oligomeric structures with different numbers of subunits (Chapman et al.,
822 2019), but further work is required to understand the functional interactions of the three
823 SEIPIN proteins in plant cells, their potential for hetero-oligomeric interactions, as well as
824 their partners in LD biogenesis.

825

826 The loss-of-function of two other *Arabidopsis* genes led to similar, large and aberrant LD
827 phenotypes in seeds, reminiscent of *seipin* mutants. These two genes encode VESICLE-
828 ASSOCIATED MEMBRANE PROTEIN-ASSOCIATED PROTEIN 27-1 (VAP27-1) and
829 LDIP, respectively, which were both shown to interact with SEIPINs and with LDs (Pyc et
830 al., 2017b; Greer et al., 2020). In other work, higher order oleosin mutants also displayed
831 aberrant formation of LDs during early seed development, which resulted from changes
832 in the fusion dynamics of very small LDs, not necessarily during LD formation at the ER
833 (Miquel et al., 2014). LDAPs also occur in seeds but at lower amounts than oleosins
834 (Kretzschmar et al., 2018). Finally, while LDAPs are interactors of LDIP (Pyc et al.,
835 2017b), their loss-of-function in *ldap* mutants did not result in dramatic alterations of LD
836 morphology in seeds (Gidda et al., 2016), although there may have been some increase
837 in LD size in the leaves of *ldap* knockdown mutants (Brocard et al., 2017). Future work
838 will be required to piece together the mechanistic associations between SEIPINs, LDIP,
839 VAP27-1, oleosins, LDAPs and other LD proteins; nevertheless, results to date support
840 the notion that these proteins play cooperative roles in the cellular process of LD formation
841 in plant cells (Greer et al, 2020; Pyc et al., 2021).

842

843 **Engineering the LD compartment**

844 Because of their high energy density and caloric value, LDs have become a target
845 compartment for metabolic engineering strategies to overproduce storage lipids in the
846 vegetative parts of plants. This process has met with remarkable success, leading to

847 tobacco plants with lipid yields from their leaves equivalent to oil yields from oilseed crops.
848 This overall engineering process has been described as the “push, pull, and protect”
849 concept for the efficient production and packaging of storage lipids in plant tissues
850 (Vanhercke et al., 2017; Vanhercke et al., 2019). Apparently, the accumulation of lipids
851 in leaves is at the expense of transient starch (Chu et al., 2020), illustrating a plasticity in
852 leaves for carbon storage that may ultimately be exploited for bioenergy and/or feed
853 energy-densification applications.

854
855 In addition to bioenergy applications, LDs offer a stable compartment for the
856 sequestration of various hydrophobic compounds. As such, several recent reports
857 indicate that manipulation of the LD machinery can be exploited for the subcellular
858 storage of secondary metabolites. For example, (Sadre et al., 2019) engineered the
859 accumulation of sesquiterpenes (patchoulol) and diterpenes (abetadiene) into
860 cytoplasmic LDs. Elsewhere, the expression of lipogenic proteins from mouse
861 dramatically elevated LD levels in *N. benthamiana* leaves and supported the increased
862 accumulation of the sesquiterpene phytoalexin, capsidiol, along with TAGs (Cai et al.,
863 2019). With the preponderance of bioactive hydrophobic secondary metabolites, these
864 studies illustrate the utility of engineering the cytoplasmic LD compartment in plants as a
865 repository for additional high-value isoprenoids in the future.

866

867 **Future prospects for LD biology**

868 In the last decade, increasing attention on cytoplasmic LDs has revealed a growing
869 inventory of proteins that support the formation, stability, and turnover of this compartment
870 in plant cells. Some proteins appear to have specific plant lineages, while others are
871 conserved across kingdoms. The identification of this LD machinery will support a
872 mechanistic examination of the interplay of these and other proteins in LD biogenesis,
873 both in oilseeds and in non-seed tissues of plants. In addition, functions beyond neutral
874 lipid storage continue to be revealed for LDs in different plant cell types, including as a
875 reservoir for membrane lipid remodeling (Xu and Shanklin, 2016), a platform for the
876 production of lipophilic signals (Shimada et al., 2014; Fernandez-Santos et al., 2020), and
877 responses to environmental stress (Yang and Benning, 2018) (Lu et al., 2020). Finally,

878 an improved understanding of the cellular processes for LD formation, neutral lipid
879 deposition, and LD stability will accelerate and expand promising applications for lipid
880 engineering.

881

882

883 **THE DYNAMIC NATURE OF PEROXISOME STRUCTURES, ABUNDANCE, AND** 884 **SUBCELLULAR INTERACTIONS**

885

886 (Written by Bethany Zolman)

887

888 Peroxisomes compartmentalize diverse oxidative reactions, allowing metabolic,
889 signaling, and detoxification roles to be carried out while limiting the potential for damage
890 (Kao et al., 2018; Pan et al., 2020). Peroxisomes are a closed system, permeable only to
891 small (300-400 Da) molecules (Charton et al., 2019; Plett et al., 2020). Membrane
892 transporters import lipid substrates and ATP, NAD⁺, and CoA cofactors into peroxisomes
893 (Charton et al., 2019; Plett et al., 2020), whereas enzymes are imported by cytosolic
894 receptors that recognize one of two Peroxisomal Targeting Signals (PTS1/PTS2;
895 (Reumann and Chowdhary, 2018; Pan et al., 2020). Plant peroxisomes are indispensable
896 during early development, when seedlings rely on lipid breakdown prior to photosynthetic
897 initiation (Graham, 2008). They are also crucial for photorespiration in leaf cells and
898 reactive oxygen species (ROS) and nitrogen species metabolism throughout
899 development and under changing conditions (Del Rio and Lopez-Huertas, 2016; Kao et
900 al., 2018; Corpas et al., 2020; Pan et al., 2020; Su et al., 2020). These organelles are
901 essential for life in all eukaryotes and have many evolutionarily conserved pathways and
902 proteins (Gabaldon, 2010).

903

904 Peroxisome abundance varies based on cell type, developmental stage, and
905 environmental conditions. Although peroxisome abundance has not been characterized
906 systematically, 10-100 peroxisomes per cell have been observed (for example, (Germain
907 et al., 2001; Orth et al., 2007; Lingard et al., 2008; Kim et al., 2013; Shibata et al., 2013).
908 Peroxisome numbers increase in response to stress, including salt (Mitsuya et al., 2010;

909 Fahy et al., 2017; Frick and Strader, 2018), light (Desai and Hu, 2008), and cadmium
910 stress (Rodríguez-Serrano et al., 2016; Terron-Camero et al., 2020), as well as prior to
911 cell division (Lingard et al., 2008). Peroxisome division occurs via fission or the budding
912 of pre-peroxisomes from the ER (Agrawal and Subramani, 2016; Kao et al., 2018; Pan et
913 al., 2020; Su et al., 2020). Peroxisomes can be degraded via pexophagy, an organelle-
914 specific type of autophagy (Young and Bartel, 2016; Su et al., 2019), as part of a natural
915 turnover (Kao et al., 2018; Yamauchi et al., 2019) or when excess organelles are not
916 necessary following stress (Calero-Muñoz et al., 2019) or developmental transitions (Kim
917 et al., 2013).

918

919 Peroxisomes are small, measuring 1-2 μm in diameter in *Arabidopsis* (Rinaldi et al., 2016)
920 but with notable variability. Larger structures can be visualized 3-4 days post imbibition
921 (Rinaldi et al., 2016), with some peroxisomes over 10 μm in diameter in 4-day-old
922 seedlings. This expansion is temporary and is thought to occur following an influx of seed-
923 storage lipids (Rinaldi et al., 2016). Although their morphology can differ, peroxisomes
924 are primarily spherical.

925

926 Since their identification, peroxisomes have been considered simple organelles, with
927 typical definitions highlighting their small size, lack of a genome, and a single membrane
928 surrounding a defined matrix. However, recent investigations by Wright and Bartel (2020)
929 have led to an enhanced description of peroxisomes, one in which extensive internal
930 membranes are present. The authors combined two high-sensitivity fluorescence
931 reporters: an mRuby3-PTS to visualize the peroxisome interior and mNeonGreen tagged
932 with an mPTS membrane peroxisomal targeting signal to label the membrane (Figure 7A-
933 B) (Wright and Bartel, 2020). This combination revealed the unexpected presence of
934 internal structures, coined intraluminal vesicles (ILVs).

935

936 In 3 to 4-day-old *Arabidopsis* seedlings, membrane reporters localized around these
937 structures, but also within the interior of the organelles (Wright and Bartel, 2020). Many
938 peroxisomes contained numerous internal vesicles, which varied in size (Figure 7A-B).
939 As discussed above, 5-day-old seedlings showed expanded organelles that rapidly

940 decreased in size. These size changes were concurrent with increasing ILV and
941 internalized membrane contents. By 8 days, the seedlings continued to show membrane
942 reporters within the peroxisome lumen, with some images showing membrane signals
943 throughout the entire structure. Following this process, dense packing likely occurred over
944 time that precluded the observation of individual vesicles, such that the membrane
945 reporter appeared uniform within the lumen at this age (Wright and Bartel, 2020). These
946 seedling experiments suggest how peroxisomes mature, beginning as larger, variable
947 structures but stabilizing at a smaller size as membranes are internalized and lipid
948 metabolism slows.

949

950 These microscopic images led to an enhanced understanding of peroxisomal structure:
951 peroxisomes have an outer membrane surrounding the luminal space that contains
952 imported matrix proteins, as well as a dynamic number of membrane-bound vesicles clear
953 of matrix proteins (Figure 7A-B) (Wright and Bartel, 2020). Indeed, two proteins with
954 unique peroxisomal localization (SNOWY COTYLEDON3/UNKNOWN PROTEIN9;
955 (Albrecht et al., 2010; Quan et al., 2013) accumulated within a subset of ILVs that lacked
956 matrix proteins (Wright and Bartel, 2020). This apparent segregation yields at least three
957 distinct spaces within peroxisomes, potentially housing unique proteins, substrates,
958 cofactors, and/or environments.

959

960 Mutants with disrupted β -oxidation showed alterations in ILV number, size, composition,
961 and orientation, suggesting that β -oxidation activity is required for inner membrane
962 formation (Wright and Bartel, 2020). Long-chain seed storage lipids are insoluble; Wright
963 and Bartel (2020) hypothesized that membrane internalization may reduce the solubility
964 challenges associated with lipid mobilization in an aqueous matrix. Lipids could be
965 degraded from the membrane, with the subsequent release and degradation of the
966 shorter, more soluble substrates, leading to the reduced organelle size common in older
967 seedlings.

968

969 **Association with other organelles**

970 Beyond this structural understanding, imaging and biochemical studies have revealed the
971 physical associations of peroxisomes with LDs, plastids, mitochondria, and the ER
972 (Figure 7C; (Shai et al., 2016) (Oikawa et al., 2019). Peroxisomal enzymes catalyze
973 specific reactions within metabolic pathways, which often extend to two (or more)
974 subcellular spaces. These organelle interactions are dynamic: peroxisomes in seedlings
975 associate with LDs, for instance, whereas peroxisomes in leaves associate with
976 chloroplasts and mitochondria (Oikawa et al., 2019). Such interaction points enhance the
977 transfer efficiency of pathway intermediates. These sites also may facilitate the transfer
978 of hydrogen peroxide and other reactive species from other organelles to peroxisomes
979 for sequestration and degradation (Shai et al., 2016; Su et al., 2019).

980

981 As detailed above, many plant species contain LDs that store TAGs for energy reserves
982 (Esnay et al., 2020). Peroxisome-LD association facilitates the efficient transfer of stored
983 material for metabolism via fatty acid β -oxidation and the glyoxylate cycle. Extended
984 interactions and peroxisomal clusters in proximity to LDs occur in β -oxidation mutants
985 (Hayashi et al., 2001; Rinaldi et al., 2016), while exogenous sucrose reduces this
986 association (Cui et al., 2016), suggesting that such interactions are critical during
987 development and are mediated by cellular requirements for lipid mobilization.

988

989 Peroxisomes and chloroplasts can form specific pairs that remain intact over time
990 (Oikawa et al., 2015). Changes in peroxisome shape expand the surface area to increase
991 chloroplast interactions. In the light, peroxisomes extend into an elliptical shape versus a
992 spherical shape in darkness. Tethering factors connecting peroxisomes and chloroplasts
993 may facilitate this interaction (Oikawa et al., 2015; Gao et al., 2016), potentially including
994 the PEROXIN10 (PEX10) RING finger protein (Schumann et al., 2003; Sparkes et al.,
995 2003; Schumann et al., 2007). A dominant-negative PEX10 line had clustered
996 peroxisomes that did not associate with chloroplasts; this line had phenotypes similar to
997 photorespiration mutants (Schumann et al., 2007), which is consistent with a role for
998 organelle association in efficient metabolic transfer.

999

1000 Mitochondria also appear in close proximity to both peroxisomes and chloroplasts in the
1001 light, which is consistent with their interactive metabolic roles (Oikawa et al., 2015).
1002 Peroxisomes associate with mitochondria under stress conditions as well; increasing
1003 interactions are seen in cells exposed to high ROS levels and might be important for ROS
1004 neutralization (Jaipargas et al., 2016; Mathur, 2021).

1005
1006 Finally, peroxisomes show a close proximity with the ER (Barton et al., 2013; Oikawa et
1007 al., 2019). Interestingly, one of the two mPTS signals used by Wright and Bartel (2020)
1008 revealed accumulation in peroxisomes and reticular membranes thought to be ER. This
1009 finding is consistent with the hypothesis that the membrane protein was trafficked through
1010 the ER or has a dual function at both sites (Wright and Bartel, 2020).

1011
1012 Another shape change in peroxisomes is the formation of thin organelle protrusions
1013 known as peroxules (Mathur, 2021). These structures are up to 15 μm in length,
1014 dramatically increasing the surface area (Sinclair et al., 2009; Barton et al., 2013). The
1015 formation of these organelle extensions is transient and dynamic (Mathur, 2021). The
1016 interactions between organelles described above may be mediated by peroxules,
1017 including the proposed interactions with LDs (Thazar-Poulot et al., 2015), chloroplasts
1018 (Schumann et al., 2007), mitochondria (Jaipargas et al., 2016), and the ER (Sinclair et
1019 al., 2009). Extended structures are seen following H_2O_2 , UV-A, and hydroxyl radical
1020 stress, but retract when stress is minimized (Sinclair et al., 2009). In addition, elongations
1021 are common during the constriction and fission steps of peroxisome division (Sinclair et
1022 al., 2009; Barton et al., 2013). Cadmium induces ROS production and leads to peroxule
1023 formation that results in division to increase peroxisome numbers (Rodríguez-Serrano et
1024 al., 2016). These ROS-induced increases in peroxule frequency led to the hypothesis that
1025 these extensions facilitate neutralization to prevent or reduce damage (Sinclair et al.,
1026 2009; Barton et al., 2013; Rodríguez-Serrano et al., 2016). Separately, peroxule-
1027 mediated contacts might assist in protein localization. The SUGAR-DEPENDENT1
1028 (SDP1) lipase (Eastmond, 2006) localizes to peroxisomal membranes and then the LD,
1029 a transition concurrent with peroxule development (Thazar-Poulot et al., 2015).

1030

1031 The refined visualization of peroxisome structures using advanced microscopy
1032 techniques and our increasing understanding of organelle interactions have led to an
1033 enhanced view of peroxisomes compared to the previously simple model. Many open
1034 questions about peroxisome biology remain. What is the mechanism for (and importance
1035 of) dynamic membrane changes for peroxisomes in adult tissues and under changing
1036 environmental conditions? How do peroxisome substructures form, and how are
1037 membrane and matrix proteins sorted to create unique environments or to provide specific
1038 functionality? Understanding such details about peroxisome structures, as well as the
1039 factors promoting and mediating peroxisome interactions with other organelles, will
1040 continue to increase our understanding of these dynamic organelles.

1041

1042

1043 **PLANT MITOCHONDRIA**

1044

1045 (Written by Shin-ichi Arimura)

1046

1047 In plants, mitochondria provide a large portion of the ATP in the cytosol through oxidative
1048 phosphorylation. In addition, these organelles are the sites of metabolism of some amino
1049 acids, nucleic acids, lipids, and plant hormones. Plant mitochondria also control redox
1050 balance when photosynthesis is on, off, or fluctuating (Noguchi and Yoshida, 2008;
1051 Finkemeier and Schwarzlander, 2018) and play roles in cellular signaling (Huang et al.,
1052 2016; Welchen et al., 2021) and in resistance to diseases (Fuchs et al., 2020). In
1053 agriculture, cytoplasmic male sterility, which is caused by genes encoded in the
1054 mitochondrial genome, is used for the production of F1 hybrid seeds in diverse crops,
1055 including vegetables. The fine structure and dynamics of plant mitochondria are briefly
1056 reviewed here.

1057

1058 Mitochondria contain two lipid bilayers that form the outer and inner membrane. Some
1059 parts of the inner membrane are invaginated to form sacs, called cristae, which increase
1060 the area of oxidative phosphorylation complexes. Five diverse eukaryotic-conserved
1061 complexes are embedded in the cristae membrane. By contrast, plant-specific proteins

1062 (alternative oxidases and extra NDH and NADH dehydrogenases) for alternative
1063 respiration pathways mainly reside in the non-cristae parts of the inner-membrane
1064 (Schwarzlander and Fuchs, 2017). Plant ATP synthase dimers (complex V) are located
1065 in the cristae membrane, where they contribute to its curvature (Zancani et al., 2020.
1066 Complexes I to V play roles in oxidative phosphorylation. Some of these complexes form
1067 super-complexes for functional efficiency and to regulate oxidative phosphorylation
1068 (Braun, 2020). Protein-protein interactions and metabolite channeling are also observed
1069 in the TCA cycle in the matrix (Zhang, 2017). Additionally, glycolysis enzymes in the
1070 cytosol dynamically associate on the outer surfaces of mitochondria (Giege et al., 2003;
1071 Graham et al., 2007), probably to more efficiently transport metabolites.

1072
1073 The mitochondrial outer membrane contains the most abundant protein in plant
1074 mitochondria, the Voltage-Dependent Anion Channel (VDAC1). A single mitochondrion
1075 contains 40,000 VDACs out of a total of 1.4 million proteins (Fuchs et al., 2020). The outer
1076 membrane does not just encapsulate the inner membrane but also sometimes extends
1077 into the cytosol and other organelles (without extending the inner-membrane);
1078 occasionally, the extensions are pinched off to form small vesicle-like structures
1079 (Yamashita et al., 2016); Figure 8A). In mammals, mitochondria-derived vesicles that do
1080 not contain inner membranes are involved in the transport of specific proteins to
1081 peroxisomes, endosomes, and multivesicular bodies (Sugiura et al., 2014) and in the
1082 biogenesis of peroxisomes (Sugiura et al., 2017).

1083
1084 Each Arabidopsis leaf cell contains 300-450 mitochondria. Many plant mitochondria move
1085 along actin microfilaments at 0.05 - 3 $\mu\text{m}/\text{sec}$ (Doniwa et al., 2007, Oikawa et al., 2021).
1086 This speed is approximately an order of magnitude faster than that of mammalian and
1087 yeast mitochondria, which mainly move along microtubules. Some plant mitochondria
1088 stop and wiggle, as if they were anchored to the cytoskeleton or other organelles, such
1089 as plastids and peroxisomes (Jaipargas et al., 2016; Oikawa et al., 2021). Moving plant
1090 mitochondria can change their speed and can also change their shapes from granular to
1091 linear to attach to other organelles in response to the presence of sucrose or light
1092 (Jaipargas et al., 2016). A single plant cell can contain mitochondria with different shapes

1093 (Jaipargas et al., 2015), different DNA contents (Figure 8B) (Arimura et al., 2004b;
1094 Preuten et al., 2010), and transiently fluctuating membrane potentials (Schwarzlander et
1095 al., 2012). In addition, as shown in Figure 8C, differently groups of mitochondria stained
1096 in different colors in a cell achieve a unified color in two hours, indicating that mitochondria
1097 undergo frequent fusion and fission, resulting in the sharing of internal proteins.
1098 Mitochondria involved in such dynamic sharing of materials in a plant cell are referred to
1099 as a dynamic syncytium (Lonsdale et al., 1988), and the collective mitochondria in a cell
1100 are thought to exist as a discontinuous whole (Logan, 2017). Fusion of mitochondria
1101 results in the formation of elongated and/or branched mitochondria in some meristematic
1102 tissues, such as shoot apices (Segui-Simarro and Staehelin, 2006), germinating seeds
1103 (Paszkiwicz et al., 2017), and dedifferentiating protoplasts (Sheahan et al., 2005; Rose
1104 and McCurdy, 2017).

1105

1106 Mitochondrial fission is achieved by dynamin-related proteins that are well-conserved in
1107 eukaryotes (e.g. DRP3A and 3B in Arabidopsis (Arimura and Tsutsumi, 2002; Arimura et
1108 al., 2004a; Arimura et al., 2004b; Fujimoto et al., 2009), Figure 8D), which polymerize to
1109 form ring-like structures outside mitochondria (Ingerman et al., 2005). Plant-specific
1110 ELM1, an outer surface protein, localizes DRP3s from the cytosol to the mitochondria
1111 (Arimura et al., 2008). An outer-membrane embedded protein that is conserved in
1112 eukaryotes (Fis1) functions as a molecular adapter for DRP in budding yeast (Okamoto
1113 and Shaw, 2005). Fis1 had been thought to carry out similar functions but is now thought
1114 to play only a rather minor and indirect role in mitochondrial fission in both mammals
1115 (Otera et al., 2010; Giacomello et al., 2020) and plants (Nagaoka et al., 2017; Arimura,
1116 2018). Other factors may be involved in plant mitochondrial fission, such as factors
1117 involved in cold-induced fission (Arimura et al., 2017) or factors that are independent of
1118 DRP and specific to Brassicaceae (Aung and Hu, 2011). On the other hand, no orthologs,
1119 factors, or molecular mechanisms are known with certainty to be involved in mitochondrial
1120 fusion in plants. However, FRIENDLY (FMT) is thought to mediate inter-mitochondrial
1121 association before mitochondrial fusion because in Arabidopsis *fmt* mutants,
1122 mitochondria gather together (Logan et al., 2003) but do not fuse (El Zawily et al., 2014).

1123

1124 Mitochondrial-specific autophagy (mitophagy) has been extensively studied in mammals
1125 and yeasts (Onishi et al., 2021), where it is involved in mitochondrial quality control. In
1126 these organisms, degraded mitochondria with low membrane potential could not fuse with
1127 other “healthy” mitochondria, but they were specifically recognized, captured, and
1128 engulfed by autophagosome membranes (Figure 8E). The engulfed mitochondria were
1129 transported to the vacuole to be digested to prevent accidental ROS generation and/or
1130 other negative effects. Therefore, mitophagy, fission, and fusion are thought to function
1131 as a quality control system for all the mitochondria in a cell (Twig et al., 2008).
1132 Mitochondrial-specific degradation in Arabidopsis has also been observed in several
1133 situations, including during leaf senescence (Broda et al., 2018), during the greening of
1134 cotyledons (Ma et al., 2021), after UV-irradiation (Nakamura et al., 2021), and after
1135 treating the inner membrane with ionophores (Ma et al., 2021). Orthologs of factors
1136 specific to mitophagy in mammals and yeasts have not yet been found in plant genomes,
1137 although FMT was recently reported to be involved in mitophagy in Arabidopsis (Ma et
1138 al., 2021).

1139
1140 Super resolution microscopy is a promising new technique that can clarify the internal
1141 structures of mitochondria, with their diverse physiology and functions, in more detail. In
1142 addition, recent trials to understand the types and numbers of molecules in an average
1143 single mitochondrion (Fuchs et al., 2020) or in a hypothetical single mitochondrion (Moller,
1144 2016) will hopefully give rise to the next stage of analysis of the exact number of individual
1145 mitochondria. Such information would help uncover the actual quantitative dynamics of
1146 molecules among diverse mitochondria underlying the functions of each cell. Until
1147 recently, the transformation of mitochondrial genomes in multicellular plants had been
1148 impossible, but new genome editing methods (Kazama et al., 2019; Arimura et al., 2020)
1149 have opened the door to analyzing the functions of mitochondrial genes, as well as
1150 regulating their expression in order to breed crops with agriculturally important
1151 characteristics.

1152

1153 **CHLOROPLAST: A PLANT’S POWERHOUSE WITH TUNABLE PERFORMANCE**

1154

1155 (Written by Helmut Kirchhoff)

1156

1157 A unique endosymbiotic event more than 900 million years ago was the starting point for
1158 the evolution of the chloroplast from a free-living cyanobacterial precursor (Sibbald and
1159 Archibald, 2020). Every second, the thylakoid membrane system of a modern chloroplast
1160 in *Viridiplantae* can convert energy from the sun into up to 80 million ATP and NADPH +
1161 H⁺ molecules. This fuels a number of anabolic reactions localized in the chloroplast
1162 stroma, including the synthesis of sugars, lipids/fatty acids, amino acids, nucleotides,
1163 pigments, alkaloids, hormones, and vitamins (Kirchhoff, 2019). Furthermore, a battery of
1164 membrane-embedded chloroplast envelope transporters makes the capacity for
1165 photosynthetic energy transformation available to the entire cell and beyond (Weber and
1166 Linka, 2011). In C3 plants, a typical leaf cell contains 20-100 chloroplasts in the palisade
1167 parenchyma and 10-50 in the spongy parenchyma (Antal et al. 2013).

1168

1169 **Chloroplast lifecycle**

1170 During the last decade, electron tomography has provided detailed structural insights into
1171 the morphological transitions from an undifferentiated, non-photosynthetic proplastid to a
1172 mature chloroplast in the shoot apical meristem for illuminated shoots (Adam et al., 2011;
1173 Charuvi et al., 2012) or via the etioplasts, with its characteristic para-crystalline
1174 prolamellar body (Kowalewska et al., 2016). The correlation between the sequential
1175 appearance of proteins such as photosystem I and II, light-harvesting complex II, CURT1
1176 proteins, ATPase, protochlorophyllide oxidoreductase, and plastidial ribosomes on the
1177 one hand and structural development of the plastid on the other hand provides a first
1178 glimpse of the roles of particular proteins in proplastid-chloroplast differentiation
1179 (Kowalewska et al., 2016; Liang et al., 2018a; Floris and Kuehlbrandt, 2021). Proplastid
1180 development requires the massive import of proteins from the cytoplasm into the
1181 chloroplast, mainly by the TOC/TIC translocase system (Aronsson and Jarvis, 2008; Ling
1182 et al., 2012), since ~95% of chloroplast proteins are encoded in the nucleus.

1183

1184 Currently, there are two major non-exclusive models describing how hydrophobic
1185 nucleus-encoded proteins (along with lipids and pigments) that are synthesized at the

1186 plastid envelope membranes are transported through the aqueous stroma to reach their
1187 thylakoid membrane destination: (1) invaginations of the inner envelope membrane/direct
1188 contact sites with thylakoids and (2) vesicle transport (Lindquist and Aronsson, 2018;
1189 Mechela et al., 2019). Evidence exists that the invagination/direct contact site pathway is
1190 realized only in the proplastid-to-chloroplast transition, whereas vesicle transport seems
1191 to be dominant in mature chloroplasts (Vothknecht and Westhoff, 2001; Andersson and
1192 D'ormann, 2008; Lindquist and Aronsson, 2018). For the latter, the roles of typical vesicle-
1193 forming proteins such as COPI, COPII, SNARE, and VIPP1 in plastid biogenesis remain
1194 to be determined (Mechela et al., 2019). However, for cyanobacterial VIPP1, a structure-
1195 based molecular understanding was recently achieved (Gupta et al., 2021).

1196
1197 In contrast to proplastids, mature chloroplasts propagate by binary fission (Osteryoung
1198 and Pyke, 2014; Yoshida, 2018). The plastid division machinery is made up of four
1199 physically connected supramolecular ring structures: two outside (an outer polyglucan
1200 plastid-dividing ring and a dynamin-related ring) and two inside the chloroplast (an inner
1201 plastid-dividing ring and a tubulin-like FtsZ-ring beneath the inner envelope membrane).
1202 In a concerted mechanism, the rings generate the mechanical force required for plastid
1203 constriction and eventually division. An example of the crucial role of regulatory proteins
1204 in plastid morphogenesis, such as the FZL-fusion protein, is visualized in Figure 9. Open
1205 questions in the field are the composition of the inner plastid-dividing ring, how thylakoid
1206 membranes divide, and how chloroplast division is coordinated with the division of cells
1207 and other organelles (Osteryoung and Pyke, 2014; Yoshida, 2018).

1208
1209 At the end of their lifespan, chloroplasts enter highly coordinated dismantling processes
1210 with the goals of minimizing ROS production and recycling their abundant
1211 macromolecules to sink tissues of the plant (Avila-Ospina et al., 2014). Strikingly,
1212 chloroplasts hold ~80% of leaf nitrogen (Makino and Osmond, 1991), making their
1213 recycling very valuable for plant resource management. It seems that ROS-dependent
1214 retrograde signaling plays a key role in coordinating chloroplast degradation via multiple
1215 breakdown pathways including chlorophagy (Woodson, 2019; Dominguez and Cejudo,
1216 2021). Current research focuses on elucidating how particular environmental conditions

1217 trigger specific dismantling pathways and deciphering the corresponding signal
1218 cascades.

1219

1220 **Interactions of chloroplasts with other organelles**

1221 Chloroplast metabolism is highly integrated into plant cell metabolism. Two prominent
1222 examples of the tight functional cooperation between chloroplasts and other organelles
1223 are photorespiration and lipid trafficking. The oxygenation of ribulose-1,5-bisphosphate by
1224 Rubisco in the chloroplast stroma can lead to a loss of up to 30% of fixed carbon (Walker
1225 et al. 2016) and the production of cell-toxic 2-phosphoglycolate (2-PG). 2-PG is detoxified
1226 by the photorespiratory pathway, which converts two 2-PG molecules into one molecule
1227 of glycerate (recycled to the Calvin-Benson cycle) and CO₂. Photorespiratory
1228 metabolization of 2-PG requires the metabolic competence of three organelles: the
1229 chloroplast, peroxisomes, and mitochondria. The efficient exchange of photorespiratory
1230 metabolites between these three organelles is tuned and controlled by organellar
1231 membrane transport proteins (Kuhnert et al. 2021) and the spatial interaction of the three
1232 organelles. For example, the area of physical contact between peroxisomes and
1233 chloroplasts increases significantly under photorespiratory conditions fostered by
1234 changes in peroxisome shape from spherical to elliptical (Oikawa et al. 2015).

1235

1236 Another intriguing example of tight organelle cooperation is lipid trafficking (Hurlock et al.
1237 2014). Chloroplast lipids are synthesized both entirely in the chloroplast (prokaryotic
1238 pathway) and by the cooperation between chloroplasts and the ER (eukaryotic pathway)
1239 (Hölz and Dörmann 2019). Some plants such as pea (*Pisum sativum*; also known as 18:3
1240 fatty acid plants) have lost their ability to synthesize lipids via the prokaryotic pathway,
1241 depending entirely on the eukaryotic one (Roughan and Slack 1984, Mongrand et al.
1242 1998). Due to their crucial roles in membrane function, integrity, and maintenance, as well
1243 as storage (triacylglycerol) and determining the composition of extracellular hydrophobic
1244 components (i.e. waxes), acclimative changes in chloroplastic fatty acid and lipid
1245 composition is key for plant survival under unfavorable conditions or during plant
1246 development (Hölz and Dörmann 2019). This plasticity of lipid composition relies heavily

1247 on the dynamic interaction between chloroplasts, the ER, lipid bodies, Golgi, and
1248 mitochondria (Hurlock et al. 2014).

1249

1250 **Structural membrane dynamics as a means to control energy conversion**

1251 The fact that photosynthetic energy conversion has to integrate and balance significant
1252 fluctuations in both cell metabolism (including CO₂ availability) and energy input by
1253 sunlight in an oxidizing environment calls for its strict regulation to minimize toxic ROS
1254 production. In the last decade, a central regulatory element for tuning photosynthetic
1255 performance in plants has been uncovered: the dynamic adjustment of lateral and
1256 transversal geometric (grana) thylakoid dimensions that regulate electron transport, light-
1257 harvesting, and protein repair (Kirchhoff et al. 2011, Herbstova et al. 2012, Hepworth et
1258 al. 2021). For example, changes in the vertical width of the thylakoid lumen as well as the
1259 lateral diameter of the grana disc were reported to control the mobility of the small electron
1260 carriers plastoquinone and the lumen-hosted plastocyanin and therefore linear electron
1261 transport from water to ferredoxin (Kirchhoff et al. 2011, Hepworth et al. 2021).
1262 Furthermore, lateral shrinkage of the grana diameter is beneficial for the repair of
1263 photodamaged, grana-hosted PSII complexes, since the shrinkage makes it easier for
1264 PSII to reach the protein repair machinery localized in distant (separated by a few hundred
1265 nanometers) unstacked thylakoid domains (Herbstova et al. 2012). It is an open question
1266 how reversible protein phosphorylation, physicochemical membrane properties, and
1267 protein composition dynamics work together to control architectural thylakoid features and
1268 subsequently energy conversion.

1269

1270 **Future perspectives**

1271 Over the next five to ten years, the rapid methodical and technological development of
1272 (cryo)electron tomography (Bussi et al. 2019, Wietrzynski et al. 2020) is expected to
1273 provide detailed new insights into chloroplast structure-function relationships not only for
1274 the mature plastid but also for its biogenesis and dismantling. Furthermore, studying
1275 chloroplast diversity in non-model, less commonly studied species as well as in
1276 specialized plant tissues and organs (including transitions between different plastid types)
1277 will gain increasing attention because it will uncover the metabolic plasticity and diversity

1278 of this organelle. Along these lines, current and future bioengineering and synthetic
1279 biology tools for chloroplasts offer the potential for improving crop plants by tuning
1280 processes such as non-photochemical quenching (Kromdijk et al. 2016) or
1281 photorespiratory pathways (South et al. 2016, Roell et al. 2021) or for using the anabolic
1282 competence of the plastid to employ these organelles as metabolic factories for valuable
1283 chemicals (Bock 2021).

1284

1285

1286 **PLANT MEMBRANE CONTACT SITES: QUESTIONS FROM THE MEMBRANE** 1287 **INTERFACE**

1288

1289 (Written by Emmanuelle Bayer, Federica Brandizzi, Yvon Jaillais, Miguel A. Botella,
1290 Pengwei Wang, and Abel Rosado)

1291

1292 **Membrane contact sites: Does one definition fit all?**

1293 Membrane Contact Sites (MCS) are evolutionarily conserved structures where the
1294 physical proximity between two or more membrane-bound organelles enables the direct
1295 exchange of molecules and facilitates coordinated inter-organelle adaptive responses
1296 (examples of MCS membrane proximity using TEM are shown in Figure 10A-B). Recent
1297 advances in plant cell imaging and the development of novel genetic and molecular tools
1298 have fueled an emerging field of research devoted to the investigation of their structural
1299 organization, dynamics, and physiological functions. This interest is uncovering plant-
1300 specific MCS structures and molecular mechanisms, but it is also exposing some
1301 limitations of the commonly accepted definitions and physiological functions inferred from
1302 different model organisms. As in yeast and animal cells, the plant ER is an interconnected
1303 organelle that establishes MCS with multiple cellular structures including the PM,
1304 mitochondria, endosomes, peroxisomes, Golgi ,and TGN (Barton et al., 2013; Stefano et
1305 al., 2014; Wang et al., 2014; Perez-Sancho et al., 2015; Wang et al., 2019b; Brandizzi,
1306 2021). Unique to plants, however, are the functional interactions at ER-plastid MCS for
1307 lipid synthesis and transport (Liu and Li, 2019), the control of intercellular communication
1308 through PD MCS-regulated intercellular bridges (Tilsner et al., 2016), and the MCS

1309 activities driven by a super-continuum that encompasses the cell wall, PM, ER, and
1310 cytoskeleton (Wang et al., 2014; Perez-Sancho et al., 2015; Zang et al., 2021). These
1311 plant-specific features are placing MCS research in plants at the forefront of discovery,
1312 broadening the definition of MCS beyond yeast and animal systems.

1313

1314 In plants, MCS can be defined as environmentally and developmentally regulated
1315 microdomains with an intermembrane gap as small as 3 nm in PD and an arbitrarily
1316 defined upper limit of 80-100 nm. Plant MCS are enriched with a variety of protein-protein,
1317 and/or protein-cytoskeleton tethering assemblies, such as those including the SYT1 and
1318 VAP27 tethers (Zang et al., 2021; Rosado and Bayer, 2021, Figure 10C-E). These
1319 complexes establish dynamic interactions with membrane phospholipids and/or the cell
1320 wall and carry out essential cellular functions, including (but not restricted to) the
1321 maintenance of membrane lipid homeostasis, cell-to-cell communication, organelle
1322 biogenesis, autophagy, endocytosis, receptor kinase signaling, and the regulation of
1323 Ca²⁺-dependent stress responses (reviewed in Perez-Sancho et al., 2016; Wang and
1324 Hussey, 2017; Liu and Li, 2019; Petit et al., 2020; Rosado and Bayer, 2021).

1325

1326 **Lipid transfer at MCS: Is that what plant tethers do?**

1327 Due to their hydrophobicity, the transport of lipids between organelles relies on either
1328 vesicle-mediated delivery mechanisms or MCS-localized lipid transport proteins (LTPs)
1329 (Scorrano et al., 2019). Most MCS-localized LTPs contain an internal hydrophobic cavity
1330 adapted to solubilize water-insoluble molecules (Wong and Levine, 2016), are anchored
1331 to the ER by either transmembrane domains or stable interactions with ER-anchored
1332 proteins (Scorrano et al., 2019), and interact with the opposing membrane, mainly through
1333 domains that bind anionic lipids (Perez-Lara and Jahn, 2015). In animal cells or yeast,
1334 direct lipid transport using MCS-localized LTPs may be one of the best characterized and
1335 documented MCS functions. The lipid species transferred using this mechanism include
1336 sterols, ceramides, phosphatidylserine (PS), phosphatidylinositol 4-phosphate (PI4P),
1337 and diacylglycerol (DAG) (Wu et al., 2018). Similarly, in plants, the emerging view is that
1338 MCS-localized LTPs participate in the delivery of lipids between the ER and organelles
1339 not linked by vesicular trafficking (e.g. mitochondria and plastids) but also in the bulk

1340 transport of lipids between organelles connected by the secretory pathway. In a recent
1341 landmark study, Ruiz-Lopez et al. showed that stress signals regulate the activity of two
1342 members of the Synaptotagmin (SYT) family of LTPs at ER-PM MCS (SYT1 and SYT3)
1343 and demonstrated their function as LTPs that transfer DAG between the PM and the ER
1344 *in vivo* (Ruiz-Lopez et al., 2021). The authors propose a geometrical model where SYT
1345 activities counteract the stress-induced build-up of conically shaped DAG at the PM and
1346 prevent the generation of areas of negative membrane curvature that could disrupt the
1347 stability of the PM during stress episodes.

1348

1349 **MCS in motion: What controls MCS plasticity and dynamics?**

1350 The molecular composition, geometry, and plasticity of inter-organelle junctions
1351 determine their ability to integrate and respond to cellular signals. Recent studies have
1352 provided an emerging picture in which MCS tethers do not act in isolation but instead
1353 interact with anionic lipids and cytoskeletal elements and regulate the plasticity, function,
1354 and dynamics of these cellular microdomains.

1355

1356 Anionic phospholipids represent only a few percent of total lipids, but they are critical
1357 biochemical and biophysical landmarks of membrane identity (Noack and Jaillais, 2020).
1358 Within the endomembrane system, anionic phospholipids, including the
1359 phosphoinositides (PIPs), phosphatidic acid (PA), and phosphatidylserine (PS),
1360 determine the electrostatic potential of each membrane, which is highest at the PM,
1361 intermediate in endosomes, and low in the ER (Platre et al., 2018; Dubois and Jaillais,
1362 2021). *In vitro* or *in silico* data for MCS tethers such as the synaptotagmins (SYTs),
1363 Multiple C2 domains and transmembrane region (MCTPs), and Vesicle-associated
1364 membrane protein (VAMP)-associated proteins (VAPs) families support the notion that
1365 anionic lipids profoundly affect the structure and function of MCSs by enabling protein-
1366 lipid interactions that regulate the association of the ER with the PM, TGN, and early
1367 endosomes (Perez-Sancho et al., 2015; Stefano et al., 2018; Brault et al., 2019; Ruiz-
1368 Lopez et al., 2021). Interestingly, these interactions appear to be mostly non-specific, the
1369 primary determinants being the negative charge carried by the anionic lipids and, in some
1370 cases, the presence of Ca²⁺ (Schapire et al., 2008). Accordingly, electrostatic interactions

1371 between phosphatidylinositol-4-phosphate (PI4P) and SYT1/SYT3 underpin the
1372 localization of SYT1/SYT3 to ER-PM MCS (Ruiz-Lopez et al., 2021), MCTP4 to PD-MCS,
1373 (Brault et al., 2019), and the remodeling of SYT1 ER-PM MCS in response to rare-earth
1374 elements (Lee et al., 2020). Similarly, the accumulation of phosphatidylinositol 4,5-
1375 biphosphate [PI(4,5)P₂] at the PM enables interactions with SYT1 and correlates with the
1376 rearrangement and expansion of ER-PM MCS in response to ionic stress (Lee et al.,
1377 2019).

1378
1379 MCS plasticity is also controlled by components that crosslink the actin cytoskeleton at
1380 MCS and create trapping mechanisms that influence MCS architecture and expansion.
1381 In plants, this cross-linking seems to be carried out by a plant-specific complex that
1382 includes the actin-associated NET3C protein and the microtubule-associated Kinesin light
1383 chain related (KLCRs) and IQ67-Domain (IQD) proteins (Zang et al., 2021) (Figure 10E).
1384 Remarkably, in plants, the presence of cell walls underlies the formation of a plant-specific
1385 supramolecular assembly known as the MCS super-continuum. This super-continuum
1386 encompasses the cell wall, PM, ER, and cytoskeleton and renders MCS with distinct
1387 kinetics, shapes, geometries, and functions (Rosado and Bayer, 2021; Zang et al., 2021).
1388 Recent studies proposed that the MCS super-continuum serves as a nexus that limits the
1389 mobility of MCS tethering assemblies (Wang et al., 2016; Lee et al., 2019; Zang et al.,
1390 2021) and controls their activities. Examples of regulation mediated by this continuum
1391 include the activity of receptor-like kinases in pollen and/or stomatal cells (Ho et al., 2016;
1392 Duckney et al., 2021) and the regulation of phospholipase C-mediated stress signals at
1393 the PM (Ruiz-Lopez et al., 2021). Finally, a unique type of regulation occurs at PD MCS
1394 where the transfer of molecules occurs parallel to the membranes, as opposed to
1395 orthogonal to them. In these ER-PM MCS, the intermembrane space may not be solely
1396 regulated by the tethers, lipids, and cytoskeleton elements in the super-continuum, but
1397 also by wall polymers (e.g. callose), which are locally synthesized around the PD structure
1398 (Petit et al., 2020).

1399

1400 **Future MCS research: What's in the plant toolkit?**

1401 MCS are microdomains with an intermembrane distance below the resolution limit of
1402 conventional fluorescence microscopy and with a dynamic behavior that requires the use
1403 of live-cell compatible techniques (McFarlane et al., 2017). In recent years, advances in
1404 super-resolution microscopy (e.g. Total Internal Reflection Fluorescence, Structure
1405 illumination microscopy, (Figure 10F), and electron tomography (Figure 10G) are
1406 providing for the first time detailed high-resolution visualizations and 3D reconstructions
1407 of the MCS ultrastructure in plants (Baillie et al., 2020). In parallel, the use of optical laser
1408 tweezers to manipulate plant MCS *in vivo* is facilitating the characterization of putative
1409 MCS components such as the AtCASP tether identified at ER-Golgi MCSs (Osterrieder
1410 et al., 2017) and the mitochondria-associated GTPase AtMiro2 at ER-mitochondria
1411 contact sites (White et al., 2020). Plant MCS research is also adopting genetically
1412 encoded tools such as synthetic tethers that bridge nearby membranes (e.g. MAPPER-
1413 GFP, (Lee et al., 2019), or split-fluorescence systems (e.g. split super-folder (sp) GFP
1414 proteins, (Li et al., 2020) to visualize MCS contacts. These artificial systems, however,
1415 have limited use in functional studies, as their expression could induce non-physiological
1416 changes in the MCS structure. Additional molecular tools with broad applications, such
1417 as inducible phosphoinositide depletion systems (Doumane et al., 2021) and
1418 phosphoinositide fluorescent markers (Simon et al., 2014) are currently being adopted for
1419 MCS research and represent promising avenues to elucidate the roles of anionic
1420 phospholipids in plant MCS function and dynamics.

1421
1422 We predict that the combination of collaborative research, technical advances, and novel
1423 molecular tools in this quickly evolving field will provide breakthroughs that will transcend
1424 plant MCS research.

1425

1426

1427

1428 **DIVERSITY IN PD FORM AND FUNCTION**

1429

1430 (Written by Tessa M. Burch-Smith)

1431

1432 **General PD structure**

1433 PD evolved multiple times in the plant lineage and are present in some groups of algae
1434 and in all land plants (Brunkard et al., 2015; Azim and Burch-Smith, 2020), 2020). In
1435 general, PD provide continuity of the PMs and cytoplasm across cell walls. In land plants
1436 and some algae, PD also include a central strand of the ER (Botha, 1992),(Ding et al.,
1437 1992; Franceschi et al., 1994; Cook et al., 1997). The cytoplasmic and membrane
1438 connectivity provided by the PD is the route for intercellular trafficking of numerous
1439 biomolecules, effectively rendering the plant a continuous cytoplasm (a symplast). PD are
1440 therefore essential for plant growth, development and environmental responses. Some
1441 molecules traffic through PD by passive diffusion, and their movement depends on the
1442 size of the molecules and the trafficking capacity of the pores. Other molecules are
1443 targeted to PD through the use of the endomembrane system (Spiegelman et al., 2019).
1444 A typical cell wall is pervaded by hundreds or thousands of PD that are often clustered
1445 into groups (pitfields), and as such the continuity between adjacent cells can be extensive.

1446
1447 PD are nanopores with outer diameters (delimited by the PMs of connected cells) ranging
1448 from 25 to 50 nm, depending on the tissue and species, and they extend for the length of
1449 cell wall thickness. Thus, much of what is known about PD structure is derived from TEM
1450 (Figure 11). The center of land plant PD is occupied by a structure called the desmotubule
1451 (DT). The DT was observed to be continuous with the cortical ER of connected cells and
1452 is now recognized as an intercellular strand of modified ER. The DT diameter is
1453 constrained to approximately 15-20 nm (Ding et al., 1992; Schulz, 1995), and so the
1454 desmotubule comprises the most tightly curved biological membranes described to date
1455 (Tilsner et al., 2011). The DT does not include a typical ER lumen. Instead, the space is
1456 largely occupied by proteins (Tilney et al., 1991), whose likely function is to enable the
1457 tight curvature of the membranes, e.g. the ER tubulating reticulon proteins (Tilsner et al.,
1458 2011; Knox et al., 2015; Kriechbaumer et al., 2015). The DT is tightly connected to the
1459 PM of the PD by structures originally described as spokes (Ding et al., 1992). The cytosol-
1460 filled space between the DT and PM is called the cytoplasmic sleeve or annulus and is
1461 likely the main route for PD trafficking, although the spoke proteins divide it into
1462 nanochannels 2-3 nm wide.

1463
1464 Analysis of PD isolated from Arabidopsis suspension cell culture identified 1,341 proteins
1465 as the putative PD proteome (Fernandez-Calvino et al., 2011). Of these, 21% were
1466 membrane proteins and included proteins previously identified as PD resident, e.g.
1467 PDLP1 (Thomas et al., 2008) and ATBG_papp (Levy et al., 2007). In addition, several
1468 GPI (glycosylphosphatidylinositol)-anchored proteins and proteins associated with the
1469 secretory pathway were identified. Further refinement of the PD proteome identified
1470 Multiple C2 domains and transmembrane region proteins (MCTPs) as PD constituents,
1471 and they have been designated as the likely spokes of PD (Brault et al., 2019). The
1472 spokes control spacing between the DT and PM, and this distance is correlated with the
1473 developmental states of PD (Nicolas et al., 2017a). Interestingly, in Arabidopsis roots, PD
1474 lacking cytoplasmic sleeves apparently had a higher trafficking capacity than PD with
1475 cytoplasmic sleeves (Nicolas et al., 2017a), raising questions about how trafficking via
1476 those PD is achieved. There are a few reports of trafficking through the DT lumen,
1477 although the DT membranes appear to provide a surface for cell-to-cell movement
1478 (Guenoune-Gelbart et al., 2008; Barton et al., 2011). The DT membranes are important
1479 conduits for the transport of at least some viruses between cells (Guenoune-Gelbart et
1480 al., 2008). The routes for PD trafficking and the contributions of the membranes and
1481 spaces to the movement of cargo molecules remain open questions in PD biology.

1482
1483 The lipid composition of the PM of PD is also distinct from the bulk PM. The PM of PD
1484 from Arabidopsis suspension cells is enriched in sterols and sphingolipids with saturated
1485 very long chain fatty acids (Grison et al., 2015), which is consistent with the presence of
1486 lipid microdomains akin to lipid rafts in PD (Raffaele et al., 2009; Tilsner et al., 2013) and
1487 GPI-anchored proteins in the PD proteome (Fernandez-Calvino et al., 2011). PD lipid
1488 composition is also important for PD protein composition and function, as changes in
1489 lipids affect the ultrastructure and permeability of PD (Grison et al., 2015; Yan et al., 2019;
1490 Iswanto et al., 2020; Liu et al., 2020). As described in the section on plant MCS, a modern
1491 view of PD considers both its unique lipid and protein composition to describe PD as
1492 specialized MCS (Brault et al., 2019; Petit et al., 2019; Ishikawa et al., 2020). A simple
1493 generalized PD structure is represented in Figure 11A.

1494

1495 **PD formation and distribution**

1496 PD are intrinsic components of the cell walls found in almost all connected cell walls in a
1497 plant. Primary PD form at the end of cell division, during cytokinesis, when strands of ER
1498 become encased in the developing cell plate. The reticulon proteins RTNLB3 and 6 and
1499 MCTPs are involved in this process (Knox et al., 2015; Brault et al., 2019). The presence
1500 of substructures like the DT in newly formed PD is uncertain, as revealed by TEM (Ehlers
1501 and van Bel, 2010). Secondary PD form across existing cell walls where cell division is
1502 not occurring. The insertion of these new PD is likely necessary to establish or maintain
1503 symplastic connectivity, as in graft unions or when cells divide and grow (Ehlers and
1504 Kollmann, 2001). Studies in *Arabidopsis* trichomes suggest that new secondary PD form
1505 in close proximity to existing PD, as described in the multiple twinning model (Faulkner et
1506 al., 2008). It is proposed that PD divide by fission, although the mechanism for this is
1507 unclear.

1508

1509 PD may also be removed from existing cell walls by a still unknown process. Studies on
1510 cambial division and vascular differentiation have shown that PD numbers can increase
1511 and decrease over the lifespan of a given cell-cell interface; this would necessarily involve
1512 the removal and insertion of PD at a given interface (Ehlers and van Bel, 2010; Fuchs et
1513 al., 2010). In other instances, PD can be drastically modified or even truncated to disrupt
1514 intercellular trafficking. For example, guard cell initials contain PD, and PD trafficking is
1515 critical for guard cell development (Guseman et al., 2010). As stomata develop, however,
1516 PD are lost from the guard-cells, rendering them symplastically isolated (Wille and Lucas,
1517 1984). It may be that PD removal is a more common occurrence in plant cell development
1518 and differentiation than previously reported. How secondary PD form and how PD are
1519 removed are other open questions that await exploration: advanced imaging approaches
1520 hold promise for generating answers to these questions.

1521

1522 **Structure-function relationships in PD**

1523 PD are often depicted as simple linear structures traversing the cell wall (Figure 11A), but
1524 PD structure is much more diversified. PD are often branched, consisting of multiple pores

1525 that connect in the vicinity of the cell wall middle lamella (Figure 11B-D). This is captured
1526 by studies on PD structure using three-dimensional approaches such as electron
1527 tomography.

1528

1529 The formation and origins of branched PD are unclear, but they likely arise through
1530 modification of existing simple PD (Burch-Smith et al., 2011). This diversity in structure
1531 suggests diversity in function. Exemplary studies of PD in tobacco leaves undergoing the
1532 sink-source transition demonstrated that simple PD were converted to branched PD
1533 contemporaneously with decreased import of fluorescent dye (Oparka et al., 1999;
1534 Roberts et al., 2001). Another common variation of PD form is the dilation of PD pores
1535 away from the PD openings or the constriction of PD at their necks (region just below the
1536 opening, Figure 11B). This PD variation seems to correlate with PD maturation (Nicolas
1537 et al., 2017b) or with trafficking capacity (Ding et al., 1992). Mathematical modeling
1538 supports the notion that dilation increases trafficking capacity as the cell wall thickens
1539 (Deinum et al., 2019), a correlation previously observed by TEM (Nicolas et al., 2017b).
1540 Another PD form that has a specialized role in trafficking is the ‘funnel PD’ in sink root
1541 tissue (Ross-Elliott et al., 2017). These PD have wide openings at the phloem sieve
1542 elements that narrow considerably as they cross the cell wall and open on the phloem-
1543 pole pericycle, creating a ‘funnel’ shape (Figure 11B). The specialized PD shape appears
1544 to facilitate the unloading of sucrose in the root phloem. Mathematical modelling supports
1545 the need for this unusual PD form to allow phloem unloading at physiological sucrose
1546 concentrations.

1547

1548 Specialized PD forms have also been reported at sites where sugars are loaded into the
1549 phloem in source tissues. For example, PD at the phloem parenchyma-companion cell
1550 interface in *Arabidopsis* leaf veins have many openings to the phloem parenchyma but
1551 only one to the companion cells (Haritatos et al., 2000). These distinct PD forms correlate
1552 with specialized functions, and they raise the possibility of PD sub-functionalization
1553 between tissues and even at a given cell-interface. PD sub-functionalization is an
1554 intriguing concept that has proven difficult to investigate due to the lack of experimental
1555 approaches that allow perturbation of specific PD. The development of appropriate

1556 genetic, imaging, and computational methods will be necessary to address this critical
1557 aspect of PD function. Undoubtedly, a comprehensive understanding of PD will enable
1558 novel approaches to engineering solutions to help overcome challenges in plant growth
1559 and development.

1560

1561

1562 **SO MUCH MORE THAN BRICKS AND MORTAR: PLANT CELL WALLS AS DYNAMIC**
1563 **EXTRACELLULAR “ORGANELLES”**

1564

1565 (Written by Charles T. Anderson)

1566

1567 Much as our skin protects us from the environment but is also itself an organ, the plant
1568 cell wall can be thought of as a protective “organelle” for the plant cell; however, it is not
1569 bound by a membrane but instead encases the PM-delimited protoplast that contains the
1570 intracellular organelles. Our understanding of cell wall composition, structure, and
1571 mechanics has expanded rapidly over the past decade due to advances in high-resolution
1572 imaging (Zeng et al., 2017; Rydahl et al., 2018; Voiniciuc et al., 2018; Zhao et al., 2019),
1573 biochemical and spectroscopic analyses of wall polymers and their interactions down to
1574 single-molecule and nanoscale levels (Voxeur et al., 2019; Zhao et al., 2020; Cai et al.,
1575 2021), and new computational modeling methods that relate wall mechanics to the
1576 deformations, movements, and interactions of individual wall polymers (Zhang et al.,
1577 2021). In contrast to its previous conception as simply “dead wood” that is the inert
1578 product of polymer secretion by plant cells, the plant cell wall is starting to be appreciated
1579 as a dynamic structure that changes over time and encompasses specialized metabolic
1580 processes, including the polymerization, coalescence, binding/unbinding, cleavage, and
1581 re-ligation of wall polymers that facilitates both plant growth and the processing of plant
1582 biomass for human use (Obro et al., 2011). Cell walls serve as conduits of intercellular
1583 transport of nutrients, secreted peptides, hormones, and other metabolites (Ramakrishna
1584 and Barberon, 2019), arenas where extracellular vesicles can deliver small RNAs to
1585 silence virulence genes in plant pathogens (Cai et al., 2018), and surveillance zones
1586 where plants can sense pathogen-generated wall fragments (Vaahtera et al., 2019) to

1587 help maintain wall integrity (Rui and Dinneny, 2020). Together, these ideas highlight how
1588 the apoplast, the extracellular compartment in which the cell wall resides, enables
1589 previously unappreciated forms of trafficking and acts as a molecular frontier in the
1590 interactions between plants and their abiotic and biotic environments.

1591

1592 **Cell wall assembly and structure**

1593 Extending the analogy with human skin, the plant cell wall can expand along with the cell
1594 it encases, and it also helps sense and transduce important environmental and
1595 mechanical information. However, the analogy is not perfect: as a biomaterial with
1596 elements approaching the tensile strength of steel, the cell wall also acts as a flexible but
1597 strong coating that shapes its occupying cell, determining its final shape. Cellulose, the
1598 most abundant biopolymer on Earth, forms the “girders” of the cell wall as its primary load-
1599 bearing component. Cellulose is extruded directly into the apoplast by multi-subunit
1600 Cellulose Synthase Complexes (Wilson et al., 2021), which move through the PM along
1601 trajectories that are likely driven by the force of polymerization and are guided by either
1602 cortical microtubules (Figure 12) or existing wall patterning (Chan and Coen, 2020). The
1603 estimated 18 catalytic subunits in each Cellulose Synthase Complex (Nixon et al., 2016)
1604 produce strands of β -1,4-linked glucose that coalesce into cable-like microfibrils that are
1605 predicted to have 18-24 chains (Yang and Kubicki, 2020). Forming the “cross-beams”
1606 and “insulation” between the cellulose “girders” are matrix polysaccharides that include
1607 pectins and hemicelluloses. Pectins are acidic polysaccharides that are composed of
1608 homogalacturonan, rhamnogalacturonan-I, and rhamnogalacturonan-II domains
1609 (Anderson, 2019), whereas hemicelluloses contain mostly neutral sugars and include
1610 xyloglucans, xylans, and mannans (Scheller and Ulvskov, 2010). In growing cells, matrix
1611 polysaccharides initially interact with cellulose upon their secretion at the cell surface,
1612 following polymerization in the Golgi lumen and post-Golgi trafficking (Hoffmann et al.,
1613 2021) (Figure 12). Both pectins and hemicelluloses can associate with the surfaces of
1614 cellulose microfibrils, potentially preventing cellulose agglomeration and thus assembling
1615 a strong but deformable wall that also contains glycoproteins, enzymes, metabolites, ions,
1616 and water (Cosgrove, 2018). In the secondary walls produced by certain cell types, a
1617 polyphenolic, hydrophobic compound called lignin is also deposited (Dixon and Barros,

1618 2019). In many cell types, the wall is deposited in layers with differing cellulose
1619 orientations, conferring multidirectional resistance to mechanical failure.

1620

1621 **Dynamics and functions of plant cell walls**

1622 What happens to the strong but flexible wall as a plant cell grows? Atomic force
1623 microscopy (Zhang et al., 2017) and coarse-grained modeling (Zhang et al., 2021)
1624 indicate that cellulose microfibrils bend, bundle, unbundle, and slide during experimentally
1625 imposed or computationally simulated wall deformation, respectively. One open question
1626 is exactly how cellulose behaves in the growing cells of living plants, where wall deposition
1627 is often ongoing, matrix polysaccharides can also undergo reorganization (Anderson et
1628 al., 2012), and wall-modifying enzymes act to modulate cell growth (Xiao et al., 2014).
1629 Also unclear is the extent to which extracellular ATP and other energetic compounds
1630 might be used in wall metabolism, in addition to their functions as signaling molecules
1631 (Pietrowska-Borek et al., 2020). PD allow for rapid communication and transport between
1632 adjacent plant cells; however, some cell types, such as stomatal guard cells, lack these
1633 connections but must nonetheless transmit and receive information with other cells,
1634 underscoring the importance of apoplastic trafficking as a mode of intercellular
1635 communication in plants. Membrane receptors on the cell surface link events in the cell
1636 wall to intracellular signaling pathways (Vaahtera et al., 2019), allowing the plant cell to
1637 adapt to changing environmental conditions and withstand pathogen attack, although the
1638 extent to which these receptors sense biochemical, chemical, and/or mechanical cues
1639 has not been fully worked out. Cell walls are highly diverse across plant tissues and taxa
1640 (Hoffmann et al., 2021) and allow cells to adopt myriad shapes and perform specialized
1641 functions that include nutrient and water absorption (e.g., root epidermal cells), transport
1642 (e.g., xylem and phloem), and secretion (e.g., aerial epidermal and nectary cells).
1643 Autodegradation of the plant cell wall allows for developmental processes that include
1644 organ abscission and pollen dehiscence, and might allow for the recycling of some wall
1645 components to produce new wall polymers (Barnes and Anderson, 2018). Overall, the
1646 plant cell wall is a fascinating biological environment, one that we are only beginning to
1647 be able to understand well enough to be able to engineer ourselves.

1648

1649

1650 **ACKNOWLEDGMENTS**

1651 The authors apologize to those whose important contributions could not be cited due to
1652 space constraints. Byung-Ho Kang thanks Drs. Gao Peng, Pengfei Wang, Juncai Ma,
1653 and Zizhen Liang for their support in preparing this review. Kai Dünser and Jürgen Kleine-
1654 Vehn are grateful to Mary Williams, David Scheuring, and Michael Sauer for critical
1655 reading as well as to Pavithran Narayanan, Marco Trujillo, Yasin Dagdas, and Liam Elliott
1656 for discussing their figure layout on Twitter. Kent Chapman gives special thanks to Payton
1657 Whitehead for acquiring confocal images and for the preparation of Figure 6, and to Dr.
1658 Eliot Herman, University of Arizona, for the EM images in Figure 6. Thanks also to
1659 Charlene Case for assistance with manuscript preparation and to Dr. Robert Mullen,
1660 University of Guelph, for comments and edits. Bethany Zolman thanks past and present
1661 members of the Zolman Lab for inspiring discussions on peroxisome structure and
1662 function. Tessa M. Burch-Smith thanks Amie Sankoh for help with figure preparation and
1663 Dr. Brandon Reagan for critical reading of the manuscript and ET model generation.
1664 Thanks to members of the Anderson Lab and the Center for Lignocellulose Structure and
1665 Formation for inspiring discussions

1666

1667 Yu Tang and Yangnan Gu's work was supported by the USDA National Institute of Food
1668 and Agriculture (HATCH project CA-B-PLB-0243-H), National Science Foundation (MCB-
1669 2049931), and start-up funds from the University of California Berkeley and the Innovative
1670 Genomics Institute (to Y.G.). Federica Brandizzi's work was funded primarily by the
1671 National Institutes of Health (GM136637), National Science Foundation (MCB1727362),
1672 the Chemical Sciences, Geosciences and Biosciences Division, Office of Basic Energy
1673 Sciences, Office of Science, US Department of Energy (award number DE-FG02-
1674 91ER20021), and AgBioResearch (MICL02598). Byung-Ho Kang's work was supported
1675 by the Hong Kong Research Grant Council (GRF14121019, 14113921, AoE/M-05/12,
1676 C4002-17G), and Chinese University of Hong Kong (Direct Grants). Research on
1677 endosomal trafficking in the Otegui Lab is supported by the National Science Foundation
1678 grant NSF MCB 2114603 to MSO. Kai Dünser and Jürgen Kleine-Vehn's work on the
1679 plant vacuole is supported by the Austrian Science Fund (FWF) (P 33044 to J.K.-V.).

1680 Peroxisome research in the Zolman lab has been funded by the National Institutes of
1681 Health (1R15GM116090-01), the University of Missouri Research Board, and the
1682 University of Missouri–St. Louis. Shin-ichi Arimura’s work was supported by the JSPS
1683 (19KK0391, 19H02927, and 20H05680). Research in the Kirchhoff lab is mainly
1684 supported by grants from the National Science Foundation (MCB-BSF-1953570) and
1685 Department of Energy (DE-SC0017160). Abel Rosado is supported by the Canada
1686 Discovery Grant RGPIN-2019-05568. Emmanuelle Bayer, Federica Brandizzi, Yvon
1687 Jaillais, Miguel A. Botella, and Pengwei Wang thank the multiple funding agencies
1688 supporting basic research projects on plant membrane contact sites. Tessa M. Burch-
1689 Smith’s work was supported by the National Science Foundation (MCB1846245). Charles
1690 T. Anderson’s work was supported as part of The Center for Lignocellulose Structure and
1691 Formation, an Energy Frontier Research Center funded by the U.S. Department of
1692 Energy, Office of Science, Basic Energy Sciences under Award # DE-SC0001090.

1693

1694 **References**

1695 **Adam, Z., Charuvi, D., Tsabari, O., Knopf, R.R., and Reich, Z.** (2011). Biogenesis of
1696 thylakoid networks in angiosperms: knowns and unknowns. *Plant Mol Biol* **76**, 221-
1697 234.

1698 **Agrawal, G., and Subramani, S.** (2016). De novo peroxisome biogenesis: Evolving
1699 concepts and conundrums. *Biochim Biophys Acta* **1863**, 892-901.

1700 **Alberts, B., Johnson, A., Lewis, J., Morgan, D., Martin, R., Roberts, K., and Walter,**
1701 **P.** (2014). Intracellular Membrane Traffic. In *Molecular Biology of the Cell* (W. W.
1702 Norton & Company; Sixth edition.

1703 **Albrecht, V., Simkova, K., Carrie, C., Delannoy, E., Giraud, E., Whelan, J., Small, I.D.,**
1704 **Apel, K., Badger, M.R., and Pogson, B.J.** (2010). The cytoskeleton and the
1705 peroxisomal-targeted snowy cotyledon3 protein are required for chloroplast
1706 development in Arabidopsis. *Plant Cell* **22**, 3423-3438.

1707 **Anderson, C.T.** (2019). Pectic Polysaccharides in Plants: Structure, Biosynthesis,
1708 Functions, and Applications. In *Extracellular Sugar-Based Biopolymers Matrices*,
1709 E. Cohen and H. Merzendorfer, eds (Springer International Publishing), pp. 487-
1710 514.

- 1711 **Anderson, C.T., Wallace, I.S., and Somerville, C.R.** (2012). Metabolic click-labeling
1712 with a fucose analog reveals pectin delivery, architecture, and dynamics in
1713 Arabidopsis cell walls. *Proc Natl Acad Sci U S A* **109**, 1329-1334.
- 1714 **Andersson, M., and D'ormann, P.** (2008). Chloroplast membrane lipid biosynthesis and
1715 transport. In *The chloroplast—Interactions with the environment*, A.S. Sandelius
1716 and H. Aronsson, eds (New York: Springer), pp. 125-158.
- 1717 **Andres, Z., Perez-Hormaeche, J., Leidi, E.O., Schlucking, K., Steinhorst, L.,**
1718 **McLachlan, D.H., Schumacher, K., Hetherington, A.M., Kudla, J., Cubero, B.,**
1719 **and Pardo, J.M.** (2014). Control of vacuolar dynamics and regulation of stomatal
1720 aperture by tonoplast potassium uptake. *Proc Natl Acad Sci U S A* **111**, E1806-
1721 E1814.
- 1722 **Appelhagen, I., Nordholt, N., Seidel, T., Spelt, K., Koes, R., Quattrochio, F.,**
1723 **Sagasser, M., and Weisshaar, B.** (2015). TRANSPARENT TESTA 13 is a
1724 tonoplast P-3A-ATPase required for vacuolar deposition of proanthocyanidins in
1725 Arabidopsis thaliana seeds. *Plant J* **82**, 840-849.
- 1726 **Appenzeller-Herzog, C., and Hauri, H.P.** (2006). The ER-Golgi intermediate
1727 compartment (ERGIC): in search of its identity and function. *J Cell Sci* **119**, 2173-
1728 2183.
- 1729 **Arimura, S., and Tsutsumi, N.** (2002). A dynamin-like protein (ADL2b), rather than FtsZ,
1730 is involved in Arabidopsis mitochondrial division. *Proc Natl Acad Sci U S A* **99**,
1731 5727-5731.
- 1732 **Arimura, S., Aida, G.P., Fujimoto, M., Nakazono, M., and Tsutsumi, N.** (2004a).
1733 Arabidopsis dynamin-like protein 2a (ADL2a), like ADL2b, is involved in plant
1734 mitochondrial division. *Plant Cell Physiol* **45**, 236-242.
- 1735 **Arimura, S., Yamamoto, J., Aida, G.P., Nakazono, M., and Tsutsumi, N.** (2004b).
1736 Frequent fusion and fission of plant mitochondria with unequal nucleoid
1737 distribution. *Proc Natl Acad Sci U S A* **101**, 7805-7808.
- 1738 **Arimura, S., Fujimoto, M., Doniwa, Y., Kadoya, N., Nakazono, M., Sakamoto, W., and**
1739 **Tsutsumi, N.** (2008). Arabidopsis ELONGATED MITOCHONDRIA1 is required for
1740 localization of DYNAMIN-RELATED PROTEIN3A to mitochondrial fission sites.
1741 *Plant Cell* **20**, 1555-1566.

- 1742 **Arimura, S.I.** (2018). Fission and Fusion of Plant Mitochondria, and Genome
1743 Maintenance. *Plant Physiol* **176**, 152-161.
- 1744 **Arimura, S.I., Kurisu, R., Sugaya, H., Kadoya, N., and Tsutsumi, N.** (2017). Cold
1745 Treatment Induces Transient Mitochondrial Fragmentation in *Arabidopsis thaliana*
1746 in a Way that Requires DRP3A but not ELM1 or an ELM1-Like Homologue, ELM2.
1747 *Int J Mol Sci* **18**.
- 1748 **Arimura, S.I., Ayabe, H., Sugaya, H., Okuno, M., Tamura, Y., Tsuruta, Y., Watari, Y.,**
1749 **Yanase, S., Yamauchi, T., Itoh, T., Toyoda, A., Takanashi, H., and Tsutsumi,**
1750 **N.** (2020). Targeted gene disruption of ATP synthases 6-1 and 6-2 in the
1751 mitochondrial genome of *Arabidopsis thaliana* by mitoTALENs. *Plant J* **104**, 1459-
1752 1471.
- 1753 **Aronsson, H., and Jarvis, P.** (2008). The chloroplast protein import apparatus, its
1754 components, and their roles. In *The Chloroplast - Interactions with the*
1755 *environment*, A.S. Sandelius and H. Aronsson, eds (New York: Springer), pp. 89-
1756 123.
- 1757 **Aung, K., and Hu, J.** (2011). The *Arabidopsis* tail-anchored protein PEROXISOMAL AND
1758 MITOCHONDRIAL DIVISION FACTOR1 is involved in the morphogenesis and
1759 proliferation of peroxisomes and mitochondria. *Plant Cell* **23**, 4446-4461.
- 1760 **Avila-Ospina, L., Moison, M., Yoshimoto, K., and Masclaux-Daubresse, C.** (2014).
1761 Autophagy, plant senescence, and nutrient recycling. *J Exp Bot* **65**, 3799-3811.
- 1762 **Azim, M.F., and Burch-Smith, T.M.** (2020). Organelles-nucleus-plasmodesmata
1763 signaling (ONPS): an update on its roles in plant physiology, metabolism and
1764 stress responses. *Curr Opin Plant Biol* **58**, 48-59.
- 1765 **Baillie, A.L., Falz, A.L., Muller-Schussele, S.J., and Sparkes, I.** (2020). It Started With
1766 a Kiss: Monitoring Organelle Interactions and Identifying Membrane Contact Site
1767 Components in Plants. *Frontiers in Plant Science* **11**.
- 1768 **Bak, G., Lee, E.J., Lee, Y., Kato, M., Segami, S., Sze, H., Maeshima, M., Hwang, J.U.,**
1769 **and Lee, Y.** (2013). Rapid Structural Changes and Acidification of Guard Cell
1770 Vacuoles during Stomatal Closure Require Phosphatidylinositol 3,5-Bisphosphate.
1771 *Plant Cell* **25**, 2202-2216

- 1772 **Barnes, W.J., and Anderson, C.T.** (2018). Release, Recycle, Rebuild: Cell-Wall
1773 Remodeling, Autodegradation, and Sugar Salvage for New Wall Biosynthesis
1774 during Plant Development. *Mol Plant* **11**, 31-46.
- 1775 **Barragan, V., Leidi, E.O., Andres, Z., Rubio, L., De Luca, A., Fernandez, J.A., Cubero,**
1776 **B., and Pardo, J.M.** (2012). Ion Exchangers NHX1 and NHX2 Mediate Active
1777 Potassium Uptake into Vacuoles to Regulate Cell Turgor and Stomatal Function in
1778 Arabidopsis. *Plant Cell* **24**, 1127-1142.
- 1779 **Barton, D.A., Cole, L., Collings, D.A., Liu, D.Y., Smith, P.M., Day, D.A., and Overall,**
1780 **R.L.** (2011). Cell-to-cell transport via the lumen of the endoplasmic reticulum. *Plant*
1781 *J* **66**, 806-817.
- 1782 **Barton, K., Mathur, N., and Mathur, J.** (2013). Simultaneous live-imaging of
1783 peroxisomes and the ER in plant cells suggests contiguity but no luminal continuity
1784 between the two organelles. *Front Physiol* **4**, 196.
- 1785 **Bassham, D.C., Laporte, M., Marty, F., Moriyasu, Y., Ohsumi, Y., Olsen, L.J., and**
1786 **Yoshimoto, K.** (2006). Autophagy in development and stress responses of plants.
1787 *Autophagy* **2**, 2-11.
- 1788 **Beebo, A., Thomas, D., Der, C., Sanchez, L., Leborgne-Castel, N., Marty, F., Schoefs,**
1789 **B., and Bouhidel, K.** (2009). Life with and without AtTIP1;1, an Arabidopsis
1790 aquaporin preferentially localized in the apposing tonoplasts of adjacent vacuoles.
1791 *Plant Mol Biol* **70**, 193-209.
- 1792 **Berger, F., Hung, C.Y., Dolan, L., and Schiefelbein, J.** (1998). Control of cell division
1793 in the root epidermis of Arabidopsis thaliana. *Dev Biol* **194**, 235-245.
- 1794 **Bi, X., Cheng, Y.J., Hu, B., Ma, X., Wu, R., Wang, J.W., and Liu, C.** (2017). Nonrandom
1795 domain organization of the Arabidopsis genome at the nuclear periphery. *Genome*
1796 *Res* **27**, 1162-1173.
- 1797 **Biel, A., Moser, M., and Meier, I.** (2020a). A Role for Plant KASH Proteins in Regulating
1798 Stomatal Dynamics. *Plant Physiol* **182**, 1100-1113.
- 1799 **Biel, A., Moser, M., and Meier, I.** (2020b). Arabidopsis KASH Proteins SINE1 and SINE2
1800 Are Involved in Microtubule Reorganization During ABA-Induced Stomatal
1801 Closure. *Front Plant Sci* **11**, 575573.

- 1802 **Bishop, J., Swan, H., Valente, F., and Nutzmann, H.W.** (2021). The Plant Nuclear
1803 Envelope and Its Role in Gene Transcription. *Front Plant Sci* **12**, 674209.
- 1804 **Boevink, P., Oparka, K., Santa Cruz, S., Martin, B., Betteridge, A., and Hawes, C.**
1805 (1998). Stacks on tracks: the plant Golgi apparatus traffics on an actin/ER network.
1806 *Plant J* **15**, 441-447.
- 1807 **Botha, C.E.** (1992). Plasmodesmatal distribution, structure and frequency in relation to
1808 assimilation in C3 and C 4 grasses in southern Africa. *Planta* **187**, 348-358.
- 1809 **Boutte, Y., Jonsson, K., McFarlane, H.E., Johnson, E., Gendre, D., Swarup, R., Friml,
1810 J., Samuels, L., Robert, S., and Bhalerao, R.P.** (2013). ECHIDNA-mediated
1811 post-Golgi trafficking of auxin carriers for differential cell elongation. *Proc Natl Acad
1812 Sci U S A* **110**, 16259-16264.
- 1813 **Brandizzi, F.** (2002). The Destination for Single-Pass Membrane Proteins Is Influenced
1814 Markedly by the Length of the Hydrophobic Domain. *THE PLANT CELL ONLINE*
1815 **14**, 1077 - 1092.
- 1816 **Brandizzi, F.** (2021). Maintaining the structural and functional homeostasis of the plant
1817 endoplasmic reticulum. *Dev Cell* **56**, 919-932.
- 1818 **Brault, M.L., Petit, J.D., Immel, F., Nicolas, W.J., Glavier, M., Brocard, L., Gaston, A.,
1819 Fouche, M., Hawkins, T.J., Crowet, J.M., Grison, M.S., Germain, V., Rocher,
1820 M., Kraner, M., Alva, V., Claverol, S., Paterlini, A., Helariutta, Y., Deleu, M.,
1821 Lins, L., Tilsner, J., and Bayer, E.M.** (2019). Multiple C2 domains and
1822 transmembrane region proteins (MCTPs) tether membranes at plasmodesmata.
1823 *EMBO Rep* **20**, e47182.
- 1824 **Brocard, L., Immel, F., Coulon, D., Esnay, N., Tuphile, K., Pascal, S., Claverol, S.,
1825 Fouillen, L., Bessoule, J.J., and Brehelin, C.** (2017). Proteomic Analysis of Lipid
1826 Droplets from Arabidopsis Aging Leaves Brings New Insight into Their Biogenesis
1827 and Functions. *Front Plant Sci* **8**, 894.
- 1828 **Broda, M., Millar, A.H., and Aken, O.V.** (2018). Mitophagy: A Mechanism for Plant
1829 Growth and Survival. *Trends in Plant Science* **23**, 434 - 450.
- 1830 **Brunkard, J.O., Runkel, A.M., and Zambryski, P.C.** (2015). The cytosol must flow:
1831 intercellular transport through plasmodesmata. *Current Opinion in Cell Biology* **35**,
1832 13 - 20.

- 1833 **Buono, R.A., Paez-Valencia, J., Miller, N.D., Goodman, K., Spitzer, C., Spalding,**
1834 **E.P., and Otegui, M.S.** (2016). Role of SKD1 Regulators LIP5 and IST1-LIKE1 in
1835 Endosomal Sorting and Plant Development. *Plant Physiol* **171**, 251-264.
- 1836 **Buono, R.A., Leier, A., Paez-Valencia, J., Pennington, J., Goodman, K., Miller, N.,**
1837 **Ahlquist, P., Marquez-Lago, T.T., and Otegui, M.S.** (2017). ESCRT-mediated
1838 vesicle concatenation in plant endosomes. *J Cell Biol* **216**, 2167-2177.
- 1839 **Burch-Smith, T.M., Stonebloom, S., Xu, M., and Zambryski, P.C.** (2011).
1840 Plasmodesmata during development: re-examination of the importance of primary,
1841 secondary, and branched plasmodesmata structure versus function. *Protoplasma*
1842 **248**, 61-74.
- 1843 **Bykov, Y.S., Schaffer, M., Dodonova, S.O., Albert, S., Plitzko, J.M., Baumeister, W.,**
1844 **Engel, B.D., and Briggs, J.A.** (2017). The structure of the COPI coat determined
1845 within the cell. *Elife* **6**.
- 1846 **Cai, Q., Qiao, L., Wang, M., He, B., Lin, F.M., Palmquist, J., Huang, S.D., and Jin, H.**
1847 (2018). Plants send small RNAs in extracellular vesicles to fungal pathogen to
1848 silence virulence genes. *Science* **360**, 1126-1129.
- 1849 **Cai, Y., Whitehead, P., Chappell, J., and Chapman, K.D.** (2019). Mouse lipogenic
1850 proteins promote the co-accumulation of triacylglycerols and sesquiterpenes in
1851 plant cells. *Planta* **250**, 79-94.
- 1852 **Cai, Y., Goodman, J.M., Pyc, M., Mullen, R.T., Dyer, J.M., and Chapman, K.D.** (2015).
1853 *Arabidopsis* SEIPIN Proteins Modulate Triacylglycerol Accumulation and Influence
1854 Lipid Droplet Proliferation. *Plant Cell* **27**, 2616-2636.
- 1855 **Cai, Y., Zhang, B., Liang, L., Wang, S., Zhang, L., Wang, L., Cui, H.L., Zhou, Y., and**
1856 **Wang, D.** (2021). A solid-state nanopore-based single-molecule approach for
1857 label-free characterization of plant polysaccharides. *Plant Commun* **2**, 100106.
- 1858 **Calero-Munoz, N., Exposito-Rodriguez, M., Collado-Arenal, A.M., Rodriguez-**
1859 **Serrano, M., Laureano-Marin, A.M., Santamaria, M.E., Gotor, C., Diaz, I.,**
1860 **Mullineaux, P.M., Romero-Puertas, M.C., Olmedilla, A., and Sandalio, L.M.**
1861 (2019). Cadmium induces reactive oxygen species-dependent pexophagy in
1862 *Arabidopsis* leaves. *Plant Cell Environ* **42**, 2696-2714.

- 1863 **Cao, P., Renna, L., Stefano, G., and Brandizzi, F.** (2016). SYP73 Anchors the ER to
1864 the Actin Cytoskeleton for Maintenance of ER Integrity and Streaming in
1865 Arabidopsis. *Curr Biol* **26**, 3245-3254.
- 1866 **Caplan, J.L., Kumar, A.S., Park, E., Padmanabhan, M.S., Hoban, K., Modla, S.,**
1867 **Czymmek, K., and Dinesh-Kumar, S.P.** (2015). Chloroplast Stromules Function
1868 during Innate Immunity. *Dev Cell* **34**, 45-57.
- 1869 **Capoen, W., Sun, J., Wysham, D., Otegui, M.S., Venkateshwaran, M., Hirsch, S.,**
1870 **Miwa, H., Downie, J.A., Morris, R.J., Ane, J.M., and Oldroyd, G.E.** (2011).
1871 Nuclear membranes control symbiotic calcium signaling of legumes. *Proc Natl*
1872 *Acad Sci U S A* **108**, 14348-14353.
- 1873 **Carpita, N.C., and McCann, M.C.** (2000). The Cell Wall. In *Biochemistry and Molecular*
1874 *Biology of Plants*, B.B. Buchanan, ed (American Society of Plant Physiologists),
1875 pp. 52 - 109.
- 1876 **Chan, J., and Coen, E.** (2020). Interaction between Autonomous and Microtubule
1877 Guidance Systems Controls Cellulose Synthase Trajectories. *Current Biology* **30**,
1878 941-+.
- 1879 **Chapman, K.D., Dyer, J.M., and Mullen, R.T.** (2012). Biogenesis and functions of lipid
1880 droplets in plants: Thematic Review Series: Lipid Droplet Synthesis and
1881 Metabolism: from Yeast to Man. *J Lipid Res* **53**, 215-226.
- 1882 **Chapman, K.D., Aziz, M., Dyer, J.M., and Mullen, R.T.** (2019). Mechanisms of lipid
1883 droplet biogenesis. *Biochem J* **476**, 1929-1942.
- 1884 **Charpentier, M., Sun, J., Vaz Martins, T., Radhakrishnan, G.V., Findlay, K.,**
1885 **Soumpourou, E., Thouin, J., Very, A.A., Sanders, D., Morris, R.J., and**
1886 **Oldroyd, G.E.** (2016). Nuclear-localized cyclic nucleotide-gated channels mediate
1887 symbiotic calcium oscillations. *Science* **352**, 1102-1105.
- 1888 **Charton, L., Plett, A., and Linka, N.** (2019). Plant peroxisomal solute transporter
1889 proteins. *J Integr Plant Biol* **61**, 817-835.
- 1890 **Charuvi, D., Kiss, V., Nevo, R., Shimoni, E., Adam, Z., and Reich, Z.** (2012). Gain and
1891 loss of photosynthetic membranes during plastid differentiation in the shoot apex
1892 of Arabidopsis. *Plant Cell* **24**, 1143-1157.

1893 **Chen, J., Stefano, G., Brandizzi, F., and Zheng, H.** (2011). Arabidopsis RHD3 mediates
1894 the generation of the tubular ER network and is required for Golgi distribution and
1895 motility in plant cells. *J Cell Sci* **124**, 2241-2252.

1896 **Chevalier, L., Bernard, S., Ramdani, Y., Lamour, R., Bardor, M., Lerouge, P., Follet-**
1897 **Gueye, M.L., and Driouich, A.** (2010). Subcompartment localization of the side
1898 chain xyloglucan-synthesizing enzymes within Golgi stacks of tobacco
1899 suspension-cultured cells. *Plant J* **64**, 977-989.

1900 **Chiaruttini, N., Redondo-Morata, L., Colom, A., Humbert, F., Lenz, M., Scheuring,**
1901 **S., and Roux, A.** (2015). Relaxation of Loaded ESCRT-III Spiral Springs Drives
1902 Membrane Deformation. *Cell* **163**, 866-879.

1903 **Choi, J., and Richards, E.J.** (2020). The role of CRWN nuclear proteins in chromatin-
1904 based regulation of stress response genes. *Plant Signal Behav* **15**, 1694224.

1905 **Chow, C.M., Neto, H., Foucart, C., and Moore, I.** (2008). Rab-A2 and Rab-A3 GTPases
1906 define a trans-golgi endosomal membrane domain in Arabidopsis that contributes
1907 substantially to the cell plate. *Plant Cell* **20**, 101-123.

1908 **Chu, K.L., Jenkins, L.M., Bailey, S.R., Kambhampati, S., Koley, S., Foley, K., Arp,**
1909 **J.J., Czymmek, K.J., Bates, P.D., and Allen, D.K.** (2020). Shifting carbon flux
1910 from non-transient starch to lipid allows oil accumulation in transgenic tobacco
1911 leaves. *Biorxiv*, 2020.2005.2015.098632.

1912 **Chung, T., Phillips, A.R., and Vierstra, R.D.** (2010). ATG8 lipidation and ATG8-
1913 mediated autophagy in Arabidopsis require ATG12 expressed from the
1914 differentially controlled ATG12A AND ATG12B loci. *Plant J* **62**, 483-493.

1915 **Concia, L., Veluchamy, A., Ramirez-Prado, J.S., Martin-Ramirez, A., Huang, Y.,**
1916 **Perez, M., Domenichini, S., Granados, N.R.Y., Kim, S., Blein, T., Duncan, S.,**
1917 **Pichot, C., Manza-Mianza, D., Juery, C., Paux, E., Moore, G., Hirt, H.,**
1918 **Bergounioux, C., Crespi, M., Mahfouz, M.M., Bendahmane, A., Liu, C., Hall,**
1919 **A., Raynaud, C., Latrasse, D., and Benhamed, M.** (2020). Wheat chromatin
1920 architecture is organized in genome territories and transcription factories. *Genome*
1921 *Biology* **21**.

- 1922 **Cook, M., Graham, L., Botha, C., and Lavin, C.** (1997). Comparative ultrastructure of
1923 plasmodesmata of Chara and selected bryophytes: toward an elucidation of the
1924 evolutionary origin of plant plasmodesmata. *Am J Bot* **84**, 1169.
- 1925 **Corpas, F.J., Gonzalez-Gordo, S., and Palma, J.M.** (2020). Plant Peroxisomes: A
1926 Factory of Reactive Species. *Front Plant Sci* **11**, 853.
- 1927 **Cosgrove, D.J.** (2018). Nanoscale structure, mechanics and growth of epidermal cell
1928 walls. *Curr Opin Plant Biol* **46**, 77-86.
- 1929 **Coulon, D., Brocard, L., Tuphile, K., and Brehelin, C.** (2020). Arabidopsis LDIP protein
1930 locates at a confined area within the lipid droplet surface and favors lipid droplet
1931 formation. *Biochimie* **169**, 29-40.
- 1932 **Cui, Y., Zhao, Q., Hu, S., and Jiang, L.W.** (2020). Vacuole Biogenesis in Plants: How
1933 Many Vacuoles, How Many Models? *Trends Plant Sci* **25**, 538-548.
- 1934 **Cui, Y., Zhao, Q., Gao, C.J., Ding, Y., Zeng, Y.L., Ueda, T., Nakano, A., and Jiang,**
1935 **L.W.** (2014). Activation of the Rab7 GTPase by the MON1-CCZ1 Complex Is
1936 Essential for PVC-to-Vacuole Trafficking and Plant Growth in Arabidopsis. *Plant*
1937 *Cell* **26**, 2080-2097.
- 1938 **Cui, Y., Cao, W.H., He, Y.L., Zhao, Q., Wakazaki, M., Zhuang, X.H., Gao, J.Y., Zeng,**
1939 **Y.L., Gao, C.J., Ding, Y., Wong, H.Y., Wong, W.S., Lam, H.K., Wang, P.F.,**
1940 **Ueda, T., Rojas-Pierce, M., Toyooka, K., Kang, B.H., and Jiang, L.W.** (2019). A
1941 whole-cell electron tomography model of vacuole biogenesis in Arabidopsis root
1942 cells. *Nat Plants* **5**, 95-105.
- 1943 **Cui, S., Hayashi, Y., Otomo, M., Mano, S., Oikawa, K., Hayashi, M., and Nishimura,**
1944 **M.** (2016). Sucrose Production Mediated by Lipid Metabolism Suppresses the
1945 Physical Interaction of Peroxisomes and Oil Bodies during Germination of
1946 Arabidopsis thaliana. *J Biol Chem* **291**, 19734-19745.
- 1947 **Day, K.J., Staehelin, L.A., and Glick, B.S.** (2013). A three-stage model of Golgi structure
1948 and function. *Histochem Cell Biol* **140**, 239-249.
- 1949 **De Angeli, A., Zhang, J.B., Meyer, S., and Martinoia, E.** (2013). AtALMT9 is a malate-
1950 activated vacuolar chloride channel required for stomatal opening in Arabidopsis.
1951 *Nat Commun* **4**. 1804

- 1952 **de Leone, M.J., Hernando, C.E., Romanowski, A., Careno, D.A., Soverna, A.F., Sun,**
1953 **H., Bologna, N.G., Vazquez, M., Schneeberger, K., and Yanovsky, M.J.** (2020).
1954 Bacterial Infection Disrupts Clock Gene Expression to Attenuate Immune
1955 Responses. *Curr Biol* **30**, 1740-1747 e1746.
- 1956 **de Vries, J., and Ischebeck, T.** (2020). Ties between Stress and Lipid Droplets Pre-date
1957 Seeds. *Trends in Plant Science* **25**, 1203-1214.
- 1958 **Deinum, E.E., Mulder, B.M., and Benitez-Alfonso, Y.** (2019). From plasmodesma
1959 geometry to effective symplasmic permeability through biophysical modelling.
1960 *eLife* **8**.
- 1961 **Del Rio, L.A., and Lopez-Huertas, E.** (2016). ROS Generation in Peroxisomes and its
1962 Role in Cell Signaling. *Plant Cell Physiol* **57**, 1364-1376.
- 1963 **Deruyffelaere, C., Purkrtova, Z., Bouchez, I., Collet, B., Cacas, J.L., Chardot, T.,**
1964 **Gallois, J.L., and D'Andrea, S.** (2018). PUX10 Is a CDC48A Adaptor Protein That
1965 Regulates the Extraction of Ubiquitinated Oleosins from Seed Lipid Droplets in
1966 Arabidopsis. *Plant Cell* **30**, 2116-2136.
- 1967 **Desai, M., and Hu, J.** (2008). Light induces peroxisome proliferation in Arabidopsis
1968 seedlings through the photoreceptor phytochrome A, the transcription factor HY5
1969 HOMOLOG, and the peroxisomal protein PEROXIN11b. *Plant Physiol* **146**, 1117-
1970 1127.
- 1971 **Dettmer, J., Hong-Hermesdorf, A., Stierhof, Y.D., and Schumacher, K.** (2006).
1972 Vacuolar H⁺-ATPase activity is required for endocytic and secretory trafficking in
1973 Arabidopsis. *Plant Cell* **18**, 715-730.
- 1974 **Ding, B., Turgeon, R., and Parthasarathy, M.V.** (1992). Substructure of Freeze-
1975 Substituted Plasmodesmata. *Protoplasma* **169**, 28-41.
- 1976 **Dixon, R.A., and Barros, J.** (2019). Lignin biosynthesis: old roads revisited and new
1977 roads explored. *Open Biol* **9**, 190215.
- 1978 **Dobro, M.J., Samson, R.Y., Yu, Z., McCullough, J., Ding, H.J., Chong, P.L., Bell, S.D.,**
1979 **and Jensen, G.J.** (2013). Electron cryotomography of ESCRT assemblies and
1980 dividing *Sulfolobus* cells suggests that spiraling filaments are involved in
1981 membrane scission. *Mol Biol Cell* **24**, 2319-2327.

- 1982 **Dominguez, F., and Cejudo, F.J.** (2021). Chloroplast dismantling in leaf senescence. *J*
 1983 *Exp Bot.*
- 1984 **Dong, Q., Li, N., Li, X., Yuan, Z., Xie, D., Wang, X., Li, J., Yu, Y., Wang, J., Ding, B.,**
 1985 **Zhang, Z., Li, C., Bian, Y., Zhang, A., Wu, Y., Liu, B., and Gong, L.** (2018).
 1986 Genome-wide Hi-C analysis reveals extensive hierarchical chromatin interactions
 1987 in rice. *Plant J* **94**, 1141-1156.
- 1988 **Donohoe, B.S., Kang, B.H., and Staehelin, L.A.** (2007). Identification and
 1989 characterization of COPIa- and COPIb-type vesicle classes associated with plant
 1990 and algal Golgi. *Proc Natl Acad Sci U S A* **104**, 163-168.
- 1991 **Donohoe, B.S., Kang, B.H., Gerl, M.J., Gergely, Z.R., McMichael, C.M., Bednarek,**
 1992 **S.Y., and Staehelin, L.A.** (2013). Cis-Golgi cisternal assembly and biosynthetic
 1993 activation occur sequentially in plants and algae. *Traffic* **14**, 551-567.
- 1994 **Doumane, M., Lebecq, A., Colin, L., Fangain, A., Stevens, F.D., Bareille, J., Hamant,**
 1995 **O., Belkhadir, Y., Munnik, T., Jaillais, Y., and Caillaud, M.C.** (2021). Inducible
 1996 depletion of PI(4,5)P2 by the synthetic iDePP system in Arabidopsis. *Nat Plants* **7**,
 1997 587-597.
- 1998 **Dubois, G.A., and Jaillais, Y.** (2021). Anionic phospholipid gradients: an
 1999 uncharacterized frontier of the plant endomembrane network. *Plant Physiol* **185**,
 2000 577-592.
- 2001 **Duckney, P., Kroon, J.T., Dixon, M.R., Hawkins, T.J., Deeks, M.J., and Hussey, P.J.**
 2002 (2021). NETWORKED2-subfamily proteins regulate the cortical actin cytoskeleton
 2003 of growing pollen tubes and polarised pollen tube growth. *New Phytol* **231**, 152-
 2004 164.
- 2005 **Dunkley, T.P., Hester, S., Shadforth, I.P., Runions, J., Weimar, T., Hanton, S.L.,**
 2006 **Griffin, J.L., Bessant, C., Brandizzi, F., Hawes, C., Watson, R.B., Dupree, P.,**
 2007 **and Lilley, K.S.** (2006). Mapping the Arabidopsis organelle proteome. *Proc Natl*
 2008 *Acad Sci U S A* **103**, 6518-6523.
- 2009 **Dunser, K., and Kleine-Vehn, J.** (2015). Differential growth regulation in plants - the acid
 2010 growth balloon theory. *Curr Opin Plant Biol* **28**, 55-59.
- 2011 **Dunser, K., Gupta, S., Herger, A., Feraru, M.I., Ringli, C., and Kleine-Vehn, J.** (2019).
 2012 Extracellular matrix sensing by FERONIA and Leucine-Rich Repeat Extensins

2013 controls vacuolar expansion during cellular elongation in *Arabidopsis thaliana*.
2014 *EMBO J* **38**. e100353

2015 **Eastmond, P.J.** (2006). SUGAR-DEPENDENT1 encodes a patatin domain
2016 triacylglycerol lipase that initiates storage oil breakdown in germinating
2017 *Arabidopsis* seeds. *Plant Cell* **18**, 665-675.

2018 **Ebine, K., Inoue, T., Ito, J., Ito, E., Uemura, T., Goh, T., Abe, H., Sato, K., Nakano, A.,**
2019 **and Ueda, T.** (2014). Plant Vacuolar Trafficking Occurs through Distinctly
2020 Regulated Pathways. *Curr Biol* **24**, 1375-1382.

2021 **Ebine, K., Okatani, Y., Uemura, T., Goh, T., Shoda, K., Niihama, M., Morita, M.T.,**
2022 **Spitzer, C., Otegui, M.S., Nakano, A., and Ueda, T.** (2008). A SNARE Complex
2023 Unique to Seed Plants Is Required for Protein Storage Vacuole Biogenesis and
2024 Seed Development of *Arabidopsis thaliana*. *Plant Cell* **20**, 3006-3021.

2025 **Ehlers, K., and Kollmann, R.** (2001). Primary and secondary plasmodesmata: structure,
2026 origin, and functioning. *Protoplasma* **216**, 1-30.

2027 **Ehlers, K., and van Bel, A.J.** (2010). Dynamics of plasmodesmal connectivity in
2028 successive interfaces of the cambial zone. *Planta* **231**, 371-385.

2029 **Eisenach, C., and De Angeli, A.** (2017). Ion Transport at the Vacuole during Stomatal
2030 Movements. *Plant Physiol* **174**, 520-530.

2031 **El Zawily, A.M., Schwarzlander, M., Finkemeier, I., Johnston, I.G., Benamar, A., Cao,**
2032 **Y., Gissot, C., Meyer, A.J., Wilson, K., Datla, R., Macherel, D., Jones, N.S., and**
2033 **Logan, D.C.** (2014). FRIENDLY regulates mitochondrial distribution, fusion, and
2034 quality control in *Arabidopsis*. *Plant Physiol* **166**, 808-828.

2035 **Emenecker, R.J., Holehouse, A.S., and Strader, L.C.** (2020). Emerging Roles for
2036 Phase Separation in Plants. *Dev Cell* **55**, 69-83.

2037 **Engel, B.D., Schaffer, M., Albert, S., Asano, S., Pitzko, J.M., and Baumeister, W.**
2038 (2015). In situ structural analysis of Golgi intracisternal protein arrays. *Proc Natl*
2039 *Acad Sci U S A* **112**, 11264-11269.

2040 **English, A.R., Zurek, N., and Voeltz, G.K.** (2009). Peripheral ER structure and function.
2041 *Curr Opin Cell Biol* **21**, 596-602.

2042 **Esnay, N., Dyer, J.M., Mullen, R.T., and Chapman, K.D.** (2020). Lipid Droplet–
2043 Peroxisome Connections in Plants. *Contact* **3**, 2515256420908765.

- 2044 **Fahy, D., Sanad, M., Duscha, K., Lyons, M., Liu, F., Bozhkov, P., Kunz, H.H., Hu, J.,**
2045 **Neuhaus, H.E., Steel, P.G., and Smertenko, A.** (2017). Impact of salt stress, cell
2046 death, and autophagy on peroxisomes: quantitative and morphological analyses
2047 using small fluorescent probe N-BODIPY. *Sci Rep* **7**, 39069.
- 2048 **Fang, X., Wang, L., Ishikawa, R., Li, Y., Fiedler, M., Liu, F., Calder, G., Rowan, B.,**
2049 **Weigel, D., Li, P., and Dean, C.** (2019). Arabidopsis FLL2 promotes liquid-liquid
2050 phase separation of polyadenylation complexes. *Nature* **569**, 265-269.
- 2051 **Faso, C., Chen, Y.N., Tamura, K., Held, M., Zemelis, S., Marti, L., Saravanan, R.,**
2052 **Hummel, E., Kung, L., Miller, E., Hawes, C., and Brandizzi, F.** (2009). A
2053 missense mutation in the Arabidopsis COPII coat protein Sec24A induces the
2054 formation of clusters of the endoplasmic reticulum and Golgi apparatus. *Plant Cell*
2055 **21**, 3655-3671.
- 2056 **Faulkner, C., Akman, O.E., Bell, K., Jeffree, C., and Oparka, K.** (2008). Peeking into
2057 pit fields: a multiple twinning model of secondary plasmodesmata formation in
2058 tobacco. *Plant Cell* **20**, 1504-1518.
- 2059 **Feeney, M., Kittelmann, M., Menassa, R., Hawes, C., and Frigerio, L.** (2018). Protein
2060 Storage Vacuoles Originate from Remodeled Preexisting Vacuoles in Arabidopsis
2061 thaliana. *Plant Physiol* **177**, 241-254.
- 2062 **Feraru, E., Paciorek, T., Feraru, M.I., Zwiewka, M., De Groot, R., De Rycke, R.,**
2063 **Kleine-Vehn, J., and Friml, J.** (2010). The AP-3 beta Adaptin Mediates the
2064 Biogenesis and Function of Lytic Vacuoles in Arabidopsis. *Plant Cell* **22**, 2812-
2065 2824.
- 2066 **Fernandez-Calvino, L., Faulkner, C., Walshaw, J., Saalbach, G., Bayer, E., Benitez-**
2067 **Alfonso, Y., and Maule, A.** (2011). Arabidopsis plasmodesmal proteome. *PLoS*
2068 *One* **6**, e18880.
- 2069 **Fernandez-Santos, R., Izquierdo, Y., Lopez, A., Muniz, L., Martinez, M., Cascon, T.,**
2070 **Hamberg, M., and Castresana, C.** (2020). Protein Profiles of Lipid Droplets during
2071 the Hypersensitive Defense Response of Arabidopsis against Pseudomonas
2072 Infection. *Plant Cell Physiol* **61**, 1144-1157.

- 2073 **Findinier, J., Delevoye, C., and Cohen, M.M.** (2019). The dynamin-like protein Fzl
2074 promotes thylakoid fusion and resistance to light stress in *Chlamydomonas*
2075 *reinhardtii*. *PLoS Genetics* **15**, e1008047 - 1008030.
- 2076 **Finkemeier, I., and Schwarzlander, M.** (2018). Mitochondrial Regulation and Signalling
2077 in the Photosynthetic Cell: Principles and Concepts. *Annu Plant Rev* **50**, 185-225.
- 2078 **Floris, D., and Kuehlbrandt, W.** (2021). Molecular landscape of etioplast inner
2079 membranes in higher plants. *Nature Plants* **7**, 514-+.
- 2080 **Franceschi, V.R., Ding, B., and Lucas, W.J.** (1994). Mechanism of Plasmodesmata
2081 Formation in Characean Algae in Relation to Evolution of Intercellular
2082 Communication in Higher-Plants. *Planta* **192**, 347-358.
- 2083 **Francisco, R.D., and Martinoia, E.** (2018). The Vacuolar Transportome of Plant
2084 Specialized Metabolites. *Plant Cell Physiol* **59**, 1326-1336.
- 2085 **Franks, P.J., Buckley, T.N., Shope, J.C., and Mott, K.A.** (2001). Guard cell volume and
2086 pressure measured concurrently by confocal microscopy and the cell pressure
2087 probe. *Plant Physiol* **125**, 1577-1584.
- 2088 **Frick, E.M., and Strader, L.C.** (2018). Kinase MPK17 and the Peroxisome Division
2089 Factor PMD1 Influence Salt-induced Peroxisome Proliferation. *Plant Physiol* **176**,
2090 340-351.
- 2091 **Fuchs, M., van Bel, A.J.E., and Ehlers, K.** (2010). Season-associated modifications in
2092 symplasmic organization of the cambium in *Populus nigra*. *Annals of Botany* **105**,
2093 375-387.
- 2094 **Fuchs, P., Rugen, N., Carrie, C., Elsasser, M., Finkemeier, I., Giese, J., Hildebrandt,**
2095 **T.M., Kuhn, K., Maurino, V.G., Ruberti, C., Schallenberg-Rudinger, M.,**
2096 **Steinbeck, J., Braun, H.P., Eubel, H., Meyer, E.H., Muller-Schussele, S.J., and**
2097 **Schwarzlander, M.** (2020). Single organelle function and organization as
2098 estimated from *Arabidopsis* mitochondrial proteomics. *Plant J* **101**, 420-441.
- 2099 **Fujimoto, M., Arimura, S., Mano, S., Kondo, M., Saito, C., Ueda, T., Nakazono, M.,**
2100 **Nakano, A., Nishimura, M., and Tsutsumi, N.** (2009). *Arabidopsis* dynamin-
2101 related proteins DRP3A and DRP3B are functionally redundant in mitochondrial
2102 fission, but have distinct roles in peroxisomal fission. *Plant J* **58**, 388-400.

- 2103 **Fyfe, I., Schuh, A.L., Edwardson, J.M., and Audhya, A.** (2011). Association of the
2104 endosomal sorting complex ESCRT-II with the Vps20 subunit of ESCRT-III
2105 generates a curvature-sensitive complex capable of nucleating ESCRT-III
2106 filaments. *J Biol Chem* **286**, 34262-34270.
- 2107 **Gabaldon T** (2010) Peroxisome diversity and evolution. *Philos Trans R Soc Lond B Biol*
2108 *Sci* **365**: 765-773.
- 2109 **Gao, C., Luo, M., Zhao, Q., Yang, R., Cui, Y., Zeng, Y., Xia, J., and Jiang, L.** (2014). A
2110 unique plant ESCRT component, FREE1, regulates multivesicular body protein
2111 sorting and plant growth. *Curr Biol* **24**, 2556-2563.
- 2112 **Gao, H., Sage, T.L., and Osteryoung, K.W.** (2006). FZL, an FZO-like protein in plants,
2113 is a determinant of thylakoid and chloroplast morphology. *Proc Natl Acad Sci U S*
2114 *A* **103**, 6759-6764.
- 2115 **Gao, H., Metz, J., Teanby, N.A., Ward, A.D., Botchway, S.W., Coles, B., Pollard, M.R.,**
2116 **and Sparkes, I.** (2016). In Vivo Quantification of Peroxisome Tethering to
2117 Chloroplasts in Tobacco Epidermal Cells Using Optical Tweezers. *Plant Physiol*
2118 **170**, 263-272.
- 2119 **Gao, X.Q., Wang, X.L., Ren, F., Chen, J., and Wang, X.C.** (2009). Dynamics of vacuoles
2120 and actin filaments in guard cells and their roles in stomatal movement. *Plant Cell*
2121 *Environ* **32**, 1108-1116.
- 2122 **Gattolin, S., Sorieul, M., and Frigerio, L.** (2011). Mapping of tonoplast intrinsic proteins
2123 in maturing and germinating Arabidopsis seeds reveals dual localization of
2124 embryonic TIPs to the tonoplast and plasma membrane. *Mol Plant* **4**, 180-189.
- 2125 **Germain V, Rylott EL, Larson TR, Sherson SM, Bechtold N, Carde JP, Bryce JH,**
2126 **Graham IA, Smith SM** (2001) Requirement for 3-ketoacyl-CoA thiolase-2 in
2127 peroxisome development, fatty acid beta-oxidation and breakdown of
2128 triacylglycerol in lipid bodies of Arabidopsis seedlings. *Plant J* **28**: 1-12.
- 2129 **Giacomello, M., Pyakurel, A., Glytsou, C., and Scorrano, L.** (2020). The cell biology
2130 of mitochondrial membrane dynamics. *Nat Rev Mol Cell Biol* **21**, 204-224.
- 2131 **Gidda, S.K., Park, S., Pyc, M., Yurchenko, O., Cai, Y., Wu, P., Andrews, D.W.,**
2132 **Chapman, K.D., Dyer, J.M., and Mullen, R.T.** (2016). Lipid Droplet-Associated

2133 Proteins (LDAPs) Are Required for the Dynamic Regulation of Neutral Lipid
2134 Compartmentation in Plant Cells. *Plant Physiol* **170**, 2052-2071.

2135 **Giege, P., Heazlewood, J.L., Roessner-Tunali, U., Millar, A.H., Fernie, A.R., Leaver,**
2136 **C.J., and Sweetlove, L.J.** (2003). Enzymes of glycolysis are functionally
2137 associated with the mitochondrion in Arabidopsis cells. *Plant Cell* **15**, 2140-2151.

2138 **Gobert, A., Isayenkov, S., Voelker, C., Czempinski, K., and Maathuis, F.J.** (2007).
2139 The two-pore channel TPK1 gene encodes the vacuolar K⁺ conductance and
2140 plays a role in K⁺ homeostasis. *Proc Natl Acad Sci U S A* **104**, 10726-1073

2141 **Goodman, K., Paez-Valencia, J., Pennington, J., Sonntag, A., Ding, X., Lee, H.N.,**
2142 **Ahlquist, P.G., Molina, I., and Otegui, M.S.** (2021). ESCRT components ISTL1
2143 andLIP5 are required for tapetal function and pollen viability. *The Plant Cell*.

2144 **Goswami, R., Asnacios, A., Milani, P., Graindorge, S., Houlne, G., Mutterer, J.,**
2145 **Hamant, O., and Chaboute, M.E.** (2020). Mechanical Shielding in Plant Nuclei.
2146 *Current Biology* **30**, 2013-+.

2147 **Goto, C., Hara-Nishimura, I., and Tamura, K.** (2021). Regulation and Physiological
2148 Significance of the Nuclear Shape in Plants. *Front Plant Sci* **12**, 673905.

2149 **Goto, C., Tamura, K., Fukao, Y., Shimada, T., and Hara-Nishimura, I.** (2014). The
2150 Novel Nuclear Envelope Protein KAKU4 Modulates Nuclear Morphology in
2151 Arabidopsis. *Plant Cell* **26**, 2143-2155.

2152 **Goto, C., Hashizume, S., Fukao, Y., Hara-Nishimura, I., and Tamura, K.** (2019).
2153 Comprehensive nuclear proteome of Arabidopsis obtained by sequential
2154 extraction. *Nucleus* **10**, 81-92.

2155 **Graham, I.A.** (2008). Seed storage oil mobilization. *Annu Rev Plant Biol* **59**, 115-142.

2156 **Graham, J.W., Williams, T.C., Morgan, M., Fernie, A.R., Ratcliffe, R.G., and**
2157 **Sweetlove, L.J.** (2007). Glycolytic enzymes associate dynamically with
2158 mitochondria in response to respiratory demand and support substrate channeling.
2159 *Plant Cell* **19**, 3723-3738.

2160 **Greer, M.S., Cai, Y., Gidda, S.K., Esnay, N., Kretzschmar, F.K., Seay, D., McClinchie,**
2161 **E., Ischebeck, T., Mullen, R.T., Dyer, J.M., and Chapman, K.D.** (2020). SEIPIN
2162 Isoforms Interact with the Membrane-Tethering Protein VAP27-1 for Lipid Droplet
2163 Formation. *Plant Cell* **32**, 2932-2950.

- 2164 **Griffis, A.H., Groves, N.R., Zhou, X., and Meier, I.** (2014). Nuclei in motion: movement
2165 and positioning of plant nuclei in development, signaling, symbiosis, and disease.
2166 *Front Plant Sci* **5**, 129.
- 2167 **Grison, M.S., Brocard, L., Fouillen, L., Nicolas, W., Wewer, V., Dormann, P., Nacir,**
2168 **H., Benitez-Alfonso, Y., Claverol, S., Germain, V., Boute, Y., Mongrand, S.,**
2169 **and Bayer, E.M.** (2015). Specific Membrane Lipid Composition Is Important for
2170 Plasmodesmata Function in Arabidopsis. *Plant Cell* **27**, 1228-1250.
- 2171 **Grob, S., Schmid, M.W., and Grossniklaus, U.** (2014). Hi-C analysis in Arabidopsis
2172 identifies the KNOT, a structure with similarities to the flamenco locus of
2173 *Drosophila*. *Mol Cell* **55**, 678-693.
- 2174 **Groves, N.R., Biel, A.M., Newman-Griffis, A.H., and Meier, I.** (2018). Dynamic
2175 Changes in Plant Nuclear Organization in Response to Environmental and
2176 Developmental Signals. *Plant Physiol* **176**, 230-241.
- 2177 **Groves, N.R., Biel, A., Moser, M., Mendes, T., Amstutz, K., and Meier, I.** (2020).
2178 Recent advances in understanding the biological roles of the plant nuclear
2179 envelope. *Nucleus* **11**, 330-346.
- 2180 **Gu, Y.** (2018). The nuclear pore complex: a strategic platform for regulating cell signaling.
2181 *New Phytol* **219**, 25-30.
- 2182 **Gu, Y., and Dong, X.** (2015). Stromules: Signal Conduits for Plant Immunity. *Dev Cell*
2183 **34**, 3-4.
- 2184 **Gu, Y., Zebell, S.G., Liang, Z., Wang, S., Kang, B.-H., and Dong, X.** (2016). Nuclear
2185 Pore Permeabilization Is a Convergent Signaling Event in Effector-Triggered
2186 Immunity. *Cell* **166**, 1526 - 1538.e1511.
- 2187 **Guenoune-Gelbart, D., Elbaum, M., Sagi, G., Levy, A., and Epel, B.L.** (2008). Tobacco
2188 mosaic virus (TMV) replicase and movement protein function synergistically in
2189 facilitating TMV spread by lateral diffusion in the plasmodesmal desmotubule of
2190 *Nicotiana benthamiana*. *Mol Plant Microbe Interact* **21**, 335-345.
- 2191 **Gumber, H.K., McKenna, J.F., Tolmie, A.F., Jalovec, A.M., Kartick, A.C., Graumann,**
2192 **K., and Bass, H.W.** (2019). MLKS2 is an ARM domain and F-actin-associated
2193 KASH protein that functions in stomatal complex development and meiotic
2194 chromosome segregation. *Nucleus* **10**, 144-166.

- 2195 **Gupta, T.K., Klumpe, S., Gries, K., Heinz, S., Wietrzynski, W., Ohnishi, N., Niemeyer,**
2196 **J., Spaniol, B., Schaffer, M., Rast, A., Ostermeier, M., Strauss, M., Pitzko,**
2197 **J.M., Baumeister, W., Rudack, T., Sakamoto, W., Nickelsen, J., Schuller, J.M.,**
2198 **Schroda, M., and Engel, B.D.** (2021). Structural basis for VIPP1 oligomerization
2199 and maintenance of thylakoid membrane integrity. *Cell* **184**, 3643-3659 e3623.
- 2200 **Guseman, J.M., Lee, J.S., Bogenschutz, N.L., Peterson, K.M., Virata, R.E., Xie, B.,**
2201 **Kanaoka, M.M., Hong, Z., and Torii, K.U.** (2010). Dysregulation of cell-to-cell
2202 connectivity and stomatal patterning by loss-of-function mutation in *Arabidopsis*
2203 *chorus* (glucan synthase-like 8). *Development* **137**, 1731-1741.
- 2204 **Haas, T.J., Sliwinski, M.K., Martinez, D.E., Preuss, M., Ebine, K., Ueda, T., Nielsen,**
2205 **E., Odorizzi, G., and Otegui, M.S.** (2007). The *Arabidopsis* AAA ATPase SKD1
2206 is involved in multivesicular endosome function and interacts with its positive
2207 regulator LYST-INTERACTING PROTEIN5. *Plant Cell* **19**, 1295-1312.
- 2208 **Hamada, T., Ueda, H., Kawase, T., and Hara-Nishimura, I.** (2014). Microtubules
2209 contribute to tubule elongation and anchoring of endoplasmic reticulum, resulting
2210 in high network complexity in *Arabidopsis*. *Plant Physiol* **166**, 1869-1876.
- 2211 **Hanson, P.I., Roth, R., Lin, Y., and Heuser, J.E.** (2008). Plasma membrane deformation
2212 by circular arrays of ESCRT-III protein filaments. *J Cell Biol* **180**, 389-402.
- 2213 **Hara-Nishimura, I., and Hatsugai, N.** (2011). The role of vacuole in plant cell death. *Cell*
2214 *Death Differ* **18**, 1298-1304.
- 2215 **Haritatos, E., Medville, R., and Turgeon, R.** (2000). Minor vein structure and sugar
2216 transport in *Arabidopsis thaliana*. *Planta* **211**, 105-111.
- 2217 **Hayashi, Y., Hayashi, M., Hayashi, H., Hara-Nishimura, I., and Nishimura, M.** (2001).
2218 Direct interaction between glyoxysomes and lipid bodies in cotyledons of the
2219 *Arabidopsis thaliana* *ped1* mutant. *Protoplasma* **218**, 83-94.
- 2220 **Heinze, L., Freimuth, N., Rossling, A.K., Hahnke, R., Riebschlager, S., Frohlich, A.,**
2221 **Sampathkumar, A., McFarlane, H.E., and Sauer, M.** (2020). EPSIN1 and MTV1
2222 define functionally overlapping but molecularly distinct trans-Golgi network
2223 subdomains in *Arabidopsis*. *Proc Natl Acad Sci U S A* **117**, 25880-25889.
- 2224 **Hepworth, C., Wood, W.H.J., Emrich-Mills, T.Z., Proctor, M.S., Casson, S., and**
2225 **Johnson, M.P.** (2021). Dynamic thylakoid stacking and state transitions work

- 2226 synergistically to avoid acceptor-side limitation of photosystem I. *Nat Plants* **7**, 87-
2227 98.
- 2228 **Herger, A., Dunser, K., Kleine-Vehn, J., and Ringli, C.** (2019). Leucine-Rich Repeat
2229 Extensin Proteins and Their Role in Cell Wall Sensing. *Curr Biol* **29**, R851-R858.
- 2230 **Herman, E.M.** (2009). Seed Oil Body Ontogeny. *Microscopy and Microanalysis* **15**, 874-
2231 875.
- 2232 **Hillmer, S., Movafeghi, A., Robinson, D.G., and Hinz, G.** (2001). Vacuolar storage
2233 proteins are sorted in the cis-cisternae of the pea cotyledon Golgi apparatus. *J Cell*
2234 *Biol* **152**, 41-50.
- 2235 **Ho, C.M., Paciorek, T., Abrash, E., and Bergmann, D.C.** (2016). Modulators of Stomatal
2236 Lineage Signal Transduction Alter Membrane Contact Sites and Reveal
2237 Specialization among ERECTA Kinases. *Dev Cell* **38**, 345-357.
- 2238 **Hoffmann, N., King, S., Samuels, A.L., and McFarlane, H.E.** (2021). Subcellular
2239 coordination of plant cell wall synthesis. *Dev Cell* **56**, 933-948.
- 2240 **Hofte, H., Hubbard, L., Reizer, J., Ludevid, D., Herman, E.M., and Chrispeels, M.J.**
2241 (1992). Vegetative and Seed-Specific Forms of Tonoplast Intrinsic Protein in the
2242 Vacuolar Membrane of *Arabidopsis thaliana*. *Plant Physiol* **99**, 561-570.
- 2243 **Horn, P.J., James, C.N., Gidda, S.K., Kilaru, A., Dyer, J.M., Mullen, R.T., Ohlrogge,**
2244 **J.B., and Chapman, K.D.** (2013). Identification of a new class of lipid droplet-
2245 associated proteins in plants. *Plant Physiol* **162**, 1926-1936.
- 2246 **Hu, B., Wang, N., Bi, X., Karaaslan, E.S., Weber, A.L., Zhu, W., Berendzen, K.W., and**
2247 **Liu, C.** (2019). Plant lamin-like proteins mediate chromatin tethering at the nuclear
2248 periphery. *Genome Biol* **20**, 87.
- 2249 **Huang, A., Tang, Y., Shi, X., Jia, M., Zhu, J., Yan, X., Chen, H., and Gu, Y.** (2020).
2250 Proximity labeling proteomics reveals critical regulators for inner nuclear
2251 membrane protein degradation in plants. *Nat Commun* **11**, 3284.
- 2252 **Huang, A.H.C.** (2018). Plant Lipid Droplets and Their Associated Proteins: Potential for
2253 Rapid Advances. *Plant Physiology* **176**, 1894-1918.
- 2254 **Huang, S., Zhu, S., Kumar, P., and MacMicking, J.D.** (2021a). A phase-separated
2255 nuclear GBPL circuit controls immunity in plants. *Nature* **594**, 424-429.

- 2256 **Huang, S., Van Aken, O., Schwarzlander, M., Belt, K., and Millar, A.H.** (2016). The
2257 Roles of Mitochondrial Reactive Oxygen Species in Cellular Signaling and Stress
2258 Response in Plants. *Plant Physiol* **171**, 1551-1559.
- 2259 **Huang, X., Chen, S., Li, W., Tang, L., Zhang, Y., Yang, N., Zou, Y., Zhai, X., Xiao, N.,**
2260 **Liu, W., Li, P., and Xu, C.** (2021b). ROS regulated reversible protein phase
2261 separation synchronizes plant flowering. *Nat Chem Biol* **17**, 549-557.
- 2262 **Ingerman, E., Perkins, E.M., Marino, M., Mears, J.A., McCaffery, J.M., Hinshaw, J.E.,**
2263 **and Nunnari, J.** (2005). Dnm1 forms spirals that are structurally tailored to fit
2264 mitochondria. *Journal of Cell Biology* **170**, 1021-1027.
- 2265 **Ischebeck, T., Krawczyk, H.E., Mullen, R.T., Dyer, J.M., and Chapman, K.D.** (2020).
2266 Lipid droplets in plants and algae: Distribution, formation, turnover and function.
2267 *Seminars in Cell & Developmental Biology* **108**, 82-93.
- 2268 **Ishikawa, K., Tamura, K., Fukao, Y., and Shimada, T.** (2020). Structural and functional
2269 relationships between plasmodesmata and plant endoplasmic reticulum-plasma
2270 membrane contact sites consisting of three synaptotagmins. *New Phytologist* **226**,
2271 798-808.
- 2272 **Isner, J.C., Begum, A., Nuehse, T., Hetherington, A.M., and Maathuis, F.J.M.** (2018).
2273 KIN7 Kinase Regulates the Vacuolar TPK1 K(+) Channel during Stomatal Closure.
2274 *Curr Biol* **28**, 466-472 e464.
- 2275 **Iswanto, A.B.B., Shon, J.C., Liu, K.H., Vu, M.H., Kumar, R., and Kim, J.Y.** (2020).
2276 Sphingolipids Modulate Secretion of Glycosylphosphatidylinositol-Anchored
2277 Plasmodesmata Proteins and Callose Deposition. *Plant Physiol* **184**, 407-420.
- 2278 **Ito, Y., and Boutte, Y.** (2020). Differentiation of Trafficking Pathways at Golgi Entry Core
2279 Compartments and Post-Golgi Subdomains. *Front Plant Sci* **11**, 609516.
- 2280 **Ito, Y., Uemura, T., and Nakano, A.** (2014). Formation and maintenance of the Golgi
2281 apparatus in plant cells. *Int Rev Cell Mol Biol* **310**, 221-287.
- 2282 **Jaipargas, E.A., Barton, K.A., Mathur, N., and Mathur, J.** (2015). Mitochondrial
2283 pleomorphy in plant cells is driven by contiguous ER dynamics. *Frontiers in Plant*
2284 *Science* **6**.

- 2285 **Jaipargas, E.A., Mathur, N., Bou Daher, F., Wasteneys, G.O., and Mathur, J.** (2016).
2286 High Light Intensity Leads to Increased Peroxule-Mitochondria Interactions in
2287 Plants. *Front Cell Dev Biol* **4**, 6.
- 2288 **Jansen, L., Roberts, I., De Rycke, R., and Beeckman, T.** (2012). Phloem-associated
2289 auxin response maxima determine radial positioning of lateral roots in maize.
2290 *Philos Trans R Soc Lond B Biol Sci* **367**, 1525-1533.
- 2291 **Jung, J.H., Barbosa, A.D., Hutin, S., Kumita, J.R., Gao, M.J., Derwort, D., Silva, C.S.,
2292 Lai, X.L., Pierre, E., Geng, F., Kim, S.B., Baek, S., Zubieta, C., Jaeger, K.E.,
2293 and Wigge, P.A.** (2020). A prion-like domain in ELF3 functions as a thermosensor
2294 in *Arabidopsis*. *Nature* **585**, 256-260.
- 2295 **Kaiser, S., and Scheuring, D.** (2020). To Lead or to Follow: Contribution of the Plant
2296 Vacuole to Cell Growth. *Front Plant Sci* **11**, 553.
- 2297 **Kaiser, S., Eisa, A., Kleine-Vehn, J., and Scheuring, D.** (2019). NET4 Modulates the
2298 Compactness of Vacuoles in *Arabidopsis thaliana*. *Int J Mol Sci* **20**, 4752.
- 2299 **Kalinowska, K., Nagel, M.K., Goodman, K., Cuyas, L., Anzenberger, F., Alkofer, A.,
2300 Paz-Ares, J., Braun, P., Rubio, V., Otegui, M.S., and Isono, E.** (2015).
2301 *Arabidopsis* ALIX is required for the endosomal localization of the deubiquitinating
2302 enzyme AMSH3. *Proc Natl Acad Sci U S A* **112**, E5543-5551.
- 2303 **Kamiya, M., Higashio, S.-Y., Isomoto, A., Kim, J.-M., Seki, M., Miyashima, S., and
2304 Nakajima, K.** (2016). Control of root cap maturation and cell detachment by
2305 BEARSKIN transcription factors in *Arabidopsis*. *Development* (Cambridge,
2306 England) **143**, 4063 - 4072.
- 2307 **Kang, B.-H.** (2011). Shrinkage and fragmentation of the trans-Golgi network in non-
2308 meristematic plant cells. *Plant signaling & behavior* **6**, 884 - 886.
- 2309 **Kang, B.-H., Nielsen, E., Preuss, M.L., Mastrorarde, D., and Staehelin, L.A.** (2011).
2310 Electron Tomography of RabA4b- and PI-4K β 1-Labeled Trans Golgi Network
2311 Compartments in *Arabidopsis*. *Traffic* (Copenhagen, Denmark) **12**, 313 - 329.
- 2312 **Kang, B.H., and Staehelin, L.A.** (2008). ER-to-Golgi transport by COPII vesicles in
2313 *Arabidopsis* involves a ribosome-excluding scaffold that is transferred with the
2314 vesicles to the Golgi matrix. *Protoplasma* **234**, 51-64.

- 2315 **Kao, Y.T., Gonzalez, K.L., and Bartel, B.** (2018). Peroxisome Function, Biogenesis, and
2316 Dynamics in Plants. *Plant Physiol* **176**, 162-177.
- 2317 **Karaaslan, E.S., Wang, N., Faiss, N., Liang, Y., Montgomery, S.A., Laubinger, S.,**
2318 **Berendzen, K.W., Berger, F., Breuninger, H., and Liu, C.** (2020). Marchantia
2319 TCP transcription factor activity correlates with three-dimensional chromatin
2320 structure. *Nat Plants* **6**, 1250-1261.
- 2321 **Kato, T., Morita, M.T., and Tasaka, M.** (2002). Role of endodermal cell vacuoles in shoot
2322 gravitropism. *J Plant Growth Regul* **21**, 113-119
- 2323 **Kazama, T., Okuno, M., Watari, Y., Yanase, S., Koizuka, C., Tsuruta, Y., Sugaya, H.,**
2324 **Toyoda, A., Itoh, T., Tsutsumi, N., Toriyama, K., Koizuka, N., and Arimura, S.I.**
2325 (2019). Curing cytoplasmic male sterility via TALEN-mediated mitochondrial
2326 genome editing. *Nat Plants* **5**, 722-730.
- 2327 **Kim, E.Y., Park, K.Y., Seo, Y.S., and Kim, W.T.** (2016). Arabidopsis Small Rubber
2328 Particle Protein Homolog SRPs Play Dual Roles as Positive Factors for Tissue
2329 Growth and Development and in Drought Stress Responses. *Plant Physiology*
2330 **170**, 2494-2510.
- 2331 **Kim, J., Lee, H., Lee, H.N., Kim, S.H., Shin, K.D., and Chung, T.** (2013). Autophagy-
2332 related proteins are required for degradation of peroxisomes in Arabidopsis
2333 hypocotyls during seedling growth. *Plant Cell* **25**, 4956-4966.
- 2334 **Kimata, Y., Kato, T., Higaki, T., Kurihara, D., Yamada, T., Segami, S., Morita, M.T.,**
2335 **Maeshima, M., Hasezawa, S., Higashiyama, T., Tasaka, M., and Ueda, M.**
2336 (2019). Polar vacuolar distribution is essential for accurate asymmetric division of
2337 Arabidopsis zygotes. *Proc Natl Acad Sci U S A* **116**, 2338-2343.
- 2338 **Kirchhoff, H.** (2019). Chloroplast ultrastructure in plants. *New Phytol* **223**, 565-574.
- 2339 **Kirchhoff, H., Hall, C., Wood, M., Herbstova, M., Tsabari, O., Nevo, R., Charuvi, D.,**
2340 **Shimoni, E., and Reich, Z.** (2011). Dynamic control of protein diffusion within the
2341 granal thylakoid lumen. *Proceedings of the National Academy of Sciences of the*
2342 *United States of America* **108**, 20248-20253.
- 2343 **Klopfenstein, D.R., Klumperman, J., Lustig, A., Kammerer, R.A., Oorschot, V., and**
2344 **Hauri, H.P.** (2001). Subdomain-specific localization of CLIMP-63 (p63) in the

2345 endoplasmic reticulum is mediated by its luminal alpha-helical segment. *J Cell Biol*
2346 **153**, 1287-1300.

2347 **Knox, K., Wang, P., Kriechbaumer, V., Tilsner, J., Frigerio, L., Sparkes, I., Hawes,**
2348 **C., and Oparka, K.** (2015). Putting the Squeeze on Plasmodesmata: A Role for
2349 Reticulons in Primary Plasmodesmata Formation. *Plant Physiol* **168**, 1563-1572.

2350 **Korbei, B., Moulinier-Anzola, J., De-Araujo, L., Lucyshyn, D., Retzer, K., Khan, M.A.,**
2351 **and Luschig, C.** (2013). Arabidopsis TOL Proteins Act as Gatekeepers for
2352 Vacuolar Sorting of PIN2 Plasma Membrane Protein. *Current Biology* **23**, 2500-
2353 2505.

2354 **Kowalewska, Ł., Mazur, R., Suski, S., Garstka, M., and Mostowska, A.** (2016). Three-
2355 Dimensional Visualization of the Tubular-Lamellar Transformation of the Internal
2356 Plastid Membrane Network during Runner Bean Chloroplast Biogenesis. *THE*
2357 *PLANT CELL ONLINE* **28**, 875 - 891.

2358 **Kretschmar, F.K., Mengel, L.A., Muller, A.O., Schmitt, K., Biersch, K.F., Valerius,**
2359 **O., Braus, G.H., and Ischebeck, T.** (2018). PUX10 Is a Lipid Droplet-Localized
2360 Scaffold Protein That Interacts with CELL DIVISION CYCLE48 and Is Involved in
2361 the Degradation of Lipid Droplet Proteins. *Plant Cell* **30**, 2137-2160.

2362 **Kriechbaumer, V., Breeze, E., Pain, C., Tolmie, F., Frigerio, L., and Hawes, C.** (2018).
2363 Arabidopsis Lunapark proteins are involved in ER cisternae formation. *New Phytol*
2364 **219**, 990-1004.

2365 **Kriechbaumer, V., Botchway, S.W., Slade, S.E., Knox, K., Frigerio, L., Oparka, K.,**
2366 **and Hawes, C.** (2015). Reticulomics: Protein-Protein Interaction Studies with Two
2367 Plasmodesmata-Localized Reticulon Family Proteins Identify Binding Partners
2368 Enriched at Plasmodesmata, Endoplasmic Reticulum, and the Plasma Membrane.
2369 *Plant Physiol* **169**, 1933-1945.

2370 **Kriegel, A., Andres, Z., Medzihradszky, A., Kruger, F., Scholl, S., Delang, S., Patir-**
2371 **Nebioglu, M.G., Gute, G., Yang, H., Murphy, A.S., Peer, W.A., Pfeiffer, A.,**
2372 **Krebs, M., Lohmann, J.U., and Schumacher, K.** (2015). Job Sharing in the
2373 Endomembrane System: Vacuolar Acidification Requires the Combined Activity of
2374 V-ATPase and V-PPase. *Plant Cell* **27**, 3383-3396.

- 2375 **Kruger, F., and Schumacher, K.** (2018). Pumping up the volume - vacuole biogenesis
2376 in *Arabidopsis thaliana*. *Semin Cell Dev Biol* **80**, 106-112.
- 2377 **Kunzl, F., Fruholz, S., Fassler, F., Li, B., and Pimpl, P.** (2016). Receptor-mediated
2378 sorting of soluble vacuolar proteins ends at the trans-Golgi network/early
2379 endosome. *Nat Plants* **2**, 16017.
- 2380 **Lai, Y.S., Stefano, G., and Brandizzi, F.** (2014). ER stress signaling requires RHD3, a
2381 functionally conserved ER-shaping GTPase. *J Cell Sci* **127**, 3227-3232.
- 2382 **Lam, S.K., Siu, C.L., Hillmer, S., Jang, S., An, G., Robinson, D.G., and Jiang, L.**
2383 (2007). Rice SCAMP1 defines clathrin-coated, trans-golgi-located tubular-
2384 vesicular structures as an early endosome in tobacco BY-2 cells. *Plant Cell* **19**,
2385 296-319.
- 2386 **Latijnhouwers, M., Hawes, C., and Carvalho, C.** (2005). Holding it all together?
2387 Candidate proteins for the plant Golgi matrix. *Curr Opin Plant Biol* **8**, 632-639.
- 2388 **Lee, E., Vanneste, S., Perez-Sancho, J., Benitez-Fuente, F., Strelau, M., Macho, A.P.,**
2389 **Botella, M.A., Friml, J., and Rosado, A.** (2019). Ionic stress enhances ER-PM
2390 connectivity via phosphoinositide-associated SYT1 contact site expansion in
2391 *Arabidopsis*. *Proc Natl Acad Sci U S A* **116**, 1420-1429.
- 2392 **Lee, E., Santana, B.V.N., Samuels, E., Benitez-Fuente, F., Corsi, E., Botella, M.A.,**
2393 **Perez-Sancho, J., Vanneste, S., Friml, J., Macho, A., Azevedo, A.A., and**
2394 **Rosado, A.** (2020). Rare earth elements induce cytoskeleton-dependent and
2395 PI4P-associated rearrangement of SYT1/SYT5 endoplasmic reticulum-plasma
2396 membrane contact site complexes in *Arabidopsis*. *J Exp Bot* **71**, 3986-3998.
- 2397 **Levy, A., Erlanger, M., Rosenthal, M., and Epel, B.L.** (2007). A plasmodesmata-
2398 associated beta-1,3-glucanase in *Arabidopsis*. *Plant J* **49**, 669-682.
- 2399 **Li, T., Xiao, Z., Li, H., Liu, C., Shen, W., and Gao, C.** (2020). A Combinatorial Reporter
2400 Set to Visualize the Membrane Contact Sites Between Endoplasmic Reticulum and
2401 Other Organelles in Plant Cell. *Front Plant Sci* **11**, 1280.
- 2402 **Li, X., and Gu, Y.N.** (2020). Structural and functional insight into the nuclear pore complex
2403 and nuclear transport receptors in plant stress signaling. *Current Opinion in Plant*
2404 *Biology* **58**, 60-68.

- 2405 **Liang, Z., Zhu, N., Mai, K.K., Liu, Z., Tzeng, D., Osteryoung, K.W., Zhong, S.,**
2406 **Staelin, L.A., and Kang, B.H.** (2018a). Thylakoid-Bound Polysomes and a
2407 Dynamin-Related Protein, FZL, Mediate Critical Stages of the Linear Chloroplast
2408 Biogenesis Program in Greening Arabidopsis Cotyledons. *Plant Cell* **30**, 1476-
2409 1495.
- 2410 **Liang, Z., Zhu, N., Mai, K.K., Liu, Z., Liu, Z., Tzeng, D., Tzeng, D.T.W., Osteryoung,**
2411 **K.W., Zhong, S., Staelin, L.A., Staelin, A., and Kang, B.-H.** (2018b).
2412 Thylakoid-Bound Polysomes and a Dynamin-Related Protein, FZL, Mediate
2413 Critical Stages of the Linear Chloroplast Biogenesis Program in Greening
2414 Arabidopsis Cotyledons. *THE PLANT CELL ONLINE* **30**, 1476 - 1495.
- 2415 **Liese, S., Wenzel, E.M., Kjos, I., Rojas Molina, R., Schultz, S.W., Brech, A.,**
2416 **Stenmark, H., Raiborg, C., and Carlson, A.** (2020). Protein crowding mediates
2417 membrane remodeling in upstream ESCRT-induced formation of intraluminal
2418 vesicles. *Proc Natl Acad Sci U S A* **117**, 28614-28624.
- 2419 **Lindquist, E., and Aronsson, H.** (2018). Chloroplast vesicle transport. *Photosynth Res*
2420 **138**, 361-371.
- 2421 **Ling, Q.H., Huang, W.H., Baldwin, A., and Jarvis, P.** (2012). Chloroplast Biogenesis Is
2422 Regulated by Direct Action of the Ubiquitin-Proteasome System. *Science* **338**,
2423 655-659.
- 2424 **Lingard, M.J., Gidda, S.K., Bingham, S., Rothstein, S.J., Mullen, R.T., and Trelease,**
2425 **R.N.** (2008). Arabidopsis PEROXIN11c-e, FISSION1b, and DYNAMIN-RELATED
2426 PROTEIN3A cooperate in cell cycle-associated replication of peroxisomes. *Plant*
2427 *Cell* **20**, 1567-1585.
- 2428 **Liu, C., Cheng, Y.J., Wang, J.W., and Weigel, D.** (2017a). Prominent topologically
2429 associated domains differentiate global chromatin packing in rice from
2430 Arabidopsis. *Nat Plants* **3**, 742-748.
- 2431 **Liu, C., Mei, M., Li, Q., Roboti, P., Pang, Q., Ying, Z., Gao, F., Lowe, M., and Bao, S.**
2432 (2017b). Loss of the golgin GM130 causes Golgi disruption, Purkinje neuron loss,
2433 and ataxia in mice. *Proc Natl Acad Sci U S A* **114**, 346-351.
- 2434 **Liu, C., Zeng, Y., Li, H., Yang, C., Shen, W., Xu, M., Xiao, Z., Chen, T., Li, B., Cao, W.,**
2435 **Jiang, L., Otegui, M.S., and Gao, C.** (2021a). A plant-unique ESCRT component,

2436 FYVE4, regulates multivesicular endosome biogenesis and plant growth. *New*
2437 *Phytol* **231**, 193-209.

2438 **Liu, L.C., and Li, J.M.** (2019). Communications Between the Endoplasmic Reticulum and
2439 Other Organelles During Abiotic Stress Response in Plants. *Frontiers in Plant*
2440 *Science* **10**.

2441 **Liu, N.J., Zhang, T., Liu, Z.H., Chen, X., Guo, H.S., Ju, B.H., Zhang, Y.Y., Li, G.Z.,**
2442 **Zhou, Q.H., Qin, Y.M., and Zhu, Y.X.** (2020). Phytosphinganine Affects
2443 Plasmodesmata Permeability via Facilitating PDLP5-Stimulated Callose
2444 Accumulation in Arabidopsis. *Mol Plant* **13**, 128-143.

2445 **Liu, Q., Shi, L., and Fang, Y.** (2012). Dicing bodies. *Plant Physiol* **158**, 61-66.

2446 **Liu, Z., Gao, J., Cui, Y., Klumpe, S., Xiang, Y., Erdmann, P.S., and Jiang, L.** (2021b).
2447 Membrane imaging in the plant endomembrane system. *Plant Physiol* **185**, 562-
2448 576.

2449 **Lofke, C., Dunser, K., and Kleine-Vehn, J.** (2013). Epidermal patterning genes impose
2450 non-cell autonomous cell size determination and have additional roles in root
2451 meristem size control. *J Integr Plant Biol* **55**, 864-875.

2452 **Lofke, C., Dunser, K., Scheuring, D., and Kleine-Vehn, J.** (2015). Auxin regulates
2453 SNARE-dependent vacuolar morphology restricting cell size. *Elife* **4**. e05868.

2454 **Logan, D.C.** (2017). The dynamic chondriome. *ANNUAL PLANT REVIEWS* **50**, 67-109.

2455 **Logan, D.C., Scott, I., and Tobin, A.K.** (2003). The genetic control of plant mitochondrial
2456 morphology and dynamics. *Plant J* **36**, 500-509.

2457 **Lonsdale, D.M., Brears, T., Hodge, T.P., Melville, S.E., and Rottmann, W.H.** (1988).
2458 The Plant Mitochondrial Genome - Homologous Recombination as a Mechanism
2459 for Generating Heterogeneity. *Philos T Roy Soc B* **319**, 149-163.

2460 **Lu, J.H., Xu, Y., Wang, J.L., Singer, S.D., and Chen, G.Q.** (2020). The Role of
2461 Triacylglycerol in Plant Stress Response. *Plants-Basel* **9** (4):472.

2462 **udevid, D., Hofte, H., Himelblau, E., and Chrispeels, M.J.** (1992). The Expression
2463 Pattern of the Tonoplast Intrinsic Protein gamma-TIP in Arabidopsis thaliana Is
2464 Correlated with Cell Enlargement. *Plant Physiol* **100**, 1633-1639.

2465 **Lundquist, P.K., Shivaiah, K.K., and Espinoza-Corral, R.** (2020). Lipid droplets
2466 throughout the evolutionary tree. *Prog Lipid Res* **78**, 101029.

- 2467 **Ma, J., Liang, Z., Zhao, J., Wang, P., Ma, W., Mai, K.K., Fernandez Andrade, J.A.,**
2468 **Zeng, Y., Grujic, N., Jiang, L., Dagdas, Y., and Kang, B.H.** (2021). Friendly
2469 mediates membrane depolarization-induced mitophagy in Arabidopsis. *Current*
2470 *Biology* **31**, 1931-1944.
- 2471 **Madison, S.L., Buchanan, M.L., Glass, J.D., McClain, T.F., Park, E., and Nebenfuhr,**
2472 **A.** (2015). Class XI Myosins Move Specific Organelles in Pollen Tubes and Are
2473 Required for Normal Fertility and Pollen Tube Growth in Arabidopsis. *Plant Physiol*
2474 **169**, 1946-1960.
- 2475 **Makarova, K.S., Yutin, N., Bell, S.D., and Koonin, E.V.** (2010). Evolution of diverse cell
2476 division and vesicle formation systems in Archaea. *Nat Rev Microbiol* **8**, 731-741.
- 2477 **Makino, A., and Osmond, B.** (1991). Effects of Nitrogen Nutrition on Nitrogen
2478 Partitioning between Chloroplasts and Mitochondria in Pea and Wheat. *Plant*
2479 *Physiology* **96**, 355-362.
- 2480 **Marsh, B.J., Mastronarde, D.N., Buttle, K.F., Howell, K.E., and McIntosh, J.R.** (2001).
2481 Organellar relationships in the Golgi region of the pancreatic beta cell line, HIT-
2482 T15, visualized by high resolution electron tomography. *Proc Natl Acad Sci U S A*
2483 **98**, 2399-2406.
- 2484 **Martinoia, E.** (2018). Vacuolar Transporters - Companions on a Longtime Journey. *Plant*
2485 *Physiol* **176**, 1384-1407.
- 2486 **Martinoia, E., Meyer, S., De Angeli, A., and Nagy, R.** (2012). Vacuolar Transporters in
2487 Their Physiological Context. *Annu Rev Plant Biol* **63**, 183-213.
- 2488 **Marty, F.** (1999). Plant vacuoles. *Plant Cell* **11**, 587-600.
- 2489 **Mathur, J.** (2021). Organelle extensions in plant cells. *Plant Physiol* **185**, 593-607.
- 2490 **Matsumoto, H., Kimata, Y, Higaki, T, Higashiyama, T, Ueda, M.** (2021) Dynamic
2491 Rearrangement and Directional Migration of Tubular Vacuoles are Required for
2492 the Asymmetric Division of the Arabidopsis Zygote. *Plant Cell Physiol* doi:
2493 10.1093/pcp/pcab075
- 2494 **McCullough, J., Colf, L.A., and Sundquist, W.I.** (2013). Membrane fission reactions of
2495 the mammalian ESCRT pathway. *Annu Rev Biochem* **82**, 663-692.

- 2496 **McFarlane, H.E., Lee, E.K., van Bezouwen, L.S., Ross, B., Rosado, A., and Samuels,**
2497 **A.L.** (2017). Multiscale Structural Analysis of Plant ER-PM Contact Sites. *Plant*
2498 *Cell Physiol* **58**, 478-484.
- 2499 **McFarlane, H.E., Mutwil-Anderwald, D., Verbancic, J., Picard, K.L., Gookin, T.E.,**
2500 **Froehlich, A., Chakravorty, D., Trindade, L.M., Alonso, J.M., Assmann, S.M.,**
2501 **and Persson, S.** (2021). A G protein-coupled receptor-like module regulates
2502 cellulose synthase secretion from the endomembrane system in Arabidopsis. *Dev*
2503 *Cell* **56**, 1484-1497 e1487.
- 2504 **McKenna, J.F., Gumber, H.K., Turpin, Z.M., Jalovec, A.M., Kartick, A.C., Graumann,**
2505 **K., and Bass, H.W.** (2021). Maize (*Zea mays* L.) Nucleoskeletal Proteins Regulate
2506 Nuclear Envelope Remodeling and Function in Stomatal Complex Development
2507 and Pollen Viability. *Frontiers in Plant Science* **12**.
- 2508 **McNew, J.A., Sondermann, H., Lee, T., Stern, M., and Brandizzi, F.** (2013). GTP-
2509 dependent membrane fusion. *Annu Rev Cell Dev Biol* **29**, 529-550.
- 2510 **Mechela, A., Schwenkert, S., and Soll, J.** (2019). A brief history of thylakoid biogenesis.
2511 *Open Biol* **9**.
- 2512 **Meents, M.J., Motani, S., Mansfield, S.D., and Samuels, A.L.** (2019). Organization of
2513 Xylan Production in the Golgi During Secondary Cell Wall Biosynthesis. *Plant*
2514 *Physiology* **181**, 527-546.
- 2515 **Meier, I., Richards, E.J., and Evans, D.E.** (2017). Cell Biology of the Plant Nucleus.
2516 *Annual Review of Plant Biology*, Vol 68 **68**, 139-172.
- 2517 **Meier, I., Griffis, A.H., Groves, N.R., and Wagner, A.** (2016). Regulation of nuclear
2518 shape and size in plants. *Curr Opin Cell Biol* **40**, 114-123.
- 2519 **Merkulova, E.A., Guiboileau, A., Naya, L., Masclaux-Daubresse, C., and Yoshimoto,**
2520 **K.** (2014). Assessment and Optimization of Autophagy Monitoring Methods in
2521 Arabidopsis Roots Indicate Direct Fusion of Autophagosomes with Vacuoles. *Plant*
2522 *Cell Physiol* **55**, 715-726.
- 2523 **Mikulski, P., Hohenstatt, M.L., Farrona, S., Smaczniak, C., Stahl, Y., Kalyanikrishna,**
2524 **Kaufmann, K., Angenent, G., and Schubert, D.** (2019). The Chromatin-
2525 Associated Protein PWO1 Interacts with Plant Nuclear Lamin-like Components to
2526 Regulate Nuclear Size. *Plant Cell* **31**, 1141-1154.

- 2527 **Miquel, M., Trigui, G., d'Andrea, S., Kelemen, Z., Baud, S., Berger, A., Deruyffelaere,**
2528 **C., Trubuil, A., Lepiniec, L., and Dubreucq, B.** (2014). Specialization of oleosins
2529 in oil body dynamics during seed development in Arabidopsis seeds. *Plant Physiol*
2530 **164**, 1866-1878.
- 2531 **Mitsuya, S., El-Shami, M., Sparkes, I.A., Charlton, W.L., Lousa Cde, M., Johnson, B.,**
2532 **and Baker, A.** (2010). Salt stress causes peroxisome proliferation, but inducing
2533 peroxisome proliferation does not improve NaCl tolerance in Arabidopsis thaliana.
2534 *PLoS One* **5**, e9408.
- 2535 **Moller, I.M.** (2016). What is hot in plant mitochondria? *Physiologia Plantarum* **157**, 256-
2536 263.
- 2537 **Mosalaganti, S., Kosinski, J., Albert, S., Schaffer, M., Strenkert, D., Salome, P.A.,**
2538 **Merchant, S.S., Plitzko, J.M., Baumeister, W., Engel, B.D., and Beck, M.**
2539 (2018). In situ architecture of the algal nuclear pore complex. *Nat Commun* **9**,
2540 2361.
- 2541 **Moser, M., Kirkpatrick, A., Groves, N.R., and Meier, I.** (2020). LINC-complex mediated
2542 positioning of the vegetative nucleus is involved in calcium and ROS signaling in
2543 Arabidopsis pollen tubes. *Nucleus* **11**, 149-163.
- 2544 **Moulinier-Anzola, J., Schwihla, M., De-Araujo, L., Artner, C., Jorg, L.,**
2545 **Konstantinova, N., Luschnig, C., and Korbei, B.** (2020). TOLs Function as
2546 Ubiquitin Receptors in the Early Steps of the ESCRT Pathway in Higher Plants.
2547 *Molecular Plant* **13**, 717-731.
- 2548 **Muller, A.O., Blersch, K.F., Gippert, A.L., and Ischebeck, T.** (2017). Tobacco pollen
2549 tubes - a fast and easy tool for studying lipid droplet association of plant proteins.
2550 *Plant J* **89**, 1055-1064.
- 2551 **Nagaoka, N., Yamashita, A., Kurisu, R., Watari, Y., Ishizuna, F., Tsutsumi, N.,**
2552 **Ishizaki, K., Kohchi, T., and Arimura, S.I.** (2017). DRP3 and ELM1 are required
2553 for mitochondrial fission in the liverwort *Marchantia polymorpha*. *Sci Rep* **7**, 4600.
- 2554 **Nakamura, S., Hagihara, S., Otomo, K., Ishida, H., Hidema, J., Nemoto, T., and Izumi,**
2555 **M.** (2021). Autophagy Contributes to the Quality Control of Leaf Mitochondria.
2556 *Plant Cell Physiol* **62**, 229-247.

- 2557 **Nakano, R.T., Matsushima, R., Ueda, H., Tamura, K., Shimada, T., Li, L., Hayashi, Y.,**
2558 **Kondo, M., Nishimura, M., and Hara-Nishimura, I.** (2009). GNOM-
2559 LIKE1/ERMO1 and SEC24a/ERMO2 are required for maintenance of endoplasmic
2560 reticulum morphology in *Arabidopsis thaliana*. *Plant Cell* **21**, 3672-3685.
- 2561 **Ndinyanka Fabrice, T., Kaech, A., Barmettler, G., Eichenberger, C., Knox, J.P.,**
2562 **Grossniklaus, U., and Ringli, C.** (2017). Efficient preparation of *Arabidopsis*
2563 pollen tubes for ultrastructural analysis using chemical and cryo-fixation. *BMC*
2564 *Plant Biol* **17**, 176.
- 2565 **Nebenfuhr, A., and Staehelin, L.A.** (2001). Mobile factories: Golgi dynamics in plant
2566 cells. *Trends Plant Sci* **6**, 160-167.
- 2567 **Nebenfuhr, A., Frohlick, J.A., and Staehelin, L.A.** (2000). Redistribution of Golgi stacks
2568 and other organelles during mitosis and cytokinesis in plant cells. *Plant Physiol*
2569 **124**, 135-151.
- 2570 **Nebenfuhr, A., Gallagher, L.A., Dunahay, T.G., and Mazurkiewicz, A.M.** (1999). Stop-
2571 and-go movements of plant Golgi stacks are mediated by the acto-myosin system.
2572 *PLANT PHYSIOLOGY* **121**, 1127 - 1142.
- 2573 **Newman-Griffis, A.H., Del Cerro, P., Charpentier, M., and Meier, I.** (2019). Medicago
2574 LINC Complexes Function in Nuclear Morphology, Nuclear Movement, and Root
2575 Nodule Symbiosis. *Plant Physiol* **179**, 491-506.
- 2576 **Nicolas, W.J., Grison, M.S., Tréput, S., Gaston, A., Fouché, M., Cordelières, F.P.,**
2577 **Oparka, K., Tilsner, J., Brocard, L., and Bayer, E.M.** (2017a). Architecture and
2578 permeability of post-cytokinesis plasmodesmata lacking cytoplasmic sleeves.
2579 *Nature Plants* **3**, 1 - 11.
- 2580 **Nicolas, W.J., Grison, M.S., Trepout, S., Gaston, A., Fouche, M., Cordelieres, F.P.,**
2581 **Oparka, K., Tilsner, J., Brocard, L., and Bayer, E.M.** (2017b). Architecture and
2582 permeability of post-cytokinesis plasmodesmata lacking cytoplasmic sleeves. *Nat*
2583 *Plants* **3**, 17082.
- 2584 **Niemes, S., Langhans, M., Viotti, C., Scheuring, D., Yan, M.S.W., Jiang, L.W.,**
2585 **Hillmer, S., Robinson, D.G., and Pimpl, P.** (2010). Retromer recycles vacuolar
2586 sorting receptors from the trans-Golgi network. *Plant Journal* **61**, 107-121.

- 2587 **Nixon, B.T., Mansouri, K., Singh, A., Du, J., Davis, J.K., Lee, J.G., Slabaugh, E.,**
2588 **Vandavasi, V.G., O'Neill, H., Roberts, E.M., Roberts, A.W., Yingling, Y.G., and**
2589 **Haigler, C.H.** (2016). Comparative Structural and Computational Analysis
2590 Supports Eighteen Cellulose Synthases in the Plant Cellulose Synthesis Complex.
2591 *Sci Rep* **6**, 28696.
- 2592 **Nixon-Abell, J., Obara, C.J., Weigel, A.V., Li, D., Legant, W.R., Xu, C.S., Pasolli, H.A.,**
2593 **Harvey, K., Hess, H.F., Betzig, E., Blackstone, C., and Lippincott-Schwartz, J.**
2594 (2016). Increased spatiotemporal resolution reveals highly dynamic dense tubular
2595 matrices in the peripheral ER. *Science* **354**.
- 2596 **Noack, L.C., and Jaillais, Y.** (2020). Functions of Anionic Lipids in Plants. *Annual Review*
2597 *of Plant Biology*, Vol 71, 2020 **71**, 71-102.
- 2598 **Noguchi, K., and Yoshida, K.** (2008). Interaction between photosynthesis and
2599 respiration in illuminated leaves. *Mitochondrion* **8**, 87-99.
- 2600 **Obro, J., Hayashi, T., and Mikkelsen, J.D.** (2011). Enzymatic Modification of Plant Cell
2601 Wall Polysaccharides. *Plant Polysaccharides, Biosynthesis and Bioengineering*
2602 **41**, 367-387.
- 2603 **Oikawa, K., Hayashi, M., Hayashi, Y., and Nishimura, M.** (2019). Re-evaluation of
2604 physical interaction between plant peroxisomes and other organelles using live-
2605 cell imaging techniques. *Journal of Integrative Plant Biology* **61**, 836-852.
- 2606 **Oikawa, K., Imai, T., Thagun, C., Toyooka, K., Yoshizumi, T., Ishikawa, K., Kodama,**
2607 **Y., and Numata, K.** (2021). Mitochondrial movement during its association with
2608 chloroplasts in *Arabidopsis thaliana*. *Commun Biol* **4**, 292.
- 2609 **Oikawa, K., Matsunaga, S., Mano, S., Kondo, M., Yamada, K., Hayashi, M., Kagawa,**
2610 **T., Kadota, A., Sakamoto, W., Higashi, S., Watanabe, M., Mitsui, T.,**
2611 **Shigemasa, A., Iino, T., Hosokawa, Y., and Nishimura, M.** (2015). Physical
2612 interaction between peroxisomes and chloroplasts elucidated by in situ laser
2613 analysis (vol 1, 15035, 2015). *Nature Plants* **1**.
- 2614 **Okamoto, K., and Shaw, J.M.** (2005). Mitochondrial morphology and dynamics in yeast
2615 and multicellular eukaryotes. *Annu Rev Genet* **39**, 503-536.
- 2616 **Onishi, M., Yamano, K., Sato, M., Matsuda, N., and Okamoto, K.** (2021). Molecular
2617 mechanisms and physiological functions of mitophagy. *EMBO J* **40**, e104705.

- 2618 **Oparka, K.J., Roberts, A.G., Boevink, P., Cruz, S.S., Roberts, I., Pradel, K.S., Imlau,**
2619 **A., Kotlizky, G., Sauer, N., and Epel, B.** (1999). Simple, but Not Branched,
2620 Plasmodesmata Allow the Nonspecific Trafficking of Proteins in Developing
2621 Tobacco Leaves. *Cell* **97**, 743-754.
- 2622 **Orth T, Reumann S, Zhang X, Fan J, Wenzel D, Quan S, Hu J** (2007) The PEROXIN11
2623 protein family controls peroxisome proliferation in Arabidopsis. *Plant Cell* **19**: 333-
2624 350
- 2625 **Osterrieder, A., Sparkes, I.A., Botchway, S.W., Ward, A., Ketelaar, T., de Ruijter, N.,**
2626 **and Hawes, C.** (2017). Stacks off tracks: a role for the golgin AtCASP in plant
2627 endoplasmic reticulum-Golgi apparatus tethering. *J Exp Bot* **68**, 3339-3350.
- 2628 **Osteryoung, K.W., and Pyke, K.A.** (2014). Division and Dynamic Morphology of
2629 Plastids. *Annual Review of Plant Biology*, Vol 65 **65**, 443-472.
- 2630 **Otegui, M.S., and Pennington, J.G.** (2018). Electron tomography in plant cell biology.
2631 *Microscopy (Oxford, England)* **68**, 69 - 79.
- 2632 **Otegui, M.S., Noh, Y.S., Martinez, D.E., Vila Petroff, M.G., Andrew Staehelin, L.,**
2633 **Amasino, R.M., and Guamet, J.J.** (2005). Senescence-associated vacuoles with
2634 intense proteolytic activity develop in leaves of Arabidopsis and soybean. *Plant J*
2635 **41**, 831-844.
- 2636 **Otera, H., Wang, C., Cleland, M.M., Setoguchi, K., Yokota, S., Youle, R.J., and**
2637 **Mihara, K.** (2010). Mff is an essential factor for mitochondrial recruitment of Drp1
2638 during mitochondrial fission in mammalian cells. *J Cell Biol* **191**, 1141-1158.
- 2639 **Owens, T., and Poole, R.J.** (1979). Regulation of Cytoplasmic and Vacuolar Volumes by
2640 Plant-Cells in Suspension Culture. *Plant Physiol* **64**, 900-904.
- 2641 **Pain, C., Kriechbaumer, V., Kittelmann, M., Hawes, C., and Fricker, M.** (2019).
2642 Quantitative analysis of plant ER architecture and dynamics. *Nat Commun* **10**, 984.
- 2643 **Pan, R.H., Liu, J., Wang, S.S., and Hu, J.P.** (2020). Peroxisomes: versatile organelles
2644 with diverse roles in plants. *New Phytologist* **225**, 1410-1427.
- 2645 **Parsons, H.T., Stevens, T.J., McFarlane, H.E., Vidal-Melgosa, S., Griss, J.,**
2646 **Lawrence, N., Butler, R., Sousa, M.M.L., Salemi, M., Willats, W.G.T., Petzold,**
2647 **C.J., Heazlewood, J.L., and Lilley, K.S.** (2019). Separating Golgi Proteins from

2648 Cis to Trans Reveals Underlying Properties of Cisternal Localization. *Plant Cell* **31**,
2649 2010-2034.

2650 **Pastor-Cantizano, N., Ko, D.K., Angelos, E., Pu, Y., and Brandizzi, F.** (2020).
2651 Functional Diversification of ER Stress Responses in Arabidopsis. *Trends*
2652 *Biochem Sci* **45**, 123-136.

2653 **Paszkiwicz, G., Gualberto, J.M., Benamar, A., Macherel, D., and Logan, D.C.** (2017).
2654 Arabidopsis Seed Mitochondria Are Bioenergetically Active Immediately upon
2655 Imbibition and Specialize via Biogenesis in Preparation for Autotrophic Growth.
2656 *Plant Cell* **29**, 109-128.

2657 **Pawar, V., Poulet, A., Detourne, G., Tatout, C., Vanrobays, E., Evans, D.E., and**
2658 **Graumann, K.** (2016). A novel family of plant nuclear envelope-associated
2659 proteins. *J Exp Bot* **67**, 5699-5710.

2660 **Peremyslov, V.V., Prokhnevsky, A.I., and Dolja, V.V.** (2010). Class XI myosins are
2661 required for development, cell expansion, and F-Actin organization in Arabidopsis.
2662 *Plant Cell* **22**, 1883-1897.

2663 **Perez-Lara, A., and Jahn, R.** (2015). Extended synaptotagmins (E-Syts): Architecture
2664 and dynamics of membrane contact sites revealed. *Proc Natl Acad Sci U S A* **112**,
2665 4837-4838.

2666 **Perez-Sancho, J., Tilsner, J., Samuels, A.L., Botella, M.A., Bayer, E.M., and Rosado,**
2667 **A.** (2016). Stitching Organelles: Organization and Function of Specialized
2668 Membrane Contact Sites in Plants. *Trends Cell Biol* **26**, 705-717.

2669 **Perez-Sancho, J., Vanneste, S., Lee, E., McFarlane, H.E., del Valle, A.E., Valpuesta,**
2670 **V., Friml, J., Botella, M.A., and Rosado, A.** (2015). The Arabidopsis
2671 Synaptotagmin1 Is Enriched in Endoplasmic Reticulum-Plasma Membrane
2672 Contact Sites and Confers Cellular Resistance to Mechanical Stresses. *Plant*
2673 *Physiology* **168**, 132-U837.

2674 **Petit, J.D., Immel, F., Lins, L., and Bayer, E.M.** (2019). Lipids or Proteins: Who Is
2675 Leading the Dance at Membrane Contact Sites? *Frontiers in Plant Science* **10**.

2676 **Petit, J.D., Li, Z.P., Nicolas, W.J., Grison, M.S., and Bayer, E.M.** (2020). Dare to
2677 change, the dynamics behind plasmodesmata-mediated cell-to-cell
2678 communication. *Curr Opin Plant Biol* **53**, 80-89.

- 2679 **Phillips, A.R., Suttangkakul, A., and Vierstra, R.D.** (2008). The ATG12-conjugating
2680 enzyme ATG10 is essential for autophagic vesicle formation in *Arabidopsis*
2681 *thaliana*. *Genetics* **178**, 1339-1353.
- 2682 **Pietrowska-Borek, M., Dobrogojski, J., Sobieszczuk-Nowicka, E., and Borek, S.**
2683 (2020). New Insight into Plant Signaling: Extracellular ATP and Uncommon
2684 Nucleotides. *Cells* **9**.
- 2685 **Platre, M.P., Noack, L.C., Doumane, M., Bayle, V., Simon, M.L.A., Maneta-Peyret, L.,**
2686 **Fouillen, L., Stanislas, T., Armengot, L., Pejchar, P., Caillaud, M.C., Potocky,**
2687 **M., Copic, A., Moreau, P., and Jaillais, Y.** (2018). A Combinatorial Lipid Code
2688 Shapes the Electrostatic Landscape of Plant Endomembranes. *Dev Cell* **45**, 465-
2689 480 e411.
- 2690 **Plett, A., Charton, L., and Linka, N.** (2020). Peroxisomal Cofactor Transport.
2691 *Biomolecules* **10**.
- 2692 **Pontvianne, F., Carpentier, M.C., Durut, N., Pavlistova, V., Jaske, K., Schorova, S.,**
2693 **Parrinello, H., Rohmer, M., Pikaard, C.S., Fojtova, M., Fajkus, J., and Saez-**
2694 **Vasquez, J.** (2016). Identification of Nucleolus-Associated Chromatin Domains
2695 Reveals a Role for the Nucleolus in 3D Organization of the *A. thaliana* Genome.
2696 *Cell Rep* **16**, 1574-1587.
- 2697 **Powers, S.K., Holehouse, A.S., Korasick, D.A., Schreiber, K.H., Clark, N.M., Jing, H.,**
2698 **Emenecker, R., Han, S., Tycksen, E., Hwang, I., Sozzani, R., Jez, J.M., Pappu,**
2699 **R.V., and Strader, L.C.** (2019). Nucleo-cytoplasmic Partitioning of ARF Proteins
2700 Controls Auxin Responses in *Arabidopsis thaliana*. *Mol Cell* **76**, 177-190 e175.
- 2701 **Preuten, T., Cincu, E., Fuchs, J., Zoschke, R., Liere, K., and Borner, T.** (2010). Fewer
2702 genes than organelles: extremely low and variable gene copy numbers in
2703 mitochondria of somatic plant cells. *Plant Journal* **64**, 948-959.
- 2704 **Pulschen, A.A., Mutavchiev, D.R., Culley, S., Sebastian, K.N., Roubinet, J.,**
2705 **Roubinet, M., Risa, G.T., van Wolferen, M., Roubinet, C., Schmidt, U., Dey, G.,**
2706 **Albers, S.V., Henriques, R., and Baum, B.** (2020). Live Imaging of a
2707 Hyperthermophilic Archaeon Reveals Distinct Roles for Two ESCRT-III Homologs
2708 in Ensuring a Robust and Symmetric Division. *Curr Biol* **30**, 2852-2859 e2854.

- 2709 **Puthiyaveetil, S., Tsabari, O., Lowry, T., Lenhert, S., Lewis, R.R., Reich, Z., and**
2710 **Kirchhoff, H.** (2014). Compartmentalization of the protein repair machinery in
2711 photosynthetic membranes. *Proceedings of the National Academy of Sciences of*
2712 *the United States of America* **111**, 15839-15844.
- 2713 **Pyc, M., Cai, Y., Greer, M.S., Yurchenko, O., Chapman, K.D., Dyer, J.M., and Mullen,**
2714 **R.T.** (2017a). Turning Over a New Leaf in Lipid Droplet Biology. *Trends Plant Sci*
2715 **22**, 596-609.
- 2716 **Pyc, M., Cai, Y., Gidda, S.K., Yurchenko, O., Park, S., Kretschmar, F.K., Ischebeck,**
2717 **T., Valerius, O., Braus, G.H., Chapman, K.D., Dyer, J.M., and Mullen, R.T.**
2718 (2017b). Arabidopsis lipid droplet-associated protein (LDAP) - interacting protein
2719 (LDIP) influences lipid droplet size and neutral lipid homeostasis in both leaves
2720 and seeds. *Plant J* **92**, 1182-1201.
- 2721 **Pyc M, Gidda SK, Seay D, Esnay N, Kretschmar FK, Cai Y, Doner NM, Greer MS,**
2722 **Hull JJ, Coulon D, Br  h  lin C, Yurchenko O, de Vries J, Valerius O, Braus**
2723 **GH, Ischebeck T, Chapman KD, Dyer JM, Mullen RT.** (2021) LDIP Cooperates
2724 with SEIPIN and LDAP to Facilitate Lipid Droplet Biogenesis in Arabidopsis. *Plant*
2725 *Cell*. doi: 10.1093/plcell/koab179.
- 2726 **Quan, S., Yang, P., Cassin-Ross, G., Kaur, N., Switzenberg, R., Aung, K., Li, J., and**
2727 **Hu, J.** (2013). Proteome analysis of peroxisomes from etiolated Arabidopsis
2728 seedlings identifies a peroxisomal protease involved in beta-oxidation and
2729 development. *Plant Physiol* **163**, 1518-1538.
- 2730 **Raffaele, S., Bayer, E., Lafarge, D., Cluzet, S., German Retana, S., Boubekeur, T.,**
2731 **Leborgne-Castel, N., Carde, J.P., Lherminier, J., Noiro, E., Satiat-**
2732 **Jeunemaitre, B., Laroche-Traineau, J., Moreau, P., Ott, T., Maule, A.J.,**
2733 **Reymond, P., Simon-Plas, F., Farmer, E.E., Bessoule, J.J., and Mongrand, S.**
2734 (2009). Remorin, a solanaceae protein resident in membrane rafts and
2735 plasmodesmata, impairs potato virus X movement. *Plant Cell* **21**, 1541-1555.
- 2736 **Ramakrishna, P., and Barberon, M.** (2019). Polarized transport across root epithelia.
2737 *Current Opinion in Plant Biology* **52**, 23-29.
- 2738 **Renna, L., Stefano, G., Slabaugh, E., Wormsbaecher, C., Sulpizio, A., Zienkiewicz,**
2739 **K., and Brandizzi, F.** (2018). TGNap1 is required for microtubule-dependent

2740 homeostasis of a subpopulation of the plant trans-Golgi network. *Nature*
2741 *Communications* **9**.

2742 **Reumann, S., and Chowdhary, G.** (2018). Prediction of Peroxisomal Matrix Proteins in
2743 Plants. *Subcell Biochem* **89**, 125-138.

2744 **Reyes, F.C., Buono, R.A., Roschzttardtz, H., Di Rubbo, S., Yeun, L.H., Russinova,**
2745 **E., and Otegui, M.S.** (2014). A novel endosomal sorting complex required for
2746 transport (ESCRT) component in *Arabidopsis thaliana* controls cell expansion and
2747 development. *J Biol Chem* **289**, 4980-4988.

2748 **Ridge, R.W., Uozumi, Y., Plazinski, J., Hurley, U.A., and Williamson, R.E.** (1999).
2749 Developmental transitions and dynamics of the cortical ER of *Arabidopsis* cells
2750 seen with green fluorescent protein. *Plant Cell Physiol* **40**, 1253-1261.

2751 **Rinaldi, M.A., Patel, A.B., Park, J., Lee, K., Strader, L.C., and Bartel, B.** (2016). The
2752 Roles of beta-Oxidation and Cofactor Homeostasis in Peroxisome Distribution and
2753 Function in *Arabidopsis thaliana*. *Genetics* **204**, 1089-1115.

2754 **Roberts, I.M., Boevink, P., Roberts, A.G., Sauer, N., Reichel, C., and Oparka, K.J.**
2755 (2001). Dynamic changes in the frequency and architecture of plasmodesmata
2756 during the sink-source transition in tobacco leaves. *Protoplasma* **218**, 31-44.

2757 **Robinson, D.G.** (2020). Plant Golgi ultrastructure. *J Microsc* **280**, 111-121.

2758 **Rodriguez-Serrano, M., Romero-Puertas, M.C., Sanz-Fernandez, M., Hu, J., and**
2759 **Sandalio, L.M.** (2016). Peroxisomes Extend Peroxules in a Fast Response to
2760 Stress via a Reactive Oxygen Species-Mediated Induction of the Peroxin PEX11a.
2761 *Plant Physiol* **171**, 1665-1674.

2762 **Rojo, E., Gillmor, C.S., Kovaleva, V., Somerville, C.R., and Raikhel, N.V.** (2001).
2763 VACUOLELESS1 is an essential gene required for vacuole formation and
2764 morphogenesis in *Arabidopsis*. *Dev Cell* **1**, 303-310.

2765 **Rosado, A., and Bayer, E.M.** (2021). Geometry and cellular function of organelle
2766 membrane interfaces. *Plant Physiol* **185**, 650-662.

2767 **Rose, R.J., and McCurdy, D.W.** (2017). New Beginnings: Mitochondrial Renewal by
2768 Massive Mitochondrial Fusion. *Trends Plant Sci* **22**, 641-643.

2769 **Rosquete, M.R., Davis, D.J., and Drakakaki, G.** (2018). The Plant Trans-Golgi Network:
2770 Not Just a Matter of Distinction. *Plant Physiol* **176**, 187-198.

- 2771 **Rosquete, M.R., Worden, N., Ren, G., Sinclair, R.M., Pflieger, S., Salemi, M., Phinney,**
2772 **B.S., Domozych, D., Wilkop, T., and Drakakaki, G.** (2019). AtTRAPPC11/ROG2:
2773 A Role for TRAPPs in Maintenance of the Plant Trans-Golgi Network/Early
2774 Endosome Organization and Function. *Plant Cell* **31**, 1879-1898.
- 2775 **Ross-Elliott, T.J., Jensen, K.H., Haaning, K.S., Wagner, B.M., Knoblauch, J., Howell,**
2776 **A.H., Mullendore, D.L., Monteith, A.G., Paultre, D., Yan, D.W., Otero, S.,**
2777 **Bourdon, M., Sager, R., Lee, J.Y., Helariutta, Y., Knoblauch, M., and Oparka,**
2778 **K.J.** (2017). Phloem unloading in Arabidopsis roots is convective and regulated by
2779 the phloem pole pericycle. *Elife* **6**.
- 2780 **Rui, Y., and Dinneny, J.R.** (2020). A wall with integrity: surveillance and maintenance of
2781 the plant cell wall under stress. *New Phytologist* **225**, 1428-1439.
- 2782 **Ruiz-Lopez, N., Perez-Sancho, J., Esteban Del Valle, A., Haslam, R.P., Vanneste, S.,**
2783 **Catala, R., Perea-Resa, C., Van Damme, D., Garcia-Hernandez, S., Albert, A.,**
2784 **Vallarino, J., Lin, J., Friml, J., Macho, A.P., Salinas, J., Rosado, A., Napier,**
2785 **J.A., Amorim-Silva, V., and Botella, M.A.** (2021). Synaptotagmins at the
2786 endoplasmic reticulum-plasma membrane contact sites maintain diacylglycerol
2787 homeostasis during abiotic stress. *Plant Cell*.
- 2788 **Rydahl, M.G., Hansen, A.R., Kracun, S.K., and Mravec, J.** (2018). Report on the
2789 Current Inventory of the Toolbox for Plant Cell Wall Analysis: Proteinaceous and
2790 Small Molecular Probes. *Frontiers in Plant Science* **9**.
- 2791 **Sadre, R., Kuo, P.Y., Chen, J.X., Yang, Y., Banerjee, A., Benning, C., and Hamberger,**
2792 **B.** (2019). Cytosolic lipid droplets as engineered organelles for production and
2793 accumulation of terpenoid biomaterials in leaves. *Nature Communications* **10**.
- 2794 **Sakamoto, Y., Sato, M., Sato, Y., Harada, A., Suzuki, T., Goto, C., Tamura, K.,**
2795 **Toyooka, K., Kimura, H., Ohkawa, Y., Hara-Nishimura, I., Takagi, S., and**
2796 **Matsunaga, S.** (2020). Subnuclear gene positioning through lamina association
2797 affects copper tolerance. *Nature Communications* **11**, 5914.
- 2798 **Schapire, A.L., Voigt, B., Jasik, J., Rosado, A., Lopez-Cobollo, R., Menzel, D.,**
2799 **Salinas, J., Mancuso, S., Valpuesta, V., Baluska, F., and Botella, M.A.** (2008).
2800 Arabidopsis Synaptotagmin 1 Is Required for the Maintenance of Plasma
2801 Membrane Integrity and Cell Viability. *Plant Cell* **20**, 3374-3388.

- 2802 **Scheller, H.V., and Ulvskov, P.** (2010). Hemicelluloses. Annual Review of Plant Biology,
2803 Vol 61 **61**, 263-289.
- 2804 **Scheuring, D., Lofke, C., Kruger, F., Kittelmann, M., Eisa, A., Hughes, L., Smith, R.S.,**
2805 **Hawes, C., Schumacher, K., and Kleine-Vehn, J.** (2016). Actin-dependent
2806 vacuolar occupancy of the cell determines auxin-induced growth repression. P Natl
2807 Acad Sci USA **113**, 452-457.
- 2808 **Scheuring, D., Viotti, C., Kruger, F., Kunzl, F., Sturm, S., Bubeck, J., Hillmer, S.,**
2809 **Frigerio, L., Robinson, D.G., Pimpl, P., and Schumacher, K.** (2011).
2810 Multivesicular Bodies Mature from the Trans-Golgi Network/Early Endosome in
2811 Arabidopsis. Plant Cell **23**, 3463-3481.
- 2812 **Schoberer, J., Konig, J., Veit, C., Vavra, U., Liebming, E., Botchway, S.W.,**
2813 **Altmann, F., Kriechbaumer, V., Hawes, C., and Strasser, R.** (2019). A signal
2814 motif retains Arabidopsis ER-alpha-mannosidase I in the cis-Golgi and prevents
2815 enhanced glycoprotein ERAD. Nat Commun **10**, 3701.
- 2816 **Schroeder, L.K., Barentine, A.E.S., Merta, H., Schweighofer, S., Zhang, Y.,**
2817 **Baddeley, D., Bewersdorf, J., and Bahmanyar, S.** (2019). Dynamic nanoscale
2818 morphology of the ER surveyed by STED microscopy. J Cell Biol **218**, 83-96.
- 2819 **Schulz, A.** (1995). Plasmodesmal Widening Accompanies the Short-Term Increase in
2820 Symplasmic Phloem Unloading in Pea Root-Tips under Osmotic-Stress.
2821 Protoplasma **188**, 22-37.
- 2822 **Schumann, U., Wanner, G., Veenhuis, M., Schmid, M., and Gietl, C.** (2003).
2823 AthPEX10, a nuclear gene essential for peroxisome and storage organelle
2824 formation during Arabidopsis embryogenesis. Proc Natl Acad Sci U S A **100**, 9626-
2825 9631.
- 2826 **Schumann, U., Prestele, J., O'Geen, H., Brueggeman, R., Wanner, G., and Gietl, C.**
2827 (2007). Requirement of the C3HC4 zinc RING finger of the Arabidopsis PEX10 for
2828 photorespiration and leaf peroxisome contact with chloroplasts. Proc Natl Acad Sci
2829 U S A **104**, 1069-1074.
- 2830 **Schwarzlander, M., and Fuchs, P.** (2017). Plant mitochondrial membranes: adding
2831 structure and new functions to respiratory physiology. Curr Opin Plant Biol **40**, 147-
2832 157.

- 2833 **Schwarzlander, M., Logan, D.C., Johnston, I.G., Jones, N.S., Meyer, A.J., Fricker,**
2834 **M.D., and Sweetlove, L.J.** (2012). Pulsing of membrane potential in individual
2835 mitochondria: a stress-induced mechanism to regulate respiratory bioenergetics in
2836 Arabidopsis. *Plant Cell* **24**, 1188-1201.
- 2837 **Scorrano, L., De Matteis, M.A., Emr, S., Giordano, F., Hajnoczky, G., Kornmann, B.,**
2838 **Lackner, L.L., Levine, T.P., Pellegrini, L., Reinisch, K., Rizzuto, R., Simmen,**
2839 **T., Stenmark, H., Ungermann, C., and Schuldiner, M.** (2019). Coming together
2840 to define membrane contact sites. *Nat Commun* **10**, 1287.
- 2841 **Segui-Simarro, J.M., and Staehelin, L.A.** (2006). Cell cycle-dependent changes in Golgi
2842 stacks, vacuoles, clathrin-coated vesicles and multivesicular bodies in
2843 meristematic cells of Arabidopsis thaliana: a quantitative and spatial analysis.
2844 *Planta* **223**, 223-236.
- 2845 **Shai, N., Schuldiner, M., and Zalckvar, E.** (2016). No peroxisome is an island -
2846 Peroxisome contact sites. *Bba-Mol Cell Res* **1863**, 1061-1069.
- 2847 **Shaw, R., Tian, X., and Xu, J.** (2021). Single-Cell Transcriptome Analysis in Plants:
2848 Advances and Challenges. *Mol Plant* **14**, 115-126.
- 2849 **Sheahan, M.B., McCurdy, D.W., and Rose, R.J.** (2005). Mitochondria as a connected
2850 population: ensuring continuity of the mitochondrial genome during plant cell
2851 dedifferentiation through massive mitochondrial fusion. *Plant J* **44**, 744-755.
- 2852 **Shemesh, T., Klemm, R.W., Romano, F.B., Wang, S., Vaughan, J., Zhuang, X.,**
2853 **Tukachinsky, H., Kozlov, M.M., and Rapoport, T.A.** (2014). A model for the
2854 generation and interconversion of ER morphologies. *Proc Natl Acad Sci U S A*
2855 **111**, E5243-5251.
- 2856 **Shibata M, Oikawa K, Yoshimoto K, Kondo M, Mano S, Yamada K, Hayashi M,**
2857 **Sakamoto W, Ohsumi Y, Nishimura M** (2013) Highly oxidized peroxisomes are
2858 selectively degraded via autophagy in Arabidopsis. *Plant Cell* **25**: 4967-4983
- 2859 **Shibata, Y., Shemesh, T., Prinz, W.A., Palazzo, A.F., Kozlov, M.M., and Rapoport,**
2860 **T.A.** (2010). Mechanisms determining the morphology of the peripheral ER. *Cell*
2861 **143**, 774 - 788.
- 2862 **Shimada, T.L., Takano, Y., Shimada, T., Fujiwara, M., Fukao, Y., Mori, M., Okazaki,**
2863 **Y., Saito, K., Sasaki, R., Aoki, K., and Hara-Nishimura, I.** (2014). Leaf Oil Body

2864 Functions as a Subcellular Factory for the Production of a Phytoalexin in
2865 Arabidopsis. *Plant Physiology* **164**, 105-118.

2866 **Shimizu, Y., Takagi, J., Ito, E., Ito, Y., Ebine, K., Komatsu, Y., Goto, Y., Sato, M.,**
2867 **Toyooka, K., Ueda, T., Kurokawa, K., Uemura, T., and Nakano, A.** (2021).
2868 Cargo sorting zones in the trans-Golgi network visualized by super-resolution
2869 confocal live imaging microscopy in plants. *Nat Commun* **12**, 1901.

2870 **Shope, J.C., DeWald, D.B., and Mott, K.A.** (2003). Changes in surface area of intact
2871 guard cells are correlated with membrane internalization. *Plant Physiol* **133**, 1314-
2872 1321.

2873 **Sibbald, S.J., and Archibald, J.M.** (2020). Genomic Insights into Plastid Evolution.
2874 *Genome Biol Evol* **12**, 978-990.

2875 **Simon, M.L., Platre, M.P., Assil, S., van Wijk, R., Chen, W.Y., Chory, J., Dreux, M.,**
2876 **Munnik, T., and Jaillais, Y.** (2014). A multi-colour/multi-affinity marker set to
2877 visualize phosphoinositide dynamics in Arabidopsis. *Plant J* **77**, 322-337.

2878 **Sinclair, A.M., Trobacher, C.P., Mathur, N., Greenwood, J.S., and Mathur, J.** (2009).
2879 Peroxule extension over ER-defined paths constitutes a rapid subcellular response
2880 to hydroxyl stress. *Plant Journal* **59**, 231-242.

2881 **Singh, M.K., Kruger, F., Beckmann, H., Brumm, S., Vermeer, J.E.M., Munnik, T.,**
2882 **Mayer, U., Stierhof, Y.D., Grefen, C., Schumacher, K., and Jurgens, G.** (2014).
2883 Protein Delivery to Vacuole Requires SAND Protein-Dependent Rab GTPase
2884 Conversion for MVB-Vacuole Fusion. *Curr Biol* **24**, 1383-1389.

2885 **Sparkes, I., Runions, J., Hawes, C., and Griffing, L.** (2009a). Movement and
2886 remodeling of the endoplasmic reticulum in nondividing cells of tobacco leaves.
2887 *Plant Cell* **21**, 3937-3949.

2888 **Sparkes, I.A., Frigerio, L., Tolley, N., and Hawes, C.** (2009b). The plant endoplasmic
2889 reticulum: a cell-wide web. *Biochem J* **423**, 145-155.

2890 **Sparkes, I.A., Brandizzi, F., Slocombe, S.P., El-Shami, M., Hawes, C., and Baker, A.**
2891 (2003). An arabidopsis pex10 null mutant is embryo lethal, implicating
2892 peroxisomes in an essential role during plant embryogenesis. *Plant Physiology*
2893 **133**, 1809-1819.

- 2894 **Spiegelman, Z., Wu, S., and Gallagher, K.L.** (2019). A role for the endoplasmic
2895 reticulum in the cell-to-cell movement of SHORT-ROOT. *Protoplasma* **256**, 1455-
2896 1459.
- 2897 **Spitzer, C., Reyes, F.C., Buono, R., Sliwinski, M.K., Haas, T.J., and Otegui, M.S.**
2898 (2009). The ESCRT-related CHMP1A and B proteins mediate multivesicular body
2899 sorting of auxin carriers in Arabidopsis and are required for plant development.
2900 *The Plant Cell* **21**, 749 - 766.
- 2901 **Spitzer, C., Schellmann, S., Sabovljevic, A., Shahriari, M., Keshavaiah, C., Bechtold,**
2902 **N., Herzog, M., Muller, S., Hanisch, F.G., and Hulskamp, M.** (2006). The
2903 Arabidopsis elch mutant reveals functions of an ESCRT component in cytokinesis.
2904 *Development* **133**, 4679-4689.
- 2905 **Staehein, L.A., and Kang, B.H.** (2008). Nanoscale architecture of endoplasmic
2906 reticulum export sites and of Golgi membranes as determined by electron
2907 tomography. *Plant Physiol* **147**, 1454-1468.
- 2908 **Staehein, L.A., Giddings, T.H., Jr., Kiss, J.Z., and Sack, F.D.** (1990). Macromolecular
2909 differentiation of Golgi stacks in root tips of Arabidopsis and Nicotiana seedlings
2910 as visualized in high pressure frozen and freeze-substituted samples. *Protoplasma*
2911 **157**, 75-91.
- 2912 **Stefano, G., Renna, L., and Brandizzi, F.** (2014). The endoplasmic reticulum exerts
2913 control over organelle streaming during cell expansion. *J Cell Sci* **127**, 947-953.
- 2914 **Stefano, G., Renna, L., Moss, T., McNew, J.A., and Brandizzi, F.** (2012). In
2915 Arabidopsis, the spatial and dynamic organization of the endoplasmic reticulum
2916 and Golgi apparatus is influenced by the integrity of the C-terminal domain of
2917 RHD3, a non-essential GTPase. *Plant J* **69**, 957-966.
- 2918 **Stefano, G., Renna, L., Wormsbaecher, C., Gamble, J., Zienkiewicz, K., and**
2919 **Brandizzi, F.** (2018). Plant Endocytosis Requires the ER Membrane-Anchored
2920 Proteins VAP27-1 and VAP27-3. *Cell Rep* **23**, 2299-2307.
- 2921 **Stefano, G., Renna, L., Lai, Y.S., Slabaugh, E., Mannino, N., Buono, R.A., Otegui,**
2922 **M.S., and Brandizzi, F.** (2015). ER network homeostasis is critical for plant
2923 endosome streaming and endocytosis. *Cell Discov* **1**, 15033.

- 2924 **Su, T., Li, W.J., Wang, P.P., and Ma, C.L.** (2019). Dynamics of Peroxisome Homeostasis
2925 and Its Role in Stress Response and Signaling in Plants. *Frontiers in Plant Science*
2926 **10**.
- 2927 **Su, T., Li, X., Yang, M., Shao, Q., Zhao, Y., Ma, C., and Wang, P.** (2020). Autophagy:
2928 An Intracellular Degradation Pathway Regulating Plant Survival and Stress
2929 Response. *Front Plant Sci* **11**, 164.
- 2930 **Sugiura, A., McLelland, G.L., Fon, E.A., and McBride, H.M.** (2014). A new pathway for
2931 mitochondrial quality control: mitochondrial-derived vesicles. *EMBO J* **33**, 2142-
2932 2156.
- 2933 **Sun, J.Q., Movahed, N., and Zheng, H.Q.** (2020a). LUNAPARK Is an E3 Ligase That
2934 Mediates Degradation of ROOT HAIR DEFECTIVE3 to Maintain a Tubular ER
2935 Network in Arabidopsis. *Plant Cell* **32**, 2964-2978.
- 2936 **Sun, J.Q., Zhang, M., Qi, X.Y., Doyle, C., and Zheng, H.Q.** (2020b). Armadillo-repeat
2937 kinesin1 interacts with Arabidopsis atlastin RHD3 to move ER with plus-end of
2938 microtubules. *Nature Communications* **11**.
- 2939 **Takagi, J., Renna, L., Takahashi, H., Koumoto, Y., Tamura, K., Stefano, G., Fukao,**
2940 **Y., Kondo, M., Nishimura, M., Shimada, T., Brandizzi, F., and Hara-Nishimura,**
2941 **I.** (2013). MAIGO5 Functions in Protein Export from Golgi-Associated Endoplasmic
2942 Reticulum Exit Sites in Arabidopsis. *Plant Cell* **25**, 4658-4675.
- 2943 **Tamura, K., Fukao, Y., Iwamoto, M., Haraguchi, T., and Hara-Nishimura, I.** (2010).
2944 Identification and characterization of nuclear pore complex components in
2945 Arabidopsis thaliana. *Plant Cell* **22**, 4084-4097.
- 2946 **Tamura, K., Iwabuchi, K., Fukao, Y., Kondo, M., Okamoto, K., Ueda, H., Nishimura,**
2947 **M., and Hara-Nishimura, I.** (2013). Myosin XI-i links the nuclear membrane to the
2948 cytoskeleton to control nuclear movement and shape in Arabidopsis. *Curr Biol* **23**,
2949 1776-1781.
- 2950 **Takemoto, K., Ebine, K., Askani, J.C., Kruger, F., Gonzalez, Z.A., Ito, E., Goh, T.,**
2951 **Schumacher, K., Nakano, A., and Ueda, T.** (2018). Distinct sets of tethering
2952 complexes, SNARE complexes, and Rab GTPases mediate membrane fusion
2953 at the vacuole in Arabidopsis. *Proc Natl Acad Sci USA* **115**, E2457-E2466.

- 2954 **Tanaka, Y., Kutsuna, N., Kanazawa, Y., Kondo, N., Hasezawa, S., and Sano, T.**
2955 **(2007). Intra-vacuolar reserves of membranes during stomatal closure: the**
2956 **possible role of guard cell vacuoles estimated by 3-D reconstruction. *Plant***
2957 ***Cell Physiol* **48**, 1159-1169.**
- 2958 **Tang, Y., Huang, A., and Gu, Y.** (2020). Global profiling of plant nuclear membrane
2959 proteome in Arabidopsis. *Nat Plants* **6**, 838-847.
- 2960 **Taurino, M., Costantini, S., De Domenico, S., Stefanelli, F., Ruano, G., Delgadillo,**
2961 **M.O., Sanchez-Serrano, J.J., Sanmartin, M., Santino, A., and Rojo, E.** (2018).
2962 SEIPIN Proteins Mediate Lipid Droplet Biogenesis to Promote Pollen Transmission
2963 and Reduce Seed Dormancy. *Plant Physiol* **176**, 1531-1546.
- 2964 **Terron-Camero, L.C., Rodriguez-Serrano, M., Sandalio, L.M., and Romero-Puertas,**
2965 **M.C.** (2020). Nitric oxide is essential for cadmium-induced peroxule formation and
2966 peroxisome proliferation. *Plant Cell and Environment* **43**, 2492-2507.
- 2967 **Thazar-Poulot, N., Miquel, M., Fobis-Loisy, I., and Gaude, T.** (2015). Peroxisome
2968 extensions deliver the Arabidopsis SDP1 lipase to oil bodies. *Proc Natl Acad Sci*
2969 *U S A* **112**, 4158-4163.
- 2970 **Thomas, C.L., Bayer, E.M., Ritzenthaler, C., Fernandez-Calvino, L., and Maule, A.J.**
2971 **(2008). Specific targeting of a plasmodesmal protein affecting cell-to-cell**
2972 **communication. *PLoS Biol* **6**, e7.**
- 2973 **Tilney, L.G., Cooke, T.J., Connelly, P.S., and Tilney, M.S.** (1991). The Structure of
2974 Plasmodesmata as Revealed by Plasmolysis, Detergent Extraction, and Protease
2975 Digestion. *Journal of Cell Biology* **112**, 739-747.
- 2976 **Tilsner, J., Amari, K., and Torrance, L.** (2011). Plasmodesmata viewed as specialised
2977 membrane adhesion sites. *Protoplasma* **248**, 39-60.
- 2978 **Tilsner, J., Nicolas, W., Rosado, A., and Bayer, E.M.** (2016). Staying Tight:
2979 Plasmodesmal Membrane Contact Sites and the Control of Cell-to-Cell
2980 Connectivity in Plants. *Annu Rev Plant Biol* **67**, 337-364.
- 2981 **Tilsner, J., Linnik, O., Louveaux, M., Roberts, I.M., Chapman, S.N., and Oparka, K.J.**
2982 **(2013). Replication and trafficking of a plant virus are coupled at the entrances of**
2983 **plasmodesmata. *Journal of Cell Biology* **201**, 981-995.**

- 2984 **Tolley, N., Sparkes, I.A., Hunter, P.R., Craddock, C.P., Nuttall, J., Roberts, L.M.,**
2985 **Hawes, C., Pedrazzini, E., and Frigerio, L.** (2008). Overexpression of a plant
2986 reticulum remodels the lumen of the cortical endoplasmic reticulum but does not
2987 perturb protein transport. *Traffic* **9**, 94-102.
- 2988 **Toyooka, K., Goto, Y., Asatsuma, S., Koizumi, M., Mitsui, T., and Matsuoka, K.**
2989 (2009). A mobile secretory vesicle cluster involved in mass transport from the Golgi
2990 to the plant cell exterior. *The Plant Cell* **21**, 1212 - 1229.
- 2991 **Twig, G., Elorza, A., Molina, A.J., Mohamed, H., Wikstrom, J.D., Walzer, G., Stiles,**
2992 **L., Haigh, S.E., Katz, S., Las, G., Alroy, J., Wu, M., Py, B.F., Yuan, J., Deeney,**
2993 **J.T., Corkey, B.E., and Shirihai, O.S.** (2008). Fission and selective fusion govern
2994 mitochondrial segregation and elimination by autophagy. *EMBO J* **27**, 433-446.
- 2995 **Ueda, H., Ohta, N., Kimori, Y., Uchida, T., Shimada, T., Tamura, K., and Hara-**
2996 **Nishimura, I.** (2018). Endoplasmic Reticulum (ER) Membrane Proteins
2997 (LUNAPARKs) are Required for Proper Configuration of the Cortical ER Network
2998 in Plant Cells. *Plant Cell Physiol* **59**, 2166.
- 2999 **Ueda, H., Yokota, E., Kutsuna, N., Shimada, T., Tamura, K., Shimmen, T., Hasezawa,**
3000 **S., Dolja, V.V., and Hara-Nishimura, I.** (2010). Myosin-dependent endoplasmic
3001 reticulum motility and F-actin organization in plant cells. *Proc Natl Acad Sci U S A*
3002 **107**, 6894-6899.
- 3003 **Ueda, H., Yokota, E., Kuwata, K., Kutsuna, N., Mano, S., Shimada, T., Tamura, K.,**
3004 **Stefano, G., Fukao, Y., Brandizzi, F., Shimmen, T., Nishimura, M., and Hara-**
3005 **Nishimura, I.** (2016). Phosphorylation of the C Terminus of RHD3 Has a Critical
3006 Role in Homotypic ER Membrane Fusion in Arabidopsis. *Plant Physiol* **170**, 867-
3007 880.
- 3008 **Uemura, T., Morita, M.T., Ebine, K., Okatani, Y., Yano, D., Saito, C., Ueda, T., and**
3009 **Nakano, A.** (2010). Vacuolar/pre-vacuolar compartment Qa-SNAREs
3010 VAM3/SYP22 and PEP12/SYP21 have interchangeable functions in Arabidopsis.
3011 *Plant J* **64**, 864-873.
- 3012 **Uemura, T., Suda, Y., Ueda, T., and Nakano, A.** (2014). Dynamic behavior of the trans-
3013 golgi network in root tissues of Arabidopsis revealed by super-resolution live
3014 imaging. *Plant Cell Physiol* **55**, 694-703.

3015 **Uemura, T., Nakano, R.T., Takagi, J., Wang, Y., Kramer, K., Finkemeier, I., Nakagami,**
3016 **H., Tsuda, K., Ueda, T., Schulze-Lefert, P., and Nakano, A.** (2019). A Golgi-
3017 Released Subpopulation of the Trans-Golgi Network Mediates Protein Secretion
3018 in Arabidopsis. *Plant Physiol* **179**, 519-532.

3019 **Vaahtera, L., Schulz, J., and Hamann, T.** (2019). Cell wall integrity maintenance during
3020 plant development and interaction with the environment. *Nat Plants* **5**, 924-932.

3021 **Valencia, J.P., Goodman, K., and Otegui, M.S.** (2016). Endocytosis and Endosomal
3022 Trafficking in Plants. *Annual Review of Plant Biology*, Vol 67 **67**, 309-335.

3023 **Van Buskirk, E.K., Decker, P.V., and Chen, M.** (2012). Photobodies in light signaling.
3024 *Plant Physiol* **158**, 52-60.

3025 **Vanhercke, T., Dyer, J.M., Mullen, R.T., Kilaru, A., Rahman, M.M., Petrie, J.R., Green,**
3026 **A.G., Yurchenko, O., and Singh, S.P.** (2019). Metabolic engineering for
3027 enhanced oil in biomass. *Prog Lipid Res* **74**, 103-129.

3028 **Vanhercke, T., Divi, U.K., El Tahchy, A., Liu, Q., Mitchell, M., Taylor, M.C., Eastmond,**
3029 **P.J., Bryant, F., Mechanicos, A., Blundell, C., Zhi, Y., Belide, S., Shrestha, P.,**
3030 **Zhou, X.R., Ral, J.P., White, R.G., Green, A., Singh, S.P., and Petrie, J.R.**
3031 (2017). Step changes in leaf oil accumulation via iterative metabolic engineering.
3032 *Metab Eng* **39**, 237-246.

3033 **Varas, J., Graumann, K., Osman, K., Pradillo, M., Evans, D.E., Santos, J.L., and**
3034 **Armstrong, S.J.** (2015). Absence of SUN1 and SUN2 proteins in Arabidopsis
3035 thaliana leads to a delay in meiotic progression and defects in synapsis and
3036 recombination. *Plant J* **81**, 329-346.

3037 **Viotti, C., Bubeck, J., Stierhof, Y.D., Krebs, M., Langhans, M., van den Berg, W., van**
3038 **Dongen, W., Richter, S., Geldner, N., Takano, J., Jurgens, G., de Vries, S.C.,**
3039 **Robinson, D.G., and Schumacher, K.** (2010). Endocytic and secretory traffic in
3040 Arabidopsis merge in the trans-Golgi network/early endosome, an independent
3041 and highly dynamic organelle. *Plant Cell* **22**, 1344-1357.

3042 **Viotti, C., Kruger, F., Krebs, M., Neubert, C., Fink, F., Lupanga, U., Scheuring, D.,**
3043 **Boutte, Y., Frescatada-Rosa, M., Wolfenstetter, S., Sauer, N., Hillmer, S.,**
3044 **Grebe, M., and Schumacher, K.** (2013). The Endoplasmic Reticulum Is the Main

3045 Membrane Source for Biogenesis of the Lytic Vacuole in Arabidopsis. *Plant Cell*
3046 **25**, 3434-3449.

3047 **Voiniciuc, C., Pauly, M., and Usadel, B.** (2018). Monitoring Polysaccharide Dynamics
3048 in the Plant Cell Wall. *Plant Physiol* **176**, 2590-2600.

3049 **Vothknecht, U.C., and Westhoff, P.** (2001). Biogenesis and origin of thylakoid
3050 membranes. *Bba-Mol Cell Res* **1541**, 91-101.

3051 **Voxeur, A., Habrylo, O., Guenin, S., Miart, F., Soulie, M.C., Rihouey, C., Pau-Roblot,**
3052 **C., Domon, J.M., Gutierrez, L., Pelloux, J., Mouille, G., Fagard, M., Hofte, H.,**
3053 **and Vernhettes, S.** (2019). Oligogalacturonide production upon Arabidopsis
3054 thaliana-Botrytis cinerea interaction. *Proceedings of the National Academy of*
3055 *Sciences of the United States of America* **116**, 19743-19752.

3056 **Wang F, Shang Y, Fan B, Yu JQ, Chen Z** (2014) Arabidopsis LIP5, a positive regulator
3057 of multivesicular body biogenesis, is a critical target of pathogen-responsive MAPK
3058 cascade in plant basal defense. *PLoS Pathog* **10**, e1004243

3059 **Wang F, Yang Y, Wang Z, Zhou J, Fan B, Chen Z** (2015) A critical role of LIP5, a positive
3060 regulator of multivesicular body biogenesis, in plant responses to heat and salt
3061 stresses. *Plant Physiol* **169**, 497-511

3062 **Wang, H., Dittmer, T.A., and Richards, E.J.** (2013). Arabidopsis CROWDED NUCLEI
3063 (CRWN) proteins are required for nuclear size control and heterochromatin
3064 organization. *BMC Plant Biol* **13**, 200.

3065 **Wang, H.J., Hsu, Y.W., Guo, C.L., Jane, W.N., Wang, H., Jiang, L., and Jauh, G.Y.**
3066 (2017a). VPS36-Dependent Multivesicular Bodies Are Critical for
3067 Plasmamembrane Protein Turnover and Vacuolar Biogenesis. *Plant Physiol* **173**,
3068 566-581.

3069 **Wang, N., Karaaslan, E.S., Faiss, N., Berendzen, K.W., and Liu, C.** (2021).
3070 Characterization of a Plant Nuclear Matrix Constituent Protein in Liverwort. *Front*
3071 *Plant Sci* **12**, 670306.

3072 **Wang, P., and Hussey, P.J.** (2017). NETWORKED 3B: a novel protein in the actin
3073 cytoskeleton-endoplasmic reticulum interaction. *J Exp Bot* **68**, 1441-1450.

3074 **Wang, P., Hawes, C., and Hussey, P.J.** (2017b). Plant Endoplasmic Reticulum-Plasma
3075 Membrane Contact Sites. *Trends Plant Sci* **22**, 289-297.

- 3076 **Wang, P., Liang, Z., and Kang, B.-H.** (2019a). Electron tomography of plant organelles
3077 and the outlook for correlative microscopic approaches. *New Phytologist* **223**, 1756
3078 - 1761.
- 3079 **Wang, P., Chen, X., Goldbeck, C., Chung, E., and Kang, B.-H.** (2017c). A distinct class
3080 of vesicles derived from the trans-Golgi mediates secretion of xylogalacturonan in
3081 the root border cell. *The Plant Journal* **92**, 596 - 610.
- 3082 **Wang, P., Richardson, C., Hawkins, T.J., Sparkes, I., Hawes, C., and Hussey, P.J.**
3083 (2016). Plant VAP27 proteins: domain characterization, intracellular localization
3084 and role in plant development. *New Phytol* **210**, 1311-1326.
- 3085 **Wang, P., Pleskot, R., Zang, J., Winkler, J., Wang, J., Yperman, K., Zhang, T., Wang,**
3086 **K., Gong, J., Guan, Y., Richardson, C., Duckney, P., Vandorpe, M., Mylle, E.,**
3087 **Fiserova, J., Van Damme, D., and Hussey, P.J.** (2019b). Plant AtEH/Pan1
3088 proteins drive autophagosome formation at ER-PM contact sites with actin and
3089 endocytic machinery. *Nat Commun* **10**, 5132.
- 3090 **Wang, P.W., Hawkins, T.J., Richardson, C., Cummins, I., Deeks, M.J., Sparkes, I.,**
3091 **Hawes, C., and Hussey, P.J.** (2014). The Plant Cytoskeleton, NET3C, and VAP27
3092 Mediate the Link between the Plasma Membrane and Endoplasmic Reticulum.
3093 *Current Biology* **24**, 1397-1405.
- 3094 **Wang, W., Zhang, X., and Niittyla, T.** (2019c). OPENER Is a Nuclear Envelope and
3095 Mitochondria Localized Protein Required for Cell Cycle Progression in
3096 Arabidopsis. *Plant Cell* **31**, 1446-1465.
- 3097 **Wanner, G., and Theimer, R.R.** (1978). Membranous appendices of spherosomes
3098 (oleosomes) : Possible role in fat utilization in germinating oil seeds. *Planta* **140**,
3099 163-169.
- 3100 **Waterman-Storer, C.M., and Salmon, E.D.** (1998). Endoplasmic reticulum membrane
3101 tubules are distributed by microtubules in living cells using three distinct
3102 mechanisms. *Curr Biol* **8**, 798-806.
- 3103 **Wattelet-Boyer, V., Brocard, L., Jonsson, K., Esnay, N., Joubes, J., Domergue, F.,**
3104 **Mongrand, S., Raikhel, N., Bhalerao, R.P., Moreau, P., and Boutte, Y.** (2016).
3105 Enrichment of hydroxylated C24- and C26-acyl-chain sphingolipids mediates PIN2
3106 apical sorting at trans-Golgi network subdomains. *Nat Commun* **7**, 12788.

- 3107 **Wear, E.E., Song, J., Zynda, G.J., LeBlanc, C., Lee, T.J., Mickelson-Young, L.,**
3108 **Concia, L., Mulvaney, P., Szymanski, E.S., Allen, G.C., Martienssen, R.A.,**
3109 **Vaughn, M.W., Hanley-Bowdoin, L., and Thompson, W.F. (2017).** Genomic
3110 Analysis of the DNA Replication Timing Program during Mitotic S Phase in Maize
3111 (*Zea mays*) Root Tips. *Plant Cell* **29**, 2126-2149.
- 3112 **Weber, A.P.M., and Linka, N. (2011).** Connecting the Plastid: Transporters of the Plastid
3113 Envelope and Their Role in Linking Plastidial with Cytosolic Metabolism. *Annual*
3114 *Review of Plant Biology*, Vol 62 **62**, 53-77.
- 3115 **Wege, S., De Angeli, A., Droillard, M.J., Kroniewicz, L., Merlot, S., Cornu, D.,**
3116 **Gambale, F., Martinoia, E., Barbier-Brygoo, H., Thomine, S., Leonhardt, N.,**
3117 **and Filleur, S. (2014).** Phosphorylation of the vacuolar anion exchanger AtCLCa
3118 is required for the stomatal response to abscisic acid. *Sci Signal* **7**, 333:ra65
- 3119 **Weigel, A.V., Chang, C.L., Shtengel, G., Xu, C.S., Hoffman, D.P., Freeman, M., Iyer,**
3120 **N., Aaron, J., Khuon, S., Bogovic, J., Qiu, W., Hess, H.F., and Lippincott-**
3121 **Schwartz, J. (2021).** ER-to-Golgi protein delivery through an interwoven, tubular
3122 network extending from ER. *Cell* **184**, 2412-2429 e2416.
- 3123 **Welchen, E., Canal, M.V., Gras, D.E., and Gonzalez, D.H. (2021).** Cross-talk between
3124 mitochondrial function, growth, and stress signalling pathways in plants. *Journal of*
3125 *Experimental Botany* **72**, 4102-4118.
- 3126 **White, R.R., Lin, C., Leaves, I., Castro, I.G., Metz, J., Bateman, B.C., Botchway, S.W.,**
3127 **Ward, A.D., Ashwin, P., and Sparkes, I. (2020).** Miro2 tethers the ER to
3128 mitochondria to promote mitochondrial fusion in tobacco leaf epidermal cells.
3129 *Commun Biol* **3**, 161.
- 3130 **Wille, A.C., and Lucas, W.J. (1984).** Ultrastructural and histochemical studies on guard
3131 cells. *Planta* **160**, 129-142.
- 3132 **Wilson, T.H., Kumar, M., and Turner, S.R. (2021).** The molecular basis of plant cellulose
3133 synthase complex organisation and assembly. *Biochemical Society Transactions*
3134 **49**, 379-391.
- 3135 **Wink, M. (1993).** The Plant Vacuole - a Multifunctional Compartment. *J Exp Bot* **44**, 231-
3136 246.

- 3137 **Witkos, T.M., Chan, W.L., Joensuu, M., Rhiel, M., Pallister, E., Thomas-Oates, J.,**
3138 **Mould, A.P., Mironov, A.A., Biot, C., Guerardel, Y., Morelle, W., Ungar, D.,**
3139 **Wieland, F.T., Jokitalo, E., Tassabehji, M., Kornak, U., and Lowe, M. (2019).**
3140 **GORAB scaffolds COPI at the trans-Golgi for efficient enzyme recycling and**
3141 **correct protein glycosylation. Nat Commun 10, 127.**
- 3142 **Wong, L.H., and Levine, T.P. (2016). Lipid transfer proteins do their thing anchored at**
3143 **membrane contact sites . . . but what is their thing? Biochemical Society**
3144 **Transactions 44, 517-527.**
- 3145 **Wong, M., and Munro, S. (2014). Membrane trafficking. The specificity of vesicle traffic**
3146 **to the Golgi is encoded in the golgin coiled-coil proteins. Science 346, (6209)**
3147 **1256898.**
- 3148 **Woodson, J.D. (2019). Chloroplast stress signals: regulation of cellular degradation and**
3149 **chloroplast turnover. Current Opinion in Plant Biology 52, 30-37.**
- 3150 **Wright, Z.J., and Bartel, B. (2020). Peroxisomes form intraluminal vesicles with roles in**
3151 **fatty acid catabolism and protein compartmentalization in Arabidopsis. Nat**
3152 **Commun 11, 6221.**
- 3153 **Wu, H.X., Carvalho, P., and Voeltz, G.K. (2018). Here, there, and everywhere: The**
3154 **importance of ER membrane contact sites. Science 361, 6401, ean5835.**
- 3155 **Xia Z, Huo Y, Wei Y, Chen Q, Xu Z, Zhang W (2016) The Arabidopsis LYST**
3156 **INTERACTING PROTEIN 5 acts in regulating abscisic acid signaling and drought**
3157 **response. Front Plant Sci 7, 758**
- 3158 **Xiao, C., Somerville, C., and Anderson, C.T. (2014). POLYGALACTURONASE**
3159 **INVOLVED IN EXPANSION1 Functions in Cell Elongation and Flower**
3160 **Development in Arabidopsis. Plant Cell 26, 1018-1035.**
- 3161 **Xu, C., and Shanklin, J. (2016). Triacylglycerol Metabolism, Function, and Accumulation**
3162 **in Plant Vegetative Tissues. Annu Rev Plant Biol 67, 179-206.**
- 3163 **Yamashita, A., Fujimoto, M., Katayama, K., Yamaoka, S., Tsutsumi, N., and Arimura,**
3164 **S. (2016). Formation of Mitochondrial Outer Membrane Derived Protrusions and**
3165 **Vesicles in Arabidopsis thaliana. PLoS One 11, e0146717.**
- 3166 **Yamashita, S., and Takahashi, S. (2020). Molecular Mechanisms of Natural Rubber**
3167 **Biosynthesis. Annu Rev Biochem 89, 821-851.**

- 3168 **Yamauchi, S., Mano, S., Oikawa, K., Hikino, K., Teshima, K.M., Kimori, Y.,**
3169 **Nishimura, M., Shimazaki, K.I., and Takemiya, A.** (2019). Autophagy controls
3170 reactive oxygen species homeostasis in guard cells that is essential for stomatal
3171 opening. *Proc Natl Acad Sci U S A* **116**, 19187-19192.
- 3172 **Yan, D., Yadav, S.R., Paterlini, A., Nicolas, W.J., Petit, J.D., Brocard, L., Belevich, I.,**
3173 **Grison, M.S., Vaten, A., Karami, L., El-Showk, S., Lee, J.Y., Murawska, G.M.,**
3174 **Mortimer, J., Knoblauch, M., Jokitalo, E., Markham, J.E., Bayer, E.M., and**
3175 **Helariutta, Y.** (2019). Sphingolipid biosynthesis modulates plasmodesmal
3176 ultrastructure and phloem unloading. *Nat Plants* **5**, 604-615.
- 3177 **Yang, H., and Kubicki, J.D.** (2020). A density functional theory study on the shape of the
3178 primary cellulose microfibril in plants: effects of C6 exocyclic group conformation
3179 and H-bonding. *Cellulose* **27**, 2389-2402.
- 3180 **Yang, Y., and Benning, C.** (2018). Functions of triacylglycerols during plant development
3181 and stress. *Curr Opin Biotechnol* **49**, 191-198.
- 3182 **Yang, Y.-d., Elamawi, R., Bubeck, J., Pepperkok, R., Ritzenthaler, C., and Robinson,**
3183 **D.G.** (2005). Dynamics of COPII Vesicles and the Golgi Apparatus in Cultured
3184 *Nicotiana tabacum* BY-2 Cells Provides Evidence for Transient Association of
3185 Golgi Stacks with Endoplasmic Reticulum Exit Sites **17**, 1513 - 1531.
- 3186 **Yoshida, Y.** (2018). Insights into the Mechanisms of Chloroplast Division. *International*
3187 *Journal of Molecular Sciences* **19**, (3):733.
- 3188 **Yoshimoto, K., and Ohsumi, Y.** (2018). Unveiling the Molecular Mechanisms of Plant
3189 Autophagy-From Autophagosomes to Vacuoles in Plants. *Plant Cell Physiol* **59**,
3190 1337-1344.
- 3191 **Young, P.G., and Bartel, B.** (2016). Pexophagy and peroxisomal protein turnover in
3192 plants. *Biochim Biophys Acta* **1863**, 999-1005.
- 3193 **Yu, F., Lou, L., Tian, M., Li, Q., Ding, Y., Cao, X., Wu, Y., Belda-Palazon, B.,**
3194 **Rodriguez, P.L., Yang, S., and Xie, Q.** (2016). ESCRT-I Component VPS23A
3195 Affects ABA Signaling by Recognizing ABA Receptors for Endosomal
3196 Degradation. *Mol Plant* **9**, 1570-1582.
- 3197 **Zancani, M., Braidot, E., Filippi, A., and Lippe, G.** (2020). Structural and functional
3198 properties of plant mitochondrial F-ATP synthase. *Mitochondrion* **53**, 178-193.

- 3199 **Zang, J., Klemm, S., Pain, C., Duckney, P., Bao, Z., Stamm, G., Kriechbaumer, V.,**
3200 **Burstenbinder, K., Hussey, P.J., and Wang, P.** (2021). A novel plant actin-
3201 microtubule bridging complex regulates cytoskeletal and ER structure at ER-PM
3202 contact sites. *Curr Biol* **31**, 1251-1260 e1254.
- 3203 **Zavaliev, R., Mohan, R., Chen, T., and Dong, X.** (2020). Formation of NPR1
3204 Condensates Promotes Cell Survival during the Plant Immune Response. *Cell*
3205 **182**, 1093-1108 e1018.
- 3206 **Zeng, Y.N., Himmel, M.E., and Ding, S.Y.** (2017). Visualizing chemical functionality in
3207 plant cell walls. *Biotechnol Biofuels* **10**.
- 3208 **Zhang, G.F., and Staehelin, L.A.** (1992). Functional compartmentation of the Golgi
3209 apparatus of plant cells : immunocytochemical analysis of high-pressure frozen-
3210 and freeze-substituted sycamore maple suspension culture cells. *Plant Physiol* **99**,
3211 1070-1083.
- 3212 **Zhang, L., Zhang, H., Liu, P., Hao, H., Jin, J.B., and Lin, J.** (2011). Arabidopsis R-
3213 SNARE proteins VAMP721 and VAMP722 are required for cell plate formation.
3214 *PLoS One* **6**, e26129.
- 3215 **Zhang, M., Wu, F., Shi, J., Zhu, Y., Zhu, Z., Gong, Q., and Hu, J.** (2013). ROOT HAIR
3216 DEFECTIVE3 family of dynamin-like GTPases mediates homotypic endoplasmic
3217 reticulum fusion and is essential for Arabidopsis development. *Plant Physiol* **163**,
3218 713-720.
- 3219 **Zhang, T., Vavylonis, D., Durachko, D.M., and Cosgrove, D.J.** (2017). Nanoscale
3220 movements of cellulose microfibrils in primary cell walls. *Nature Plants* **3**.
- 3221 **Zhang, X., Ding, X., Marshall, R.S., Paez-Valencia, J., Lacey, P., Vierstra, R.D., and**
3222 **Otegui, M.S.** (2020). Reticulon proteins modulate autophagy of the endoplasmic
3223 reticulum in maize endosperm. *Elife* **9**.
- 3224 **Zhang, Y., Yu, J.Y., Wang, X., Durachko, D.M., Zhang, S.L., and Cosgrove, D.J.**
3225 (2021). Molecular insights into the complex mechanics of plant epidermal cell
3226 walls. *Science* **372**, 706-+.
- 3227 **Zhao, W.C., Fernando, L.D., Kirui, A., Deligey, F., and Wang, T.** (2020). Solid-state
3228 NMR of plant and fungal cell walls: A critical review. *Solid State Nucl Mag* **107**.

- 3229 **Zhao, Y.Y., Man, Y., Wen, J.L., Guo, Y.Y., and Lin, J.X.** (2019). Advances in Imaging
3230 Plant Cell Walls. *Trends in Plant Science* **24**, 867-878.
- 3231 **Zheng, H.Q., and Staehelin, L.A.** (2011). Protein Storage Vacuoles Are Transformed
3232 into Lytic Vacuoles in Root Meristematic Cells of Germinating Seedlings by
3233 Multiple, Cell Type-Specific Mechanisms. *Plant Physiol* **155**, 2023-2035.
- 3234 **Zhou, X., Groves, N.R., and Meier, I.** (2015). SUN anchors pollen WIP-WIT complexes
3235 at the vegetative nuclear envelope and is necessary for pollen tube targeting and
3236 fertility. *J Exp Bot* **66**, 7299-7307.
- 3237 **Zhou, X., Graumann, K., Wirthmueller, L., Jones, J.D., and Meier, I.** (2014).
3238 Identification of unique SUN-interacting nuclear envelope proteins with diverse functions
3239 in plants. *J Cell Biol* **205**, 677-692.
- 3240 **Zwiewka, M., Feraru, E., Moller, B., Hwang, I., Feraru, M.I., Kleine-Vehn, J., Weijers,**
3241 **D., and Friml, J.** (2011). The AP-3 adaptor complex is required for vacuolar
3242 function in Arabidopsis. *Cell Res* **21**, 1711-1722.

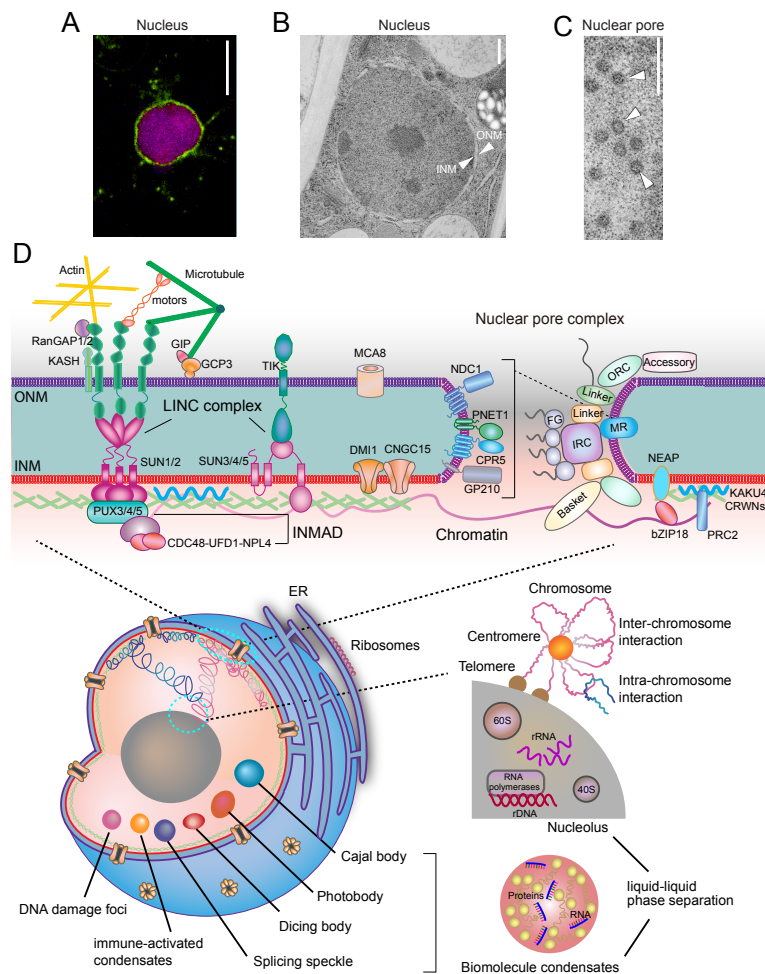


Figure 1. The nucleus and its constituents. A, A fluorescence micrograph of a nucleus in a *Nicotiana benthamiana* epidermal cell. The nuclear envelope (NE)-localized CPR5 protein (pseudo-colored in green) was coexpressed with the nucleoplasmic-localized cyclin kinase inhibitor SIM (pseudo-colored in magenta). B, An electron micrograph of a nucleus in an Arabidopsis root cell. Arrowheads indicate the outer nuclear membrane (ONM) and the inner nuclear membrane (INM) of the NE. C, An electron micrograph showing a tangential section through the nuclear envelope in an Arabidopsis root cell. Arrowheads indicate nuclear pores distributed at the surface of the NE. Scale bars are 10 μm in A and 500 nm in B and C. D, The nucleus is defined by the double-layered NE composed of the ONM and the INM, which join at the nuclear pore membrane. The NE hosts a specific population of proteins. SUN and KASH proteins comprise the LINC complex and function in various aspects of plant cell biology and physiology, as discussed in the main text. CPR5, PNET1, GP210, and NDC1 are structural components of the plant nuclear pore complex (NPC) membrane ring (MR). CNGC15, DMI1, and MCA8 regulate nuclear calcium transport and signaling and affect symbiotic interaction with arbuscular mycorrhiza. GCP3 and GIP proteins are part of the microtubule nucleation complex and regulate nuclear stiffness. CRWN and KAKU4 proteins assemble the plant nuclear skeleton and also function as a platform to interact with INM proteins and regulate chromatin organization by binding to chromatin-associating proteins (such as the PRC2 complex). NEAP proteins bind to the transcription factor bZIP18 and may also influence chromatin organization. The CDC48-UFD1-NPL4 trimeric complex and PUX3/4/5 proteins mediate plant INM-associated protein degradation (INMAD). The nuclear interior is organized heterogeneously. Heterochromatic regions and chromocenters are typically located near the nuclear periphery and the nucleolus. Other multivalent biomolecules (e.g., proteins and RNAs) aggregate to form various types of membrane-less condensates via the liquid-liquid phase separation mechanism.

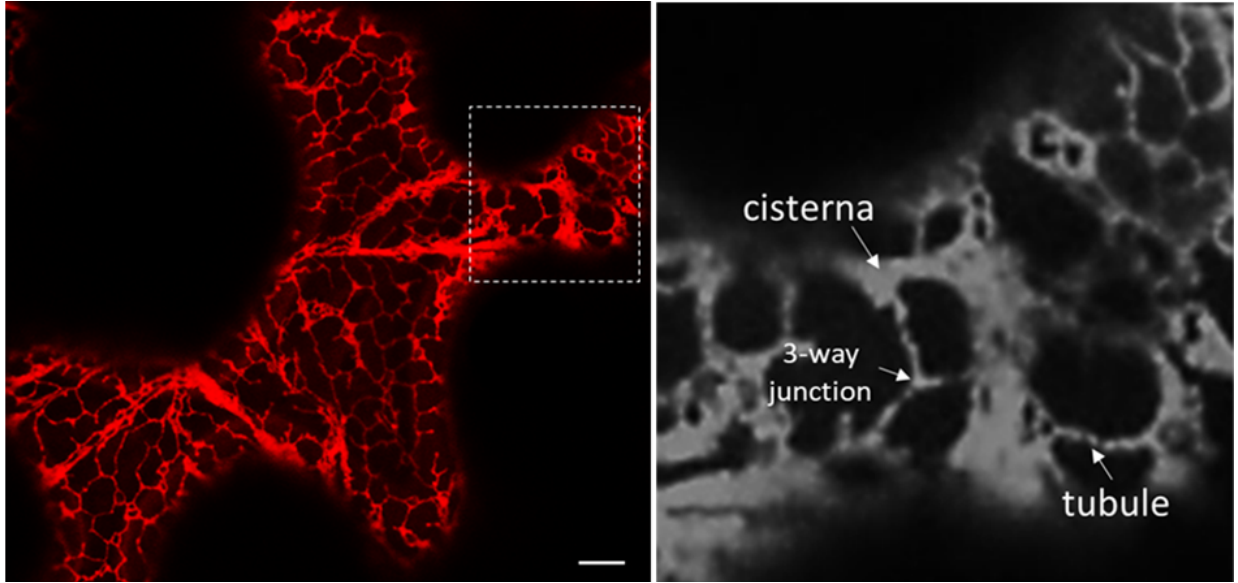


Figure 2. The plant ER forms a distinctive network of membranes at the cell cortex. Left panel: Confocal microscopy image of a *Nicotiana benthamiana* leaf epidermal cell transiently expressing the fluorescent luminal marker ER-mCherry (Nelson et al., 2007), which labels the lumen of the bulk ER network. Scale bar = 40 mm. Right panel: magnified view of the boxed region in the left panel highlighting some of the characteristic ER structures discussed in the main text.

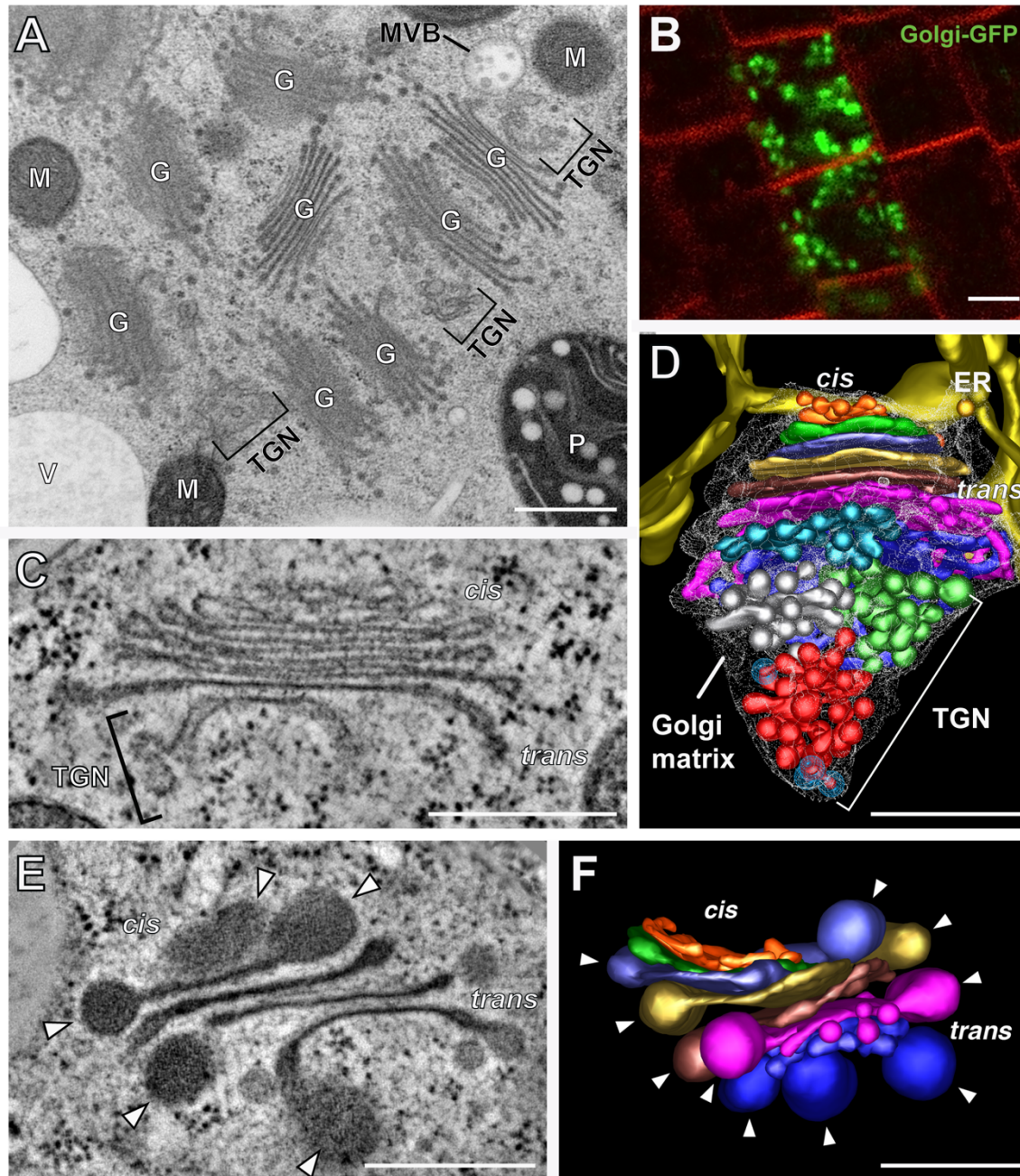


Figure 3. Plant Golgi stacks. A, Transmission electron micrograph showing a cluster of Golgi stacks in an Arabidopsis root tip cell. Plastids (P), mitochondria (M), and vacuoles (V) are marked. B, Confocal laser scanning micrograph of Arabidopsis root tip cells expressing a Golgi-localized green fluorescent protein. The plasma membrane was counterstained. C, ET slice image of a Golgi stack. The cis-side, trans-side and trans-Golgi network (TGN) are labeled. D, ET model of an Arabidopsis Golgi stack associated with the endoplasmic reticulum (ER). The entire Golgi and TGN are encompassed by a ribosome-ribosome excluding matrix (Golgi matrix). E, ET slice image of a Golgi stack in a root cap border cell. F, ET model of the Golgi in E. Swollen distal margins containing mucilage are marked with arrowheads in E and F. Scale bars in A, B, D, E, and F: 500 nm. Scale bar in C: 10 μ m.

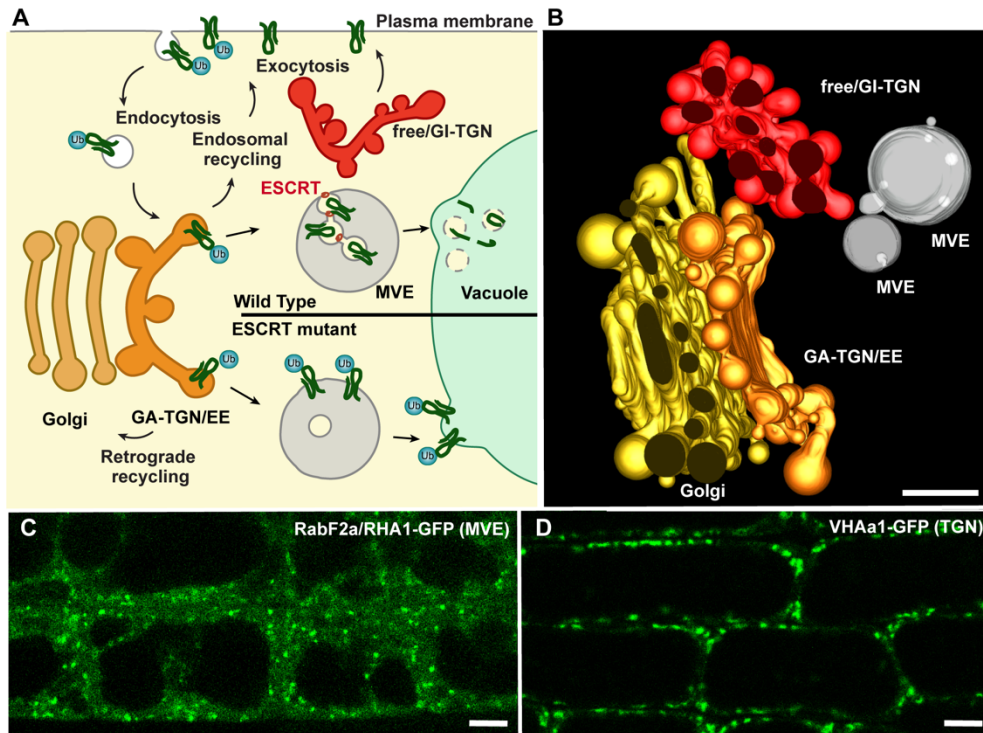


Figure 4. Plant endosomes. A, Diagram of plant endosomes and the major associated pathways, highlighting the effects on MVE mis-sorting in ESCRT mutants. B, Tomographic reconstructions of a Golgi stack, Golgi-associated TGN (GA-TGN), and free/Golgi independent (GI-TGN) in an Arabidopsis embryo cells. C-D, Confocal images of MVE-localized RabF2a/RHA1-GFP (C) and TGN-localized VHAA1-GFP (D) in Arabidopsis root cells. Scale bar = 200 nm in (B) and 5 mm in (C) and (D).

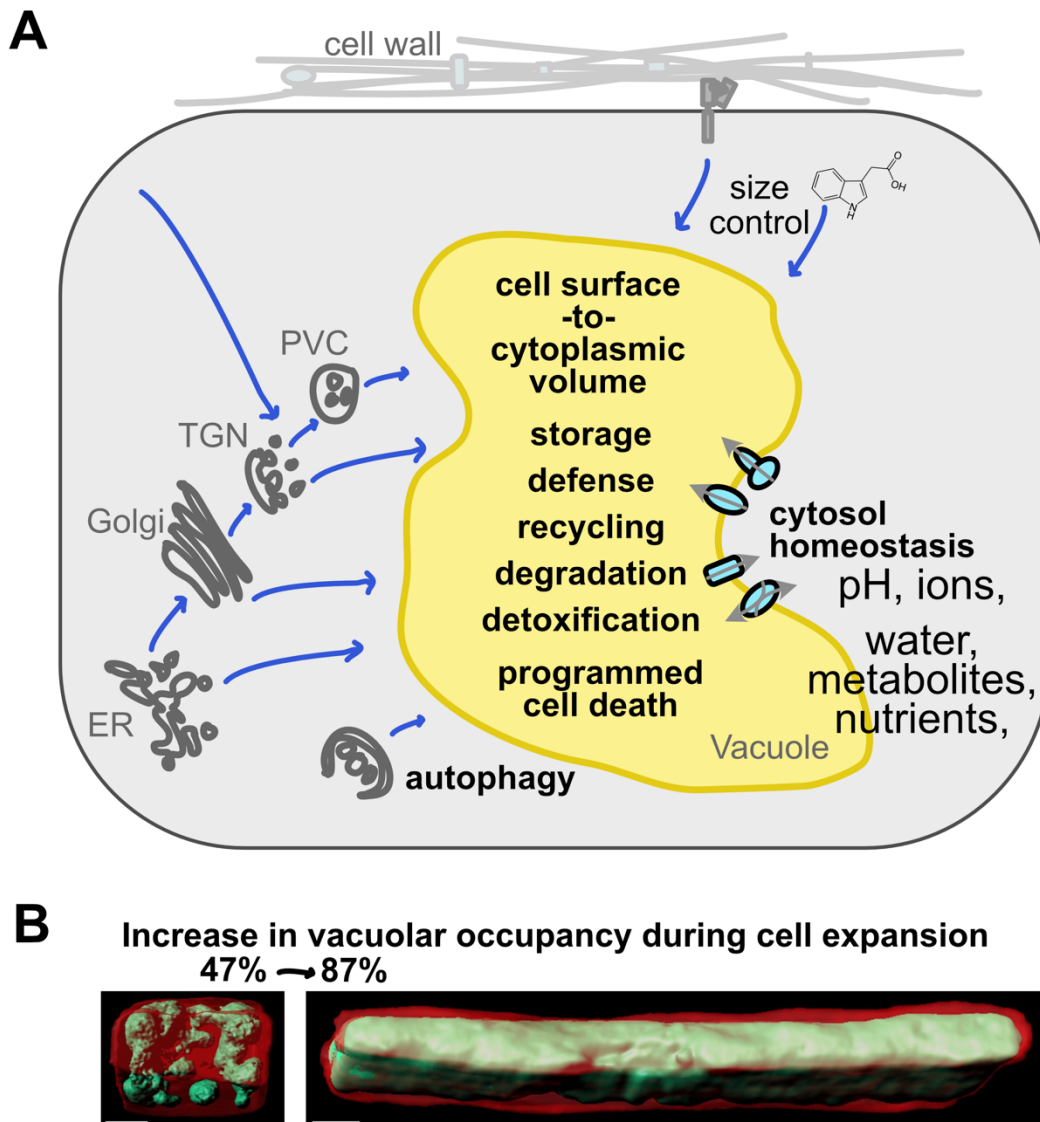


Figure 5. The multifunctional roles of the plant vacuole. A, There are various trafficking routes towards the vacuole, including pathways from the pre-vacuolar compartment (PVC), trans-Golgi network (TGN), Golgi, endoplasmic reticulum (ER), and autophagosomes. The vacuole carries out numerous indispensable functions as indicated. B, Confocal-based 3D reconstruction of the cell (in purple, based on cell wall staining with propidium iodide) and the vacuole (in green, based on BCECF-AM staining) visualizes the vacuolar occupancy of meristematic (left) and elongating cells (right). Scale bars: 6 μ m.

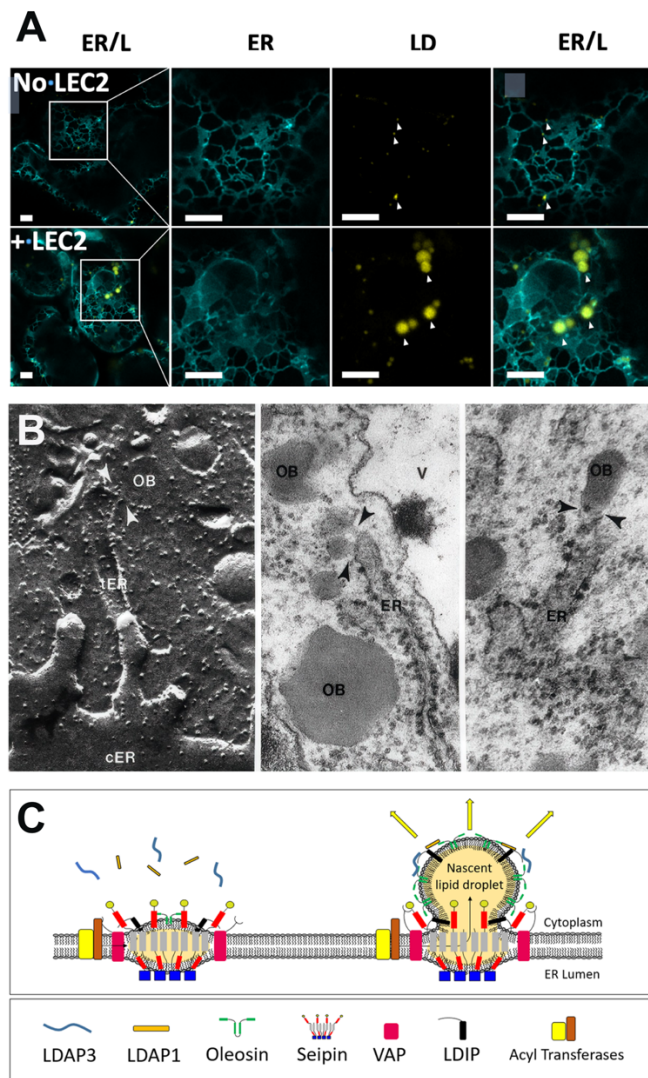


Figure 6. Spatial association of LDs with the ER and a model of LD biogenesis. A, Enhanced-resolution fluorescence imaging of the relationship of the ER to LDs in leaf mesophyll cells of *N. benthamiana* infiltrated with an ER marker and stained with the LD-specific fluorescent dye BODIPY 493/503. The ER network was marked in cyan with the ER-lumen marker protein Kar2-CFP-HDEL, and LDs are false-colored in yellow (white arrows). In leaves, small LDs are normally associated with the ER (top row). In this system, LDs were induced to proliferate by expressing lipogenic factors to study LD formation proteins and their roles in LD formation (second row). Here this process is illustrated by expressing LEAFY COTYLEDON2 (LEC2) in these leaves; this transcription factor is preferentially expressed in developing seeds and promotes storage lipid synthesis and LD formation. Under semi-normal conditions, the LD phenotype of tobacco shows few small LD's intimately connected to the ER. Scale bars: 5 μ m. B, TEM micrographs showing LDs (labeled as OB for oil body) emerging from the ER in cells of developing soybean (*Glycine max*) cotyledons. Left to right- freeze-fracture; cryofixation; chemical fixation. Arrows mark ER-LD junctions. For scale, ribosomes on the ER membrane are approximately 20 nm in diameter. Electron micrographs are courtesy of Dr. Eliot Herman, University of Arizona. C, Diagram illustrating the current, general model for LD biogenesis. Initial LD formation begins with the coalescence of the "lipid lens" within the ER bilayer. Various LD-associated proteins such as SEIPINs, LDIP, LDAPs, VAP27-1, oleosins (in seeds), and LDIP are recruited, which together facilitate the formation and stabilization of the nascent LD as it emerges into the cytoplasm. Adapted in part from a model presented and described in Greer et al. (2020).

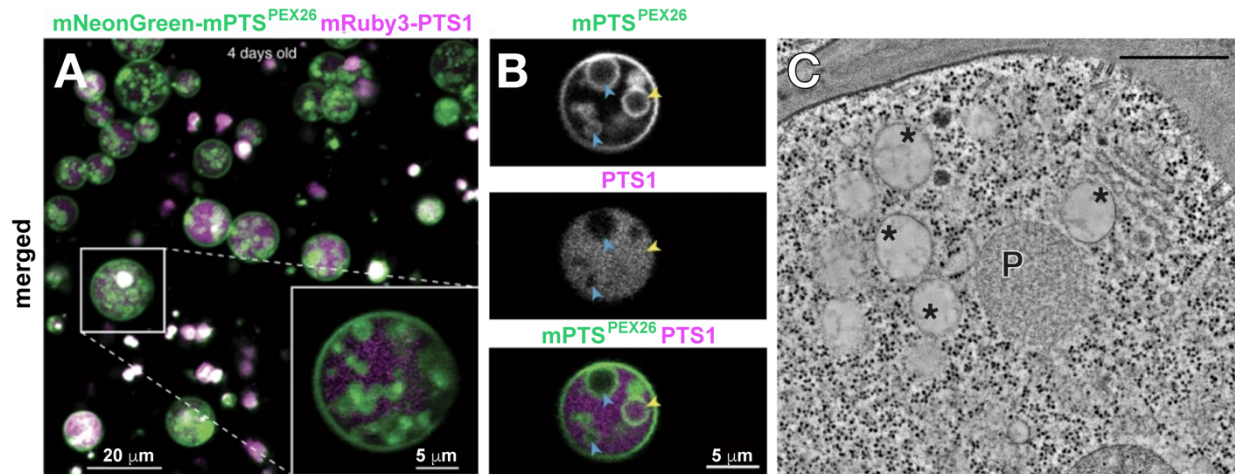


Figure 7. Microscopic images of peroxisomal structures in Arabidopsis cells. A, Microscopic image of 4-day-old Arabidopsis cotyledons expressing mNeonGreen with a membrane peroxisomal targeting signal (mNeonGreen-mPTS^{PEX26}; green) and mRuby with a matrix-bound peroxisomal targeting signal (mRuby3-PTS1; magenta) showing the presence of intralumenal vesicles (ILVs) in peroxisomes. The close-up image highlights the variable sizes of the vesicles. B, Separate images of fluorescent molecules in the membrane (green) and matrix (magenta) highlight the different substructures within the peroxisome, including ILVs with (yellow arrowheads) or without (blue arrowheads) matrix proteins and a separate area with denser membrane accumulation. Images in (A) and (B) are Figures 1G and 6A from Wright and Bartel (2020; reprinted with permission). C, ET slice image of a young root cell highlighting the interactions between a peroxisome (P), lipid droplets (*), and other organelles. Scale bar: 500 nm.

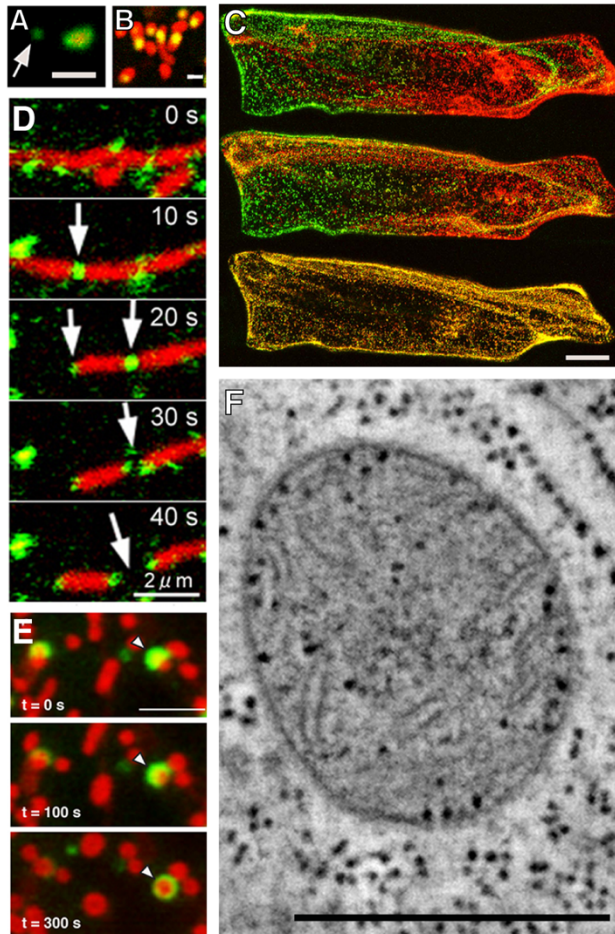


Figure 8. Microscopy imaging of plant mitochondrial dynamics. A, An apparent mitochondrial outer-membrane derived vesicle (MDV) (arrow) in an Arabidopsis cell. On the right is a mitochondrion whose outer membrane was stained with ELM1-GFP and whose matrix was stained with RFP. The MDV contains only the outer membranes and no matrix (Yamashita et al., 2016, reprinted with permission). B, Heterogeneity of DNA contents in mitochondria. The mitochondria were stained red with MitoTracker Red and DNA was stained with SYBR Green I. Green signals in red regions are shown in yellow. Therefore, red particles with yellow dots represent mitochondria containing DNA, and red mitochondria without yellow dots represent mitochondria lacking DNA (Arimura et al., 2004, reprinted with permission). C, Fusion of mitochondria in an onion bulb epidermal cell. The cell contains thousands of mitochondria. The mitochondria on the left and right sides of the cell were labeled green and red, respectively, by the (irreversibly) color-changing fluorescent protein Kaede. The photographs show the movement and mixing of the mitochondria after 10 minutes (upper), one hour (middle), and two hours (bottom). Yellow mitochondria are the result of fusion between green and red mitochondria (Arimura et al., 2004, reprinted with permission). D, Five consecutive frames showing mitochondria fission in a tobacco BY-2 cell. The mitochondria were stained with MitoTracker Red and dynamin-related protein 3A was labeled with GFP (Arimura 2018, reprinted with permission). E, Progression of mitophagy in an Arabidopsis cell, in which the mitochondria were stained with MitoTracker Red and autophagosomes were visualized by expression of YFP-ATG8e. The autophagosome on the right (arrowhead) is shown engulfing a mitochondrion over a 300 s interval (Ma et al., 2021, reprinted with permission). F, ET image of a mitochondrion in an Arabidopsis root meristematic cell. Black dots in the cytosol and mitochondrial matrix are ribosomes. Scale bars. A, D, and E, 2 μ m; B, 1 μ m; C, 40 μ m; F, 500 nm.

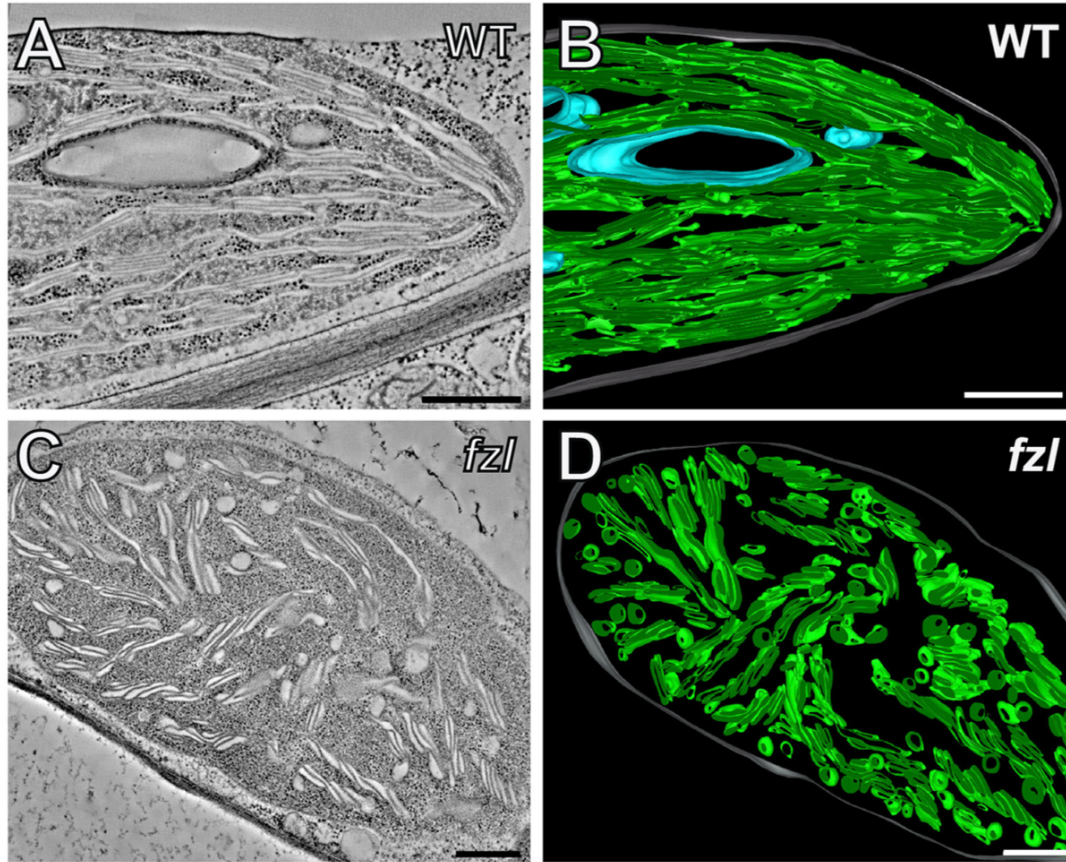


Figure 9. Chloroplast morphogenesis is a highly regulated process. A, ET slice image of a normal-sized wild-type (WT) chloroplast with typical thylakoid differentiation into stacked (grana) and unstacked domains. B, 3D model based on the chloroplast in (A). Green represents thylakoid membrane; blue represents starch grains. C, ET slice image of an oversized chloroplast (compare scale bars) with aberrant thylakoid membrane organization in an *Arabidopsis fzl* mutant (Liang et al., 2018b). FLZ is a dynamin-like protein, and thylakoid fusion is inhibited in the mutant (Gao et al., 2006; Findinier et al., 2019). Instead of a stroma-wide network, thylakoids form discrete spirals in the mutant. D, 3D model based on the chloroplast in (C). Scale bars = 500 nm.

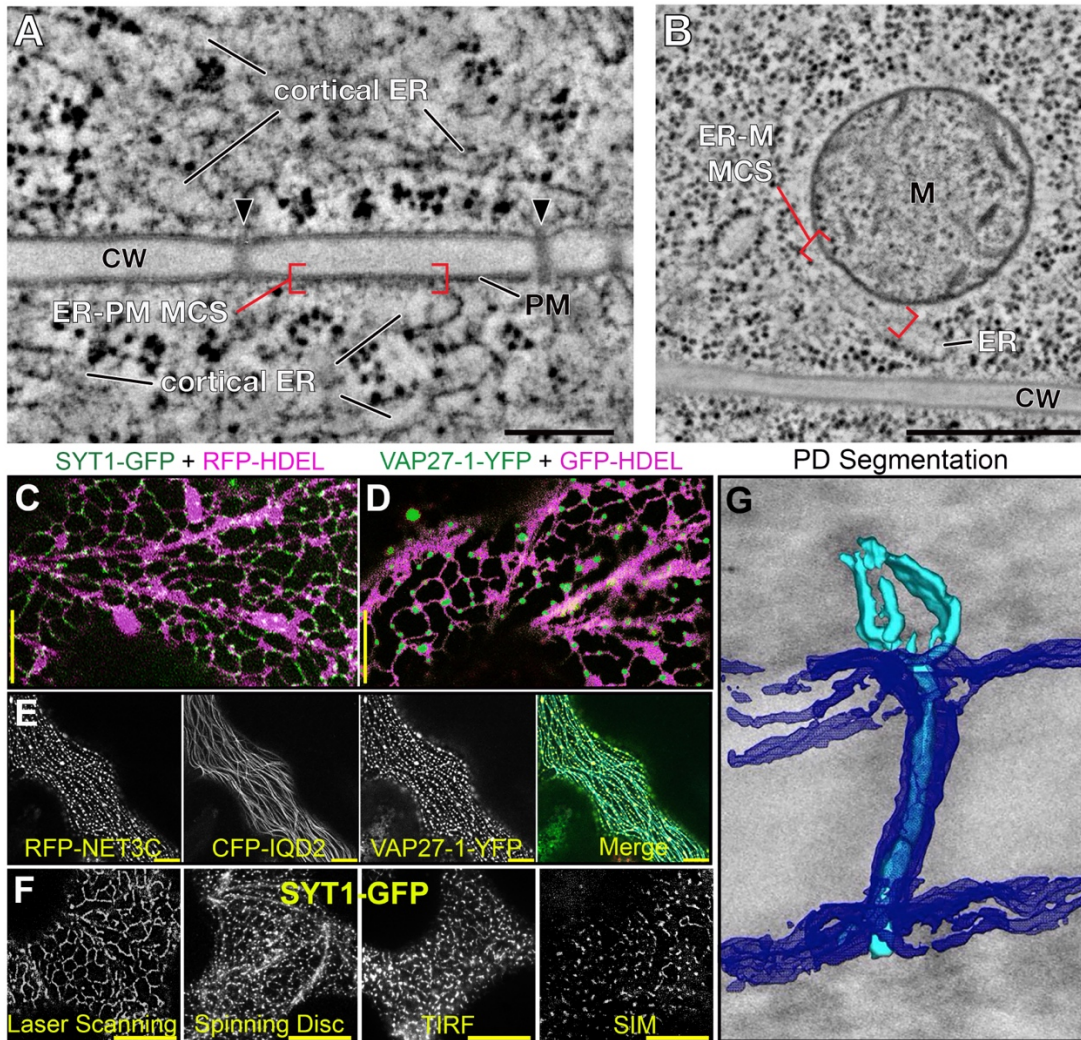


Figure 10. Examples of membrane contact sites in plants. A-B, ET slice images showing different MCS present in plant cells; an ER-PM contact site (A) and an ER-mitochondrion contact site (B) are shown. Arrowheads mark plasmodesmata. CW: cell wall, M: mitochondrion. Scale bars = 500 nm. C-D, The distribution of SYT1-GFP- and VAP27-1-YFP-labelled tethering assemblies in different regions of the cortical ER (indicated by the RFP-HDEL or GFP-HDEL markers) highlights the presence of spatially separated ER-PM MCS within the cell. E, The co-expression of the actin-associated NET3C cytoskeletal adaptor, the microtubule-associated IQ67-domain 2 (IQD2) bridging component, and the VAP27-1 tether highlights the interaction of the Arabidopsis ER-PM MCS with the cortical cytoskeleton. Scale bars in (C-E) = 10 μ M. F, The appearance of putative SYT1-GFP labelled ER-PM contact sites changes depending on the microscopy technique used. The intermembrane distances at MCS are below the light diffraction limit and are not properly resolved using conventional confocal microscopy (Laser Scanning/Spinning Disc, left two panels). More accurate visualizations are obtained using super-resolution techniques (TIRF/SIM, right two panels). Scale bar in (F) = 20 μ M. G, Advances in electron tomography techniques are enabling accurate 3D reconstructions of PD MCS. In the current functional models, the cytosolic space between the ER and the PM inside the PD serves as a trafficking conduit for mobile molecules, and the adjustment of its width is believed to regulate their flow rate, effectively controlling inter-cellular trafficking. Dark blue: Plasma Membrane. Light Blue: Cortical ER across the PD pore. (Panel E is from Zang et al. 2021, reprinted with permission.)

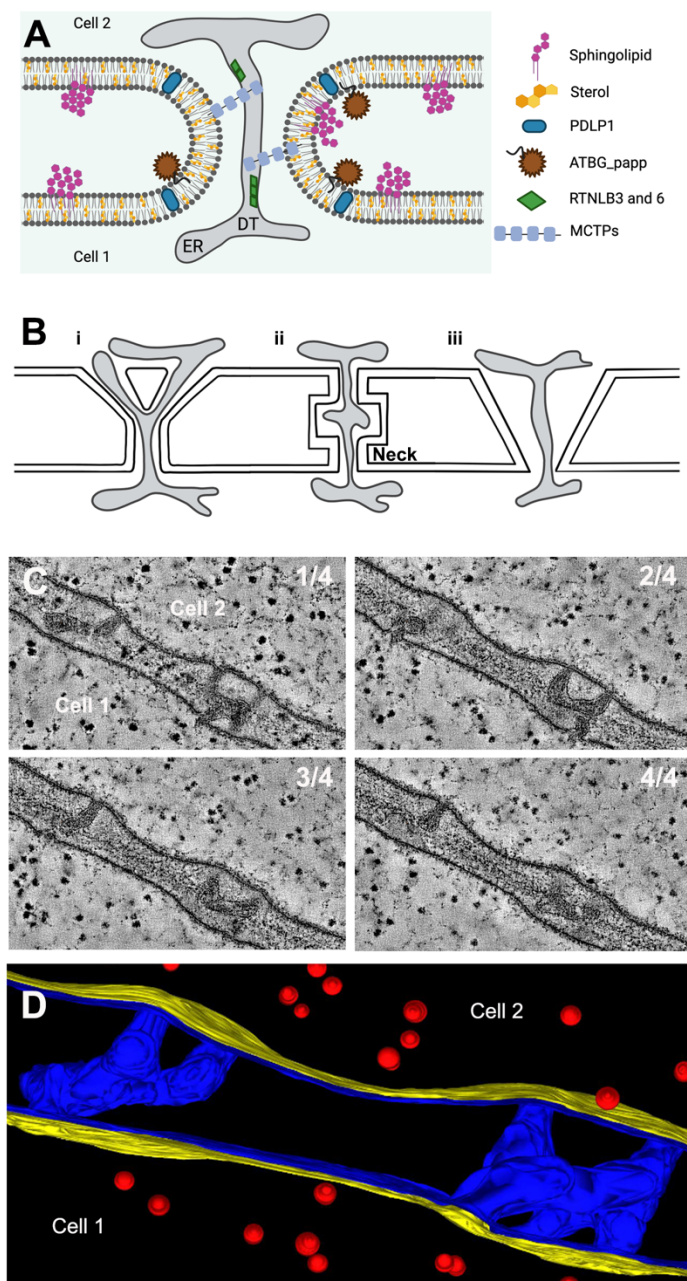


Figure 11. Structural diversity in PD and their constituents. A, A cartoon depiction of a simple plasmodesma showing details of the plasma membrane, lipid composition, and select protein constituents as described in the text. ER, endoplasmic reticulum; DT, desmotubule. B, Cartoons depicting some PD morphologies. (i) is a branched PD with a 'Y' shape, (ii) represents a simple pore with constrictions near the openings (necks) and dilation of the central region of the DT; (iii) is a funnel plasmodesma. (A) and (B) were drawn with BioRender. C-D, Structure of branched PD in Arabidopsis leaf tissue revealed by ET. (C) Four representative individual frames from a tomogram (1/4 - 4/4). While the PM is readily visible in these images, the desmotubule is difficult to discern. Central cavities are found in the vicinity of the middle lamella. (D) 3D model of PD generated by tracing the inner (yellow) and outer (blue) leaflets of the PM in the tomogram in (C). The PD on the left consists of two pores in Cell 2 and one in Cell 1. The PD on the right has two openings to Cell 2 but three to Cell 1. Ribosomes (red) are shown for scale. (C) and (D) were generated in the author's lab.

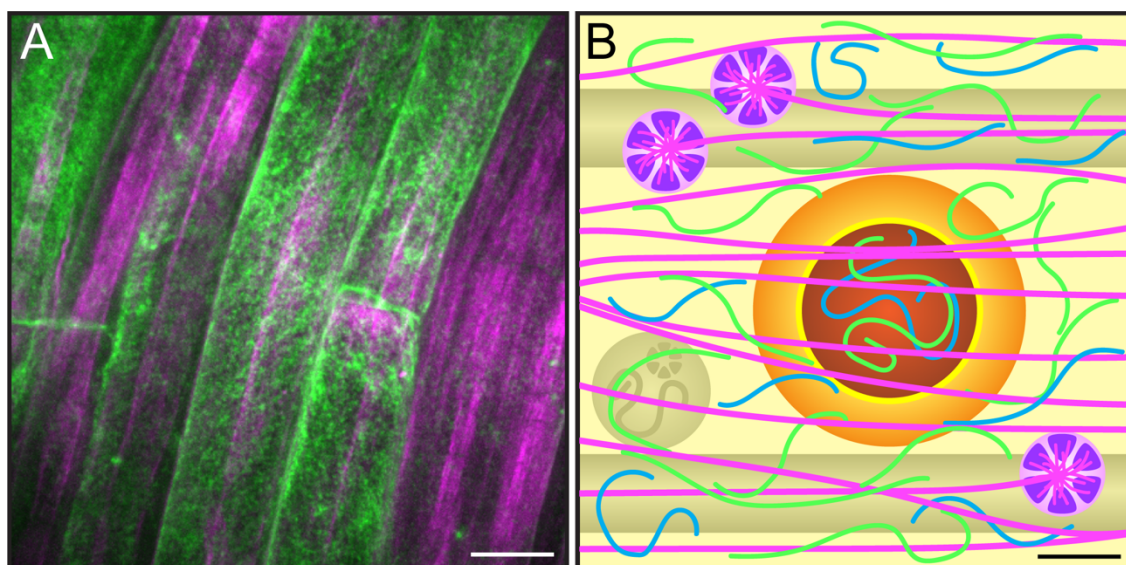


Figure 12.

Micrograph and model of the plant cell wall, showing wall patterning at the tissue and nanometer scales. A, Cellulose labelled with Pontamine Fast Scarlet 4B (S4B, magenta) and newly synthesized pectin labelled with fucose-alkyne and Alexa488-azide (green) in epidermal cells of the root differentiation zone in a 5-day-old Arabidopsis seedling. Note oblique, punctate labelling of the Alexa488 signal, predominantly longitudinal labelling of the S4B signal, and variation in intensity of the Alexa488 signal between different cells. Bar = 10 μm . B, Model of cell wall assembly viewed from outside the plasma membrane (yellow), showing Cellulose Synthase Complexes (purple) producing cellulose microfibrils (magenta) and a vesicle (orange) fusing with the plasma membrane to deliver pectin (green) and hemicellulose (cyan) to the wall. Cortical microtubules and an intracellular vesicle are shown in grey in the background. Objects are drawn approximately to scale, bar = 25 nm. Part B of this figure was inspired by a dynamic model of cell wall assembly created by Drew Berry for the Australian Research Council Center of Excellence in Plant Cell Walls and directed by Tony Bacic (University of Melbourne), Monika Doblin (University of Melbourne), and Mike Gidley (University of Queensland), which can be viewed on YouTube (<https://youtu.be/zp2WW2TYcng>).